ROYAL INSTITUTE
OF TECHNOLOGY

Coordination, Consensus and Communication in Multi-Robot Control Systems

ALBERTO SPERANZON

PhD Thesis
Stockholm, Sweden 2006

Academic thesis, which with the approval of Kungliga Tekniska Högskolan, will be presented for public review in fulfillment of the requirements for a Doctorate of Engineering in Automatic Control. The public review is held on May 24, 2006 at 10:00 at Kungliga Tekniska Högskolan, room F3, Lindstedtsvägen 26, Stockholm, Sweden.

Abstract

Analysis, design and implementation of cooperative control strategies for multi-robot systems under communication constraints is the topic of this thesis. Motivated by a rapidly growing number of applications with networked robots and other vehicles, fundamental limits on the achievable collaborative behavior are studied for large teams of autonomous agents. In particular, a problem is researched in detail in which the group of agents is supposed to agree on a common state without any centralized coordination. Due to the dynamics of the individual agents and their varying connectivity, this problem is an extension of the classical consensus problem in computer science. It captures a crucial component of many desirable features of multi-robot systems, such as formation, flocking, rendezvous, synchronizing and covering.

Analytical bounds on the convergence rate to consensus are derived for several system configurations. It is shown that static communication networks that exhibit particular symmetries yield slow convergence, if the connectivity of each agent does not scale with the total number of agents. On the other hand, some randomly varying networks allow fast convergence even if the connectivity is low. It is furthermore argued that if the data being exchanged between the agents are quantized, it may heavily degrade the performance. The extent to which certain quantization schemes are more suitable than others is quantified through relations between the number of agents and the required total network bit rate.

The design of distributed coordination and estimation schemes based on the consensus algorithm is presented. A receding horizon coordination strategy utilizing subgradient optimization is developed. Robustness and implementation aspects are discussed. A new collaborative estimation method is also proposed.

The implementation of multi-robot control systems is difficult due to the high system complexity. In the final part of this thesis, a hierarchical control architecture appropriate for a class of coordination tasks is therefore suggested. It allows a formal verification of the correctness of the implemented control algorithms.

Acknowledgments

Completing a PhD is truly a marathon event, and I would not have been able to complete this journey without the aid and support of countless people over the past five years.

First and foremost I would like to thank my advisor Karl Henrik Johansson for his guidance, support and encouragement throughout my years as PhD student. His interest, sharp mind, and patience have been very helpful during the entire time working on this thesis. I feel very honored of having become his first graduate student and I am very grateful for the past five years.

I owe my gratitude to Bo Wahlberg who accepted me as a graduate student at the Automatic Control Group and for the co-supervision.

I would like also to thank Fabio Fagnani and Sandro Zampieri for the possibility of working with them. Their never-ending enthusiasm and competence in solving research problems has been very inspiring for me. In particular I owe my gratitude to Sandro Zampieri for hosting me for five months at University of Padova.

The thesis is based on papers I have been published with different co-authors. I am indebted with all of them: Ruggero Carli, Fabio Fagnani, Carlo Fischione, Marco Focoso, Björn Johansson, Karl Henrik Johansson, Mikael Johansson , Jorge Silva, João Borges de Sousa and Sandro Zampieri.

I feel deep gratitude to everybody at the Automatic Control Group for creating a great research environment that I had the privilege to work in. In particular, I would like to thank Carlo Fischione, Björn Johansson, Mikael Johansson, Niel Möller, Michael Rotkowitz and Bo Wahlberg for reading and commenting parts of the thesis. To Karin Karlsson Eklund, I owe you gratitude for helping me with all the administrative matters.

I would like to thank Ruggero Carli, Marco Focoso and Paolo Santesso for the memorable moments spent in Padova during my five month visit.

To all the friends I met here in Stockholm, who have given me many great moments far away from control and robotics: thank you.

To my family in Italy I am especially grateful for encouraging and supporting me during all these years far from home.

Writing this thesis has required incredible teamwork with the most important people in my life, my wife Jovita and my daughter Alice. Without their patience, continuous support and encouragement I would probably have given up after 2Km of this marathon. Thank you! *Aš jus myliu.*

CONTENTS

1

INTRODUCTION

Over the past decade, the advent of networked control systems has begun to challenge the design and analysis methods in control theory. Examples of such systems are found in ad-hoc sensor networks, swarms of cooperative mobile robots and power distribution grids. Indeed, the presence of a communication network, linking the different components of the system, adds new levels of complexity to the control problem. The facts that communication links have intrinsic limitations and that few components of the system can directly communicate require the design of control strategies that can cope with such constraints and are decentralized. Mathematical models that capture both control and communication aspects are particularly important in systems where the control objective requires active coordination among the components. Typical examples of such control tasks are formation maintaining, where robots need to keep specific relative distances, or monitoring of a geographical area, by measuring the temperature or humidity of the area, or exploration.

As is typical for many complex systems, when building mathematical models one needs to tradeoff tractability and accuracy. However, for systems comprising communicating robots, vehicles, or sensors, the difficulty of finding good tradeoffs is enhanced by the fact that control and communication theory have little in common. In control theory one is concerned with designing control laws such that a given control objective is achieved, possibly minimizing some performance index. In contrast communication theory is studying a reliable way of transmitting information from a source to a destination, without considering what the information represents and if it will be reused at the source. For example, in a digital communication system one might consider rather complicated channel models so that a suitable quantization scheme (coding) can be
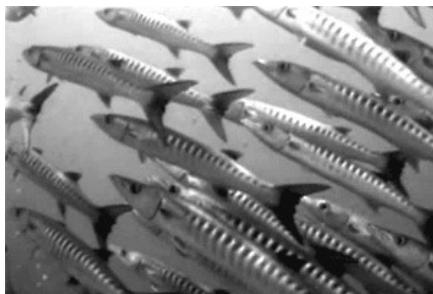
(a) A school of fish. The fish swim in a cluster to improve safety from predators.

(b) A flock of birds. Notice the "V" shape of the formation. In this way each bird can save energy from drag reduction.

Figure 1.1: Coordination in nature. (Courtesy of Harun Yahya International, `http://www.harunyahya.com/`).

designed for reliable transmission of data. From a control perspective however, a control design based on a detailed model of, for example, the robots might be useless in the presence of quantized information.

The main contribution of this thesis is the development of analytical tools and design methods for the coordination of multi-robot control systems under communication constraints. These tools are used to answer questions on the stability and performance of coordination algorithms in presence of limited network connectivity and quantization. In the first part of the thesis we will be mostly considering simplified models of the robot dynamics and communication networks, but detailed enough to capture important interactions. In the last part of the thesis we will propose and discuss a possible way for handling the complexity of a real system. In particular we will propose a layered architecture that, because of its modularity, allows detailed layer models without that the complexity of the overall system is exploding. For specific classes of coordination strategies we will show that the proposed architecture allows formal verification of the correctness of the implemented control algorithms.

The remainder of this chapter is organized as follows. In the next section we motivate why systems of multiple robots and sensors are of interest. In Section 1.2 some relevant application scenarios will be presented. In Section 1.3 we will formulate a bit more in detail the type of problems we are going to present in the thesis. Related work are summarized in Section 1.4. In Section 1.5 the contributions and the outline of the thesis will be presented.
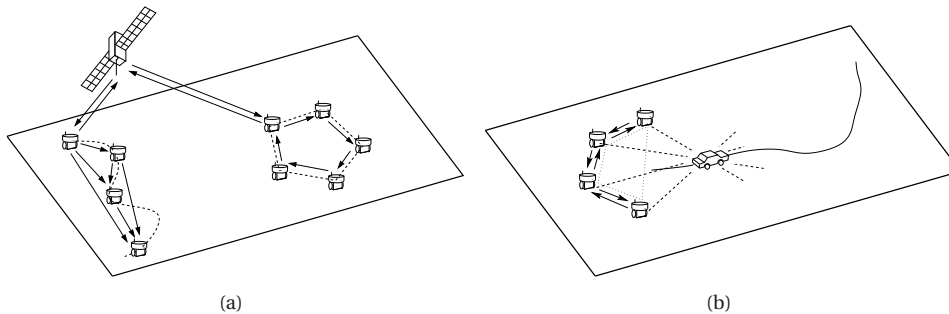
Figure 1.2: Examples of multi-agents tasks. On the left two groups of robots are engaged in a formation maintaining task. Active communication is indicated with arrows. On the right agents cooperate for tracking a moving vehicle. Each agent has limited sensing capabilities. Exchanging information the multi-agent system can obtain a precise estimate of the vehicle position.

1.1 Multi-agent systems

Coordination among interacting agents with a common group behavior is not only a recent engineering problem, but it is something that happens everyday in nature. Typical examples of such systems are schools of fish as shown in Figure 1.1(a), where fish swim in clusters in order to improve safety against predators or flocks of birds that are formed for improving the aerodynamic efficiency of the single birds in the flock, as it appears from the "V" shape of the flock in Figure 1.1(b). With agent we denote any system with sensing, computing and communicating capabilities, such as a robot, a sensor, etc. The interest in multi-agents systems has grown in the last decade, mostly because a group of collaborating agents can often deal with tasks that are difficult, or even impossible, to be accomplished by an individual agent. A team of agents typically provides flexibility, redundancy and efficiency beyond what is possible with single agents. Having several agents deployed often means that they can be flexibly organized into groups performing tasks at different locations. Robustness is ensured by the numerousness of the group, if an agent fails the other can continue the task. Having many agents rather than one can allow to perform tasks in a faster and more precise way. Figures 1.2(a) and 1.2(b) show multi-agent systems employed in two cooperative tasks. In the first example, agents are split in different groups performing different tasks. The communication network (line with arrows) allows the exchange of critical information for the task execution and to coordinate the different groups. In the second example agents with limited sensor capabilities (only bearing measurements) are used to estimate the position and follow a moving vehicle. Interagent communication enables a precise reconstruction of the vehicle position, which would never be possible using a single agent.

1.2 Motivating applications

We consider here two realistic scenarios where multi-agents system could be used.

Search and rescue operations

The problem of search and rescue is a typical application where the flexibility and redundancy of a multi-robot system would be peculiar for a successful mission. Recently robots have been used during the rescue operations of a Russian submarine trapped in the Pacific Ocean [CNN 2005]. In future applications we can foresee the use of collaborating autonomous robots in such missions.

Let us discuss a scenario as shown in Figure 1.3. A team of autonomous underwater vehicles (AUVs) is deployed in order to localize a wreck. The AUVs can communicate (dashed lines) with each other and with buoys using an acoustic modem. The deployed buoys are also used for localization of the underwater vehicle. An autonomous surface vessel (ASV) can receive data from the underwater vehicles and send them back to the remote station. The ASV works also as gateway to some unmanned aerial vehicles (UAVs). The UAVs give an approximate position of the wreck from aerial view of the area. An accurate localization of the wreck can be achieved with an active communication of measurements and a precise motion coordination of the AUVs. After some time they will reach a consensus on the position of the wreck which they communicate to the ASV through the buoys.

In the scenario there are heterogeneous agents (AUVs, ASVs and UAVs) that need to communicate and coordinate their tasks. The challenge is on the design of coordination strategies, but also on a modular architecture that allows us to handle heterogeneity.

Hazard prevention

An interesting application of multi-agent systems is the monitoring of hazards in specific geographical areas, such as natural parks and forests. In a recent report from the United Nation Environment Program [UNEP 2003] it it reported that every year wildland fires burn an area the size of Australia with consequences on deforestation and climate change. The possibility of having a multi-agent system, comprised of both stationary and moving sensors, placed on a large area would allow an alarm to be raised as soon as an hazard occurs and an effective prevention could be carried out by continuous temperature and humidity monitoring.

Figure 1.4 shows an example of such a scenario. A network of nodes (sensors with communication capabilities) and robots are deployed over a large area in order to detect a fire. Internode communication of temperature data allows the nodes to determine the location of the fire and propagate such information through the network to the nodes that are closer to a long-range communication antenna, which forward the alarm. Mobile robots are used to interact with the environment, for example, moving toward the fire to gather more detailed information or even for an extinguishing operation. Impor-
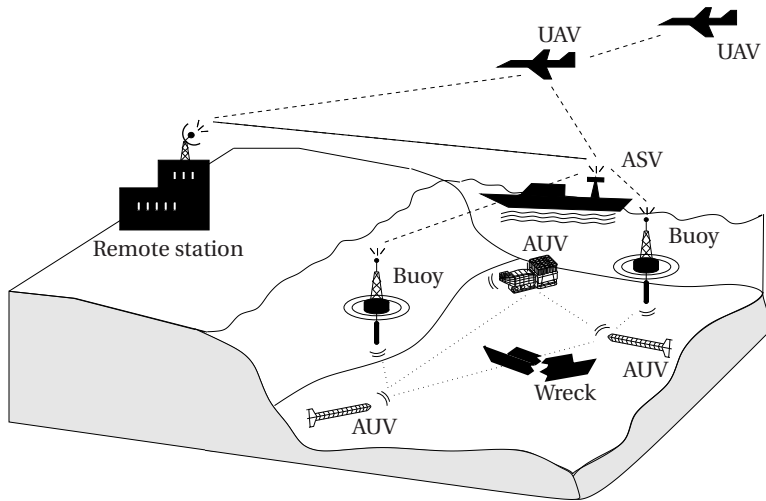
Figure 1.3: Search and rescue scenario. Heterogenous autonomous vehicles deployed for the rescue operation of a wreck.

tant in this scenario is that the sensors would reach a fast agreement on the position of the hazard from different measurements, so that a prompt action can be undertaken.

1.3 Problem formulation

A fundamental role in a problem of coordination is the definition and management of shared information among the agents. In cooperative control problems the shared information may take the form of relative positions or velocity information, as it could be in a search and rescue task, or an environment map, as in a hazard prevention scenario. A cooperative control strategy is effective if each agent is able to take advantage of the information received, so that the team of agents is able to carry out the cooperative task in an efficient and robust way, for example completing the task with minimum energy consumption and being able to respond to unanticipated situations or changes in the environment. A direct consequence of the assumption that shared information is a necessary to achieve coordination in an efficient way is that cooperation requires the group of agents to reach consensus on the coordination data. In other words, agent's state must asymptotically approach a common value. This is the case, for example, in the two scenarios we discussed previously, where the consensus on the position of a wreck, in the first case, and of a fire, in the second, is critical for the accomplishment of the task.

The mathematical formulation of such cooperative control strategies yields to the consensus or state-agreement problem. The consensus problem can be stated as follows. Let x_i represent the information state of vehicle i, i.e., the information needed to
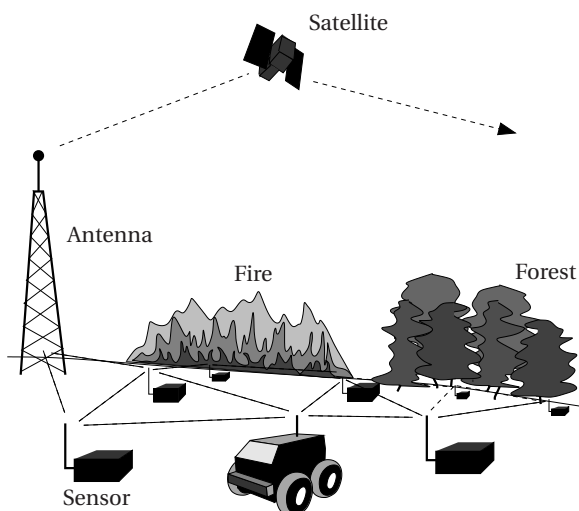
Figure 1.4: Hazard prevention scenario. A wireless sensor network is deployed over a large area in order to detect possible fires. Moving sensors (as the wheeled robot in the figure) are used for more detailed information and first aid operations.

coordinate the agents. The consensus dynamics is

$$x_i(t+1) = \sum_{i=1}^{N} \alpha_{i,j}(t) \, x_j(t)$$

where N is the number of agents. The consensus problem is then to choose the control laws $\alpha_{i,j}(t)$, at each time instance t, such that the information state $x_i(t)$ of all vehicles converge to the same value, called the consensus point. If $\alpha_{i,j} = 0$ agent j is not communicating with agent i. The scalars $\alpha_{i,j}$ define the arc set of a graph with vertexes corresponding to the agents. There is an arc between vertex j and vertex i if and only if $\alpha_{i,j}$ is nonzero. Thus the graph is a model of the communication network linking the agents.

We associate to the consensus dynamics a cost function, in order to measure the control performance of a given control strategy. In this context, an interesting problem is the characterization of the relationship between control and communication. More precisely, given a communication network, specified by the connectivity of each vertex, that is, the number of neighbors of each agent, determine the values of $\alpha_{i,j}$ that guarantee convergence and that the cost function is minimized. This will be the focus of Chapter 3. Since agents interacts via a digital communication network, where the information is quantized to cope with bandwidth limitations, an interesting problem is to study the consensus problem in this setting. In particular the problem is to determine $\alpha_{i,j}$ so that converge of the state to the consensus point is guaranteed. Quantization and consensus are discussed in Chapter 4.

An interesting question is on the choice of the consensus point. In particular, a design problem is that of determining the values $\alpha_{i,j}$, for a given communication network, so that a cost function that depends on the consensus point is minimized. In Chapter 5 we will consider such problem. The generality of the consensus, allows also to consider problems related to collaborative estimation. Extending the consensus problem to a stochastic setting we can choose as performance the variance of the estimate. The problem is then to design $\alpha_{i,j}$, for a given communication network, so that a distributed minimum variance estimator is obtained. This problem is tackled in Chapter 6.

One of the main limitations of the consensus problem is that the dynamics considered are typically too simple to model complex agents, as vehicles or robots. Indeed mobile robots are generally nonholonomic mechanical systems, roughly speaking systems that cannot move in an arbitrary direction in their configuration space. Also the effect of data exchange over a network are not restricted to limited connectivity or quantization, but data losses and delays should also be considered. Thus one needs either to consider more complex models, with the risk that the overall problem becomes difficult to be tackled formally or providing a framework that could handle such complexity. In this context the problem is that of designing an architecture which allows the implementation of coordination algorithms for more realistic scenarios. The architecture needs to be flexible, modular and it should be possible to verify the correctness of the algorithms implemented. More precisely, the architecture needs to fulfill a set of specifications that describes the class of coordination algorithms that can be correctly implemented. In Chapter 7 we propose and discuss such architecture.

1.4   Related work

A brief review of related work within the area of multi-agent control will be presented here. The discussion is focused on the recent literature in the area of control. More details will be given in relation to the contribution in each chapter.

Many frameworks and mathematical models have been proposed over the past years in order to solve coordination problems for multiple robots. Recent examples include virtual potential functions [Leonard and Fiorelli 2001; Tanner et al. 2005], Voronoi partitions [Cortés et al. 2004b; Lindhé et al. 2005], graphs [Olfati-Saber et al. 2003; Tanner et al. 2005], probabilistic methods [Hespanha et al. 1999; Vidal et al. 2002; Speranzon and Johansson 2003], model predictive control [Dunbar and Murray 2005; Borrelli et al. 2005]. In some of these frameworks the communication among the different agents is explicitly considered, in others the data exchange is assumed to be perfect.

A coordination problem, in which the communication is modelled as a graph, is the consensus problem. In the classical framework, each agent shares its information with other agents inside a predefined neighborhood, namely the agents are modelled as omnidirectional antennas with a short reliable communication range [Jadbabaie et al. 2003; Olfati-Saber and Murray 2004; Cortés et al. 2004a]. In this case the communication is modelled as a disc graph. When such communication is available among moving agents, the network topology changes with the position of the agents. The overall dy-

namical system exhibits a quite complex behavior that is hard to analyze. One of the difficulties is that connectivity properties of the communication network are, in general, not guaranteed to be preserved under dynamical constraints. Simplified models have been proposed in [Jadbabaie et al. 2003; Olfati-Saber and Murray 2004; Ren and Beard 2005] where the authors consider switching systems in which, anyway, the switching rule does not dependent on the position of the agents. With such models they are able to derive sufficient conditions for state agreement. In [Tanner et al. 2003] the authors use tools from non-smooth analysis to design a control strategy that leads to agreement and allows the vehicle to avoid collisions. Robustness to communication link failure [Cortés et al. 2004a] and the effects of time delays [Olfati-Saber and Murray 2004] have been also considered. The consensus problem with time-invariant communication networks have been studied in [Smith et al. 2005; Ferrari-Trecate et al. 2005]. Also randomly time-varying networks have been analyzed recently in [Hatano and Mesbahi 2004].

In most of the frameworks the vehicles dynamic considered are rather simple, such as a first or second order model [Leonard and Fiorelli 2001; Jadbabaie et al. 2003; Speranzon and Johansson 2003; Olfati-Saber and Murray 2004; Tanner et al. 2005]. More complex dynamics are considered, for example, in in [Egerstedt and Hu 2001; Ren and Beard 2004; Dunbar and Murray 2005; Borrelli et al. 2005], however the communication among the vehicle is assumed to be perfect. A way of dealing with the increasing complexity of a system where the agents are described by nonlinear differential equations is that of considering hierarchical control structures [Godbole et al. 1994; Varaiya 2000; Koo and Sastry 2002; Campbell et al. 2003; Mazo et al. 2004]. The main advantage of a hierarchical control structure is its flexibility, modularity that can be used to tackle rather complex problems. Moreover verification analysis can be carried out on such systems [Lygeros et al. 1996]. On the other hand there are few examples where such architecture has been used in for modelling multi-agent systems with communication capabilities and in particular to model communication limitations such as data losses.

1.5   Outline of the thesis and contributions

The main contribution of the thesis is given in five chapters. The material is organized as follows

Chapter 3 and 4	Analysis of consensus coordination under communication constraints, in particular, connectivity and quantization.
Chapter 5 and 6	Design of consensus coordination strategies for control and estimation.
Chapter 7	Implementation of coordination strategies for multi-agent systems through a hierarchical control architecture.

In more detail, the outline of the thesis is as follows.

Chapter 2: Mathematical background

In this chapter some mathematical concepts used throughout the thesis are reviewed. The main objective of the chapter is to show that for a Markov chain defined on a finite Abelian group is possible to bound the convergence rate by the Fourier transform of the probability measure that defines the chain. We present results from harmonic analysis and Markov chains on finite Abelian groups.

Chapter 3: Consensus coordination under limited communication

In this chapter the consensus problem is introduced together with a model for the communication network linking the agents. An optimization problem based on the essential spectral radius of the closed loop state transition matrix is considered. Such cost function is a measure of the convergence rate to the consensus. Under some suitable constraints, it captures the tradeoffs between connectivity of the communication network and control performance. Restricting to doubly stochastic matrices compatible with time-invariant communication networks with symmetries, we compute a tight bound on the essential spectral radius. It is shown that the convergence rate to the consensus decreases as the number of agents increases if the connectivity is kept constant. An analysis of the performance in time-varying communication graphs is also carried out. Averaging over classes of graphs, it is shown that the convergence rate is much higher compared to time-invariant communication graphs. The content of this chapter will appear in

> R. Carli, F. Fagnani, M. Focoso, A. Speranzon and S. Zampieri. Symmetries in the Coordinated Consensus Problem. In P.J. Antsaklis and P. Tabuada, Ed., NESC: Networked Embedded Sensing and Control, Lecture Notes in Control and Information Sciences, Springer, 2006. To appear.

and partially also in

> R. Carli, F. Fagnani, A. Speranzon and S. Zampieri. Communication Constraints in Coordinated Consensus Problems. In Proceedings of American Control Conference, 2006. To appear.

> R. Carli, F. Fagnani, A. Speranzon and S. Zampieri. Communication Constraints in the State Agreement Problem. Internal Report 32, Department of Mathematics, Politecnico di Torino. Submitted for journal publication, 2005.

Chapter 4: Quantization in consensus coordination

Data exchange over digital communication channels requires quantization. In this chapter we analyze the effects of quantized data exchange in the consensus problem. Considering a weaker concept of consensus, with respect to the one introduced in the previous chapter, we analyze various control strategies for solving the problem. We consider the effect of two quantization schemes: uniform and logarithmic. Scenarios where data

are either uniformly or logarithmically or uniformly and logarithmically quantized are analyzed. A comparison between the different scenarios is made considering the total amount of data that is circulating in the network at each time instance. The results of the first part of this chapter have been extended from the papers

> K. H. Johansson, A. Speranzon and S. Zampieri. On Quantization and Communication Topologies in Multi-vehicle Rendezvous. In Proceedings of 16th IFAC World Congress, 2005.

> F. Fagnani and K. H. Johansson and A. Speranzon and S. Zampieri. On Multi-vehicle Rendezvous under Quantized Communication. In Proceedings of International Symposium on Mathematical Theory of Networks and Systems, 2004.

The second part is based on the following two papers

> R. Carli, F. Fagnani, A. Speranzon and S. Zampieri. Communication constraints in coordinated consensus problems. In Proceedings of American Control Conference, 2006. To appear.

> R. Carli, F. Fagnani, A. Speranzon and S. Zampieri. Communication Constraints in the State Agreement Problem. Internal Report 32, Department of Mathematics, Politecnico di Torino. Submitted to for journal publication, 2005.

Chapter 5: Model predictive consensus

A finite time horizon consensus problem where the consensus point is negotiated by the agents is considered in this chapter. The control action is computed solving a receding horizon optimization problem. Distributed implementation is obtained through primal decomposition techniques and incremental subgradient methods. We show that, for particular communication networks, the problem can be efficiently solved by a multi-agent system. In the end of the chapter some extensions to cases when noise and limited data rate affects the system are presented. The results of this work will appear as

> B. Johansson, A. Speranzon, M. Johansson, and K. H. Johansson. Distributed Model Predictive Consensus. In Proceedings of International Symposium on Mathematical Theory of Networks and Systems, 2006. To appear.

Chapter 6: Collaborative estimation

The consensus algorithm is used in this chapter to design a minimum variance estimator. The problem is to estimate a time-varying signal measured by the agents. Each agent builds an estimate from estimates and measurements received by neighboring agents. Such information is weighted so that the variance of the estimate at each agent is minimized, maintaining global stability of the estimator. The time-varying weights are computed online through a distributed filter. Simulation results show improvements of performance compared to other methods proposed in the literature. This chapter is partially based on

A. Speranzon, C. Fischione and K. H. Johansson. Distributed and Collaborative Estimation over Wireless Sensor Networks. Submitted to IEEE Conference on Decision and Control, 2006.

B. Johansson, A. Speranzon, M. Johansson, and K. H. Johansson. Distributed Model Predictive Consensus. In Proceedings of International Symposium on Mathematical Theory of Networks and Systems, 2006. To appear.

Chapter 7: Hierarchical coordination architecture

Implementation of coordination strategies for multi-agent systems is addressed in this chapter. proposing a hierarchical coordination architecture. A control architecture composed of three-layer systems connected in a network is proposed. Event-driven coordination strategies are mapped onto the top layer, which provides waypoints for the agents. The maneuver that an agent needs to perform in order to reach its waypoint is generated by the two lower layers. The middle layer maps commands from the top layer to a finite set of maneuvers. The execution of each maneuver is done at the bottom layer which generates and tracks suitable trajectories. Issues related to the verification of the architecture with respect to a given overall specification is considered. Part of the results has been presented as

J. Silva and A. Speranzon and J. Borges de Sousa and K. H. Johansson. Hierarchical Search Strategy for a Team of Autonomous Vehicles. In Proceedings of the 5th IFAC Symposium on Intelligent Autonomous Vehicles, 2004.

J. Borges de Sousa, K. H. Johansson, A. Speranzon, and J. Silva. A Control Architecture for Multiple Submarines in Coordinated Search Missions. In Proceedings of 16th IFAC World Congress, 2005.

The chapter is based on

J. Borges de Sousa, K. H. Johansson, J. Silva and A. Speranzon. A Verified Hierarchical Control Architecture for Coordinated Multi-Vehicle Operations. International Journal of Adaptive Control and Signal Processing, 2006. Special issue on autonomous adaptive control of vehicles. To appear.

Chapter 8: Conclusions and future work

This chapter summarizes the results of the thesis and concludes by suggesting possible future extensions to the presented work.

Contributions by the author

The present thesis is a monograph. It is partially based on papers written with co-authors. In the joint papers the author has actively contributed both to the development of the theory as well as the paper writing.

1.6 Other publications

The author of the thesis has been co-author of other publications in the field of robotics and automatic control, which have influenced the contents of this thesis. The publication include the following:

M. Mazo, A. Speranzon, K. H. Johansson and X. Hu: "Multi-robot Tracking of a Moving Object Using Directional Sensors". IEEE International Conference on Robotics and Automation, 2004.

E. Pagello, A. D'Angelo, C. Ferrari, R. Polesel, R. Rosati and A. Speranzon: "Emergent Behaviors of a Robot Team Performing Cooperative Tasks". *Advanced Robotics*, Vol. 15, No. 1, 3-20, 2003.

A. Speranzon and K. H. Johansson: "On Some Communication Schemes for Distributed Pursuit-Evasion Games". In Proceedings of IEEE Conference on Decision and Control, 2003.

C. Altafini, A. Speranzon and K. H. Johansson: "Hybrid Control of a Truck and Trailer Vehicle". In Hybrid Systems: Computation and Control, C.J. Tomlin and M.R. Greenstreet, Ed. - Lecture Notes in Computer Science, Springer-Verlag. 2002.

P. de Pascalis, M. Ferraresso, M. Lorenzetti, A. Modolo, M. Peluso, R. Polesel, R. Rosati, N. Scattolin, A. Speranzon and W. Zanette: "Golem Team in Middle-Sized Robots League". In RoboCup-2000: Robot Soccer World Cup IV, P. Stone, T. Balch, and G. Kraetszchmar, Ed. - Springer-Verlag, Berlin, 2001.

C. Altafini, A. Speranzon and B. Wahlberg: "A Feedback Control Scheme for Reversing a Truck and Trailer Vehicle". *IEEE Transactions on Robotics and Automation*, 2001.

R. Polesel, R. Rosati, A. Speranzon, C. Ferrari and E. Pagello: "Using Collision Avoidance Algorithms for Designing Multi-robot Emergent Behaviors".
IEEE/RSJ International Conference on Intelligent Robots and Systems, 2000.

MATHEMATICAL BACKGROUND

2.1 Introduction

In this chapter we introduce the mathematical framework upon which the results presented in the next chapters of the thesis are based. The main objective is to present a bound on the mixing rate of finite Markov chains when the chain is defined on finite Abelian groups. The presentation is based on [Diaconis 1988; Aldous and Fill 200X; Fraleigh 1998; Behrends 1999; Terras 1999; Bremaud 2001; Saloff-Coste 2004]. All the proofs of the results presented here are taken from the previous list of references.

2.2 Harmonic analysis on finite groups

The main objective of this section is that of reviewing some concepts on harmonic analysis on finite groups.

2.2.1 Finite Abelian groups

We start by recalling the definition of a finite Abelian group.

Definition 2.1 *A finite Abelian group G of order N, is a set G of cardinality $|G| = N$, closed under a binary operation $+$, such that the following axioms are satisfied*[1]

---

[1] In the following we will use $|.|$ to denote both the cardinality of a set and the absolute value operator.

(i) *(Associativity) For all $g, h, \ell \in G$, we have that*

$$(g + h) + \ell = g + (h + \ell)\,.$$

(ii) *(Commutativity) The binary operation $+$ is commutative, for any $g, h \in G$ if we have that $g + h = h + g$.*

(iii) *(Neutral element) There is a neutral element $e \in G$ such that for all $g \in G$*

$$g + e = g\,,$$

In the following we will indicate with 0 such element.

(iv) *(Inverse element) Corresponding to each $g \in G$ there is an element $g' \in G$ such that*

$$g + g' = 0\,,$$

In the following we will indicate such element with $-g$.

From now on when we refer to a group we will implicitly consider finite Abelian groups. We will assume the operation to be the addition if not otherwise stated.

Example 2.1 Let us consider the set $\mathbb{Z}_N = \{0, 1, \ldots, N - 1\}$. If we consider as binary operation the addition modulo N, all the previous axioms are satisfied, and thus it represents a finite Abelian group. ◇

Let G and H be two Abelian groups. The two groups, in general, need not to be finite. An *homomorphism* is a map $\varphi : G \to H$ satisfying

$$\varphi(g + h) = \varphi(g) + \varphi(h)$$

with $g \in G$ and $h \in H$. An homomorphism that is bijective is called *isomorphism*. Two Abelian groups are isomorphic if there is an isomorphism between them. Isomorphic groups are regarded as "equal" from a structural or group-theoretic point of view, even though their elements might be quite different kinds of object. In the following we will write $G \cong H$ to denote that G is isomorphic to H.

Example 2.2 Let us consider the finite additive group $\mathbb{Z}_4 = \{0, 1, 2, 3\}$ and the binary group $B = \{00, 01, 10, 11\}$ with operation the 2-bits binary sum. If we consider the map

$$\varphi : G \to H : g \mapsto \varphi(g) = \mathrm{binary}_2(g)$$

where $\mathrm{binary}_2(g)$ is the binary representation in two bits of the integer g, then we see immediately that it is an isomorphism. Thus $G \cong H$. ◇

Given a finite group G a subgroup H of G is a subset of G that also forms a group under the same binary operation $+$.

Example 2.3 Let us consider $\mathbb{Z}_8$, and let $H = \{0, 4\} \subset \mathbb{Z}_8$. It is easy to see that H is also a group with respect to the addition modulo eight. ◇

Given a finite group G let us consider a subset S of the group. Then $\langle S \rangle$, the subgroup generated by S, is the smallest subgroup of G containing every element of S. Equivalently, $\langle S \rangle$ is the subgroup of all elements of G that can be expressed as the finite product of elements in S and their inverses.

Example 2.4 Let us consider the group

$$\mathbb{Z}_3 \times \mathbb{Z}_3 = \{(0,0), (0,1), (0,2), (1,0), (2,0), (1,1), (1,2), (2,1)\}.$$

Let consider $S = \{(0,0)\}$. It is clear that $\langle S \rangle = S$ is a subgroup of G. Let us consider $S = \{(0,0), (0,1)\}$ then we see that $S \subset \langle S \rangle = \{(0,0), (0,1), (0,2)\}$ is smallest subgroup of G containing S. ◇

If $G = \langle S \rangle$, then we say S generates G; and the elements in S are called generators or group generators.

Example 2.5 Let us consider again group $\mathbb{Z}_3 \times \mathbb{Z}_3$. Then we see that if we choose $S = \{(0,0), (0,1), (1,0)\}$ then $\langle S \rangle = G$. ◇

Definition 2.2 *An finite Abelian group G is called cyclic group if its elements are all of the form kg for $k \in \mathbb{Z}$ for some fixed $g \in G$. The element g is called the generator of the group G, and we will write that $\langle g \rangle = G$.*

It turns out that a finite cyclic group is a group generated by a single element. In a finite cyclic group of order N, the generator satisfies $Ng = 0$, and N is the smallest positive integer with this property, and N is called the order of the generator. Thus the order of the generator is equal to the order of the group (even if the sense of the word "order" is different). It is then easy to see that any two finite cyclic groups of the same order are isomorphic.

Example 2.6 Let us consider the group $\mathbb{Z}_4$. Then we have that

$$\langle 1 \rangle = \langle 3 \rangle = \mathbb{Z}_4.$$

Notice that $\langle 2 \rangle = \{0, 2\}$ which, clearly, is not $\mathbb{Z}_4$. The group $\mathbb{Z}_4$ is the called the cyclic group of the integers modulo four. ◇

The direct sum $G \oplus H$ of two Abelian groups G and H is the set of all ordered pairs (g, h), with $g \in G$ and $h \in H$. If we define the following addition operation

$$(g_1, h_1) + (g_2, h_2) = (g_1 + g_2, h_1 + h_2)$$

then it is easy to see that $G \oplus H$ is an Abelian group whose neutral element is $(0, 0)$ and the inverse of (g, h) is $(-g, -h)$. The definition of direct sum is easily extended to more than two Abelian groups.

We then have the following fundamental result.

Theorem 2.1 (Fundamental theorem of finite Abelian groups) *Let G be a finite Abelian group. There exist cyclic groups $\mathbb{Z}_{q_1}, \mathbb{Z}_{q_2}, \ldots, \mathbb{Z}_{q_r}$ of orders $q_1, q_2, \ldots, q_r > 1$, respectively, where the q_i are prime powers, for $1 \leq i \leq r$, such that*

$$G \cong \mathbb{Z}_{q_1} \oplus \mathbb{Z}_{q_2} \oplus \cdots \oplus \mathbb{Z}_{q_r}.$$

Thus G is isomorphic to the direct sum of cyclic groups.

Example 2.7 Let us consider the group $\mathbb{Z}_6 = \{0, 1, 2, 3, 4, 5\}$. Using the previous theorem we have that

$$\mathbb{Z}_6 \cong \mathbb{Z}_2 \oplus \mathbb{Z}_3.$$

Indeed, let us consider the following map

$$\varphi : \mathbb{Z}_2 \oplus \mathbb{Z}_3 \to \mathbb{Z}_6 : (g, h) \mapsto (3g + 2h) \bmod 6,$$

with $g \in \mathbb{Z}_2$ and $h \in \mathbb{Z}_3$. It is easy to see that φ is an isomorphism, and thus $\mathbb{Z}_6 \cong \mathbb{Z}_2 \oplus \mathbb{Z}_3$.

$\diamond$

2.2.2   Group characters

Let G an finite Abelian group of order N. We can define the character of the group G as follows.

Definition 2.3 *A character of G is a homomorphism $\chi : G \to \mathbb{C}^\times$ where $\mathbb{C}^\times = \mathbb{C} \setminus \{0\}$, which maps G to the non-zero multiplicative group of complex numbers.*

Since χ is a homomorphism then have that

$$\chi(g + h) = \chi(g)\chi(h), \qquad g, h \in G.$$

In particular, we have that

$$\chi(g)^N = \chi(Ng) = \chi(0) = 1, \quad g \in G,$$

and so the values of χ are the Nth roots of the unity. Notice moreover that

$$\chi(-g) = \chi(g)^{-1} = \overline{\chi(g)}$$

where the bar indicates the complex conjugate. The character defined by

$$\chi(g) = 1, \quad \forall g \in G,$$

is called the *trivial* (or principal) character of the group G. All the others are called non-trivial characters.

Example 2.8 Consider the group $\mathbb{Z}_N$. We have that the characters of $\mathbb{Z}_N$ are

$$\chi_\ell : g \mapsto \exp\left(i2\pi \frac{\ell}{N} g\right),$$

with $\ell = 0, \ldots, N-1$ and $g \in \mathbb{Z}_N$. It is easy to see that the trivial character of the group $\mathbb{Z}_N$ is $\chi_0(g)$. $\diamond$

The characters of a finite Abelian group have many properties. We summarize here some important facts.

Proposition 2.1 *For any nontrivial character χ of G,*

$$\sum_{g \in G} \chi(g) = 0.$$

Proof. Let $h \in G$ be that $\chi(h) \neq 1$, h is not a trivial character of G. Let $L = \sum_{g \in G} \chi(g)$ with χ non trivial, then we have

$$\chi(h) L = \sum_{g \in G} \chi(h)\chi(g) = \sum_{g \in G} \chi(h+g) = L.$$

We then have

$$L(\chi(h) - 1) = 0$$

which implies $L = 0$ since $\chi(h) \neq 0$. This concludes the proof. $\square$

Let us now denote $\hat{G}$ the set of all characters. Let us define the following operation between two characters, χ and φ, of a group G

$$(\chi\varphi)(g) = \chi(g)\varphi(g). \tag{2.1}$$

It is easy to see that this set forms an Abelian group under the operation defined by (2.1). The conjugation represent the inversion in the group $\hat{G}$. The group of the characters $\hat{G}$ is called the *dual group* of G.

Proposition 2.2 *Let χ and φ be two characters of the group G. Then we have*

$$\sum_{g \in G} \chi(g)\overline{\varphi(g)} = \begin{cases} N & \text{if } \chi = \varphi \\ 0 & \text{otherwise}. \end{cases}$$

Proof. If $\chi = \varphi$ then this follows from the fact that $\overline{\chi(g)} = \chi(g)^{-1}$. If $\chi \neq \varphi$, then $\chi\overline{\varphi}$ is a nontrivial character of G and using Proposition 2.1 the result follows. $\square$

Example 2.9 Consider the group $\mathbb{Z}_N$. The characters of the group are

$$\chi_\ell(g) = \exp(i2\pi \frac{\ell}{N} g)$$

$\ell = 0, \ldots, N-1$ and $g \in \mathbb{Z}_N$. Then the dual group of $\mathbb{Z}_N$ is

$$\hat{\mathbb{Z}}_N = \{\chi_0, \ldots, \chi_{N-1}\}.$$

$\Diamond$

Lemma 2.1 $\hat{\mathbb{Z}}_N \cong \mathbb{Z}_N$.

Proof. Since $\mathbb{Z}_N$ is a cyclic group then $\langle 1 \rangle = \mathbb{Z}_N$. The characters of $\mathbb{Z}_N$ then have the form

$$\chi_\ell(k) = \exp\left(i2\pi\frac{\ell}{N}k\right)$$

where $k \in \mathbb{Z}$, $\ell = 0,\ldots,N-1$. But this shows that χ_1 is a generator of $\hat{\mathbb{Z}}_N$. Since two cyclic groups of the same order are isomorphic then we can conclude. $\square$

Lemma 2.2 *If the group G is expressed as direct sum, namely $G = G_1 \oplus G_2$ and $\varphi_i : G_i \rightarrow \mathbb{C}^\times$ is a character of G_i, $i = 1,2$, then $\chi = \varphi_1 \oplus \varphi_2$, defined as*

$$\chi(g_1,g_2) = \varphi_1(g_1)\varphi_2(g_2),\tag{2.2}$$

is a character of G. Moreover, all characters of G are of this form. Thus we have that

$$\hat{G} \cong \hat{G}_1 \oplus \hat{G}_2.$$

Proof. It is easy to show that χ is a character of G since it defines an homomorphism between G and $\mathbb{C}^\times \times \mathbb{C}^\times$ and

$$\chi(g + h) = \chi((g_1,g_2) + (h_1,h_2)) = \chi(g_1 + h_1, g_2 + h_2) = \varphi(g_1 + h_1)\varphi(g_2 + h_2)$$
$$= \varphi(g_1)\varphi(h_1)\varphi(g_2)\varphi(h_2) = \varphi(g_1 + g_2)\varphi(h_1 + h_2) = \varphi(g)\varphi(h)$$

where we used the fact that φ_i is a character of G_i. It is clear that $\hat{G}_1 \oplus \hat{G}_2 \rightarrow \hat{G}$ defined by (2.2) is injective. We need to show then that if we consider $\chi(\tilde{(g_1)}, g_2) = \chi(g_1,g_2)$ then $\varphi_1(\tilde{g}_1) = \varphi_1(g_1)$. It follows that

$$0 = \chi(\tilde{g}_1,g_2) - \chi(g_1,g_2) = \varphi(\tilde{g}_1)\varphi_2(g_2) - \varphi(g_1)\varphi_2(g_2) = \varphi_2(g_2)\left(\varphi(\tilde{g}_1) - \varphi(g_1)\right).$$

Since $\varphi_2(g_2) = 0$ then it follows that $\varphi(\tilde{g}_1) = \varphi(g_1)$ as we wanted. Let us now consider $\chi \in \hat{G}$. Then the restriction $\varphi_i = \chi|_{G_i}$ is a character of G_i, and it easy to verify that $\chi = \varphi_1 \oplus \varphi_2$. $\square$

Theorem 2.2 *For arbitrary finite Abelian groups $\hat{G} \cong G$.*

Proof. From Theorem 2.1 we have that $G \cong \mathbb{Z}_{q_1} \oplus \cdots \oplus \mathbb{Z}_{q_r}$. We know that $\hat{\mathbb{Z}}_{q_i} \cong \mathbb{Z}_{q_i}$ by Lemma 2.1. From Lemma 2.2 follows that the direct sum $\hat{G} \cong \hat{\mathbb{Z}}_{N_1} \oplus \cdots \oplus \hat{\mathbb{Z}}_{N_k} \cong G$. $\square$

Let $\mathbb{C}^G$ denote the space of functions $f : G \rightarrow \mathbb{C}$. This represents an N-dimensional linear space over $\mathbb{C}$. We introduce an inner product over this space

$$\langle f_1, f_2 \rangle = \frac{1}{N}\sum_{g \in G} f_1(g)\overline{f_2(g)}, \quad f_1, f_2 \in \mathbb{C}^G.$$

We then have the following result.

Theorem 2.3 *The elements of the set $\hat{G}$ forms an orthonormal basis in $\mathbb{C}^G$.*

Proof. Orthogonality follows directly from Lemma 2.2. Completeness follows from that $G \cong \hat{G}$, which implies that $|\hat{G}| = N = \dim \mathbb{C}^G$.

$\qquad\qquad\qquad\qquad\qquad\qquad\qquad\qquad\qquad\qquad\qquad\qquad\qquad\qquad\qquad\qquad\square$

Let $\chi_0, \ldots, \chi_{N-1}$ be the characters of $G = \{g_0, \ldots, g_{N-1}\}$. We can then consider the following matrix

$$[C]_{ij} = \chi_i(g_j)$$

which is called the character table of G.

2.2.3   Fourier transform on groups

We now introduce the Fourier transform of functions defined on an Abelian group G.

Definition 2.4 *Let $f : G \to \mathbb{C}$ be any function. We define the Fourier transform $\hat{f} : \hat{G} \to \mathbb{C}$ of f by*

$$\hat{f}(\chi) = \sum_{g \in G} f(g)\overline{\chi(g)}, \quad \chi \in \hat{G}. \qquad\qquad (2.3)$$

Example 2.10 Let us consider again the group $\mathbb{Z}_N$. The characters, as we seen before, are given by

$$\chi_\ell(g) = e^{i\frac{2\pi}{N}\ell g}, \quad g \in \mathbb{Z}_N, \quad \ell = 0, \ldots, N-1.$$

The correspondence $\ell \to \chi_\ell$ yields an explicit isomorphism between $\mathbb{Z}_N$ and $\hat{\mathbb{Z}}_N$. Given any function $f : \mathbb{Z}_N \to \mathbb{C}$, its Fourier transform is given by

$$\hat{f}(\chi_\ell) = \sum_{g=0}^{N-1} f(g)e^{-i\frac{2\pi}{N}\ell g}.$$

$$\diamond$$

This transformation is easily inverted, and we define the inverse Fourier transform as follows

$$f = \frac{1}{N}\sum_{\chi \in \hat{G}} \hat{f}(\chi)\chi(g), \qquad g \in G. \qquad\qquad (2.4)$$

An important fact about the Fourier transform is that it is an isometry with respect to a (suitably normalized) L_2-norm. Indeed we have the following result.

Theorem 2.4 (Plancherel's formula) *For any $f_1, f_2 \in \mathbb{C}^G$,*

$$\langle \hat{f}_1, \hat{f}_2 \rangle = N\langle f_1, f_2 \rangle.$$

Proof. Let us define the following vectors

$$f_1 = (f_1(g_0), \ldots, f_1(g_{N-1}))) \qquad f_2 = (f_2(g_0), \ldots, f_2(g_{N-1}))$$
$$\hat{f}_1 = (\hat{f}_1(\chi_0), \ldots, \hat{f}_1(\chi_{N-1}))) \qquad \hat{f}_2 = (\hat{f}_2(\chi_0), \ldots, \hat{f}_2(\chi_{N-1})).$$

Let C be the character table of G. Then we have that $\hat{f}_1 = f_1 C$ and $\hat{f}_2 = f_2 C$, and thus

$$\langle \hat{f}_1, \hat{f}_2 \rangle = \frac{1}{N} \hat{f}_1 \hat{f}_2^* = \frac{1}{N} f_1 CC^* f_2^* = f_1 f_2^* = N \langle f_1, f_2 \rangle,$$

where we used the fact that $CC^* = N \cdot I$, and where the start indicates the transpose and complex conjugation operator. □

Corollary 2.1 (Parceval's formula) *For any $f \in \mathbb{C}^G$,*

$$\langle \hat{f}, \hat{f} \rangle = N \langle f, f \rangle.$$

2.3   Convergence rates of Markov chains

We first recall her some definition and properties of finite Markov chains.

A Markov chain consists of

- a non-empty finite set S, called the state space,

- a stochastic matrix $[P]_{ij} = p_{j,i}$, with $i, j \in S$ such that $p_{j,i} \geqslant 0$ and $\sum_{i \in S} p_{j,i} = 1$ for all j. The matrix P is called the transition matrix of the Markov chain[2] and the element p_{ij} is the probability of jumping from state i to state j.

Let us assume that $|S| = N$, then given an initial probability vector $\zeta^{(0)} = (\zeta_1^{(0)}, \ldots, \zeta_N^{(0)})^T$ we have that for any $k > 0$ the probability vector $\zeta^{(k)}$ is given by

$$\zeta^{(k)} = P^k \zeta^{(0)}.$$

We can rewrite the previous equation in a iterative form

$$\zeta^{(k+1)} = P \zeta^{(k)}, \quad \zeta^{(0)} = (\zeta_1^{(0)}, \ldots, \zeta_N^{(0)})^T.$$

A column vector ζ_{eq} is said to be an equilibrium distribution if it satisfies

$$\zeta_{\text{eq}} = P \zeta_{\text{eq}}.$$

---

[2]Notice that we have decided to associate to the element (i, j) of the matrix P the number $p_{j,i}$. This notation allows to consider column vectors instead of row vectors.

Definition 2.5 *A Markov chain with state space $S = \{0, \ldots, N-1\}$ and with transition probability P is said to be irreducible if for all $i, j \in S$ we can find an n such that $[P^n]_{i,j} > 0$.*

Let us denote with $\gcd\{a_1, \ldots, a_r\}$ the greatest common divisor of $a_1, a_2, \ldots, a_r$. We can then define the period of a state i of the chain as

$$d(i) = \gcd\{n \geqslant 1 : [P^n]_{i,i} > 0\},$$

namely it is the greatest common divisor of the set of times the chain returns to the initial state i. The we have the following definition.

Definition 2.6 *A Markov chain is aperiodic if for all states i it holds $d(i) = 1$.*

A very important result is the following.

Theorem 2.5 (Existence and uniqueness of the equilibrium distribution) *For any irreducible and aperiodic Markov chain there is always a unique equilibrium distribution.*

Proof. See [Bremaud 2001] for details. □

Example 2.11 Let us consider the following Markov chain with state space $S = \{0, 1\}$ and transition matrix

$$P = \frac{1}{2} \begin{pmatrix} 1 & 1 \\ 1 & 1 \end{pmatrix}.$$

We see that the matrix P has all elements non-zero and this its powers are all non-zero. Thus the chain is irreducible. Notice that

$$d(i) = \gcd\{1, 2, 3, \ldots, n\}, \quad i = 0, 1,$$

and thus $d(i) = 1$ for all i. This implies that the chain is also aperiodic. This could be easily seen noticing from each state there is a non-zero probability of jumping to the same state. Its equilibrium distribution then exists and is unique

$$\zeta_{\text{eq}} = \left(\frac{1}{2}, \frac{1}{2}\right)^T.$$

$\Diamond$

A consequence of the previous facts (see [Bremaud 2001] for details) are that the powers P^k of the transition matrix P converge componentwise to a stochastic matrix W in which all the columns are equal. Moreover a column, ζ, of W is the unique vector such that $\zeta = P\zeta$, which then is the equilibrium distribution.

2.3.1   Markov chain on Abelian groups

Let us now assume that state space S is a finite Abelian group G. Every probability measure $\pi : G \to [0,1]$ gives rise to a Markov chain with state space G if we define the transition probabilities as

$$P_{g,h} = \pi(g-h), \quad g,h \in G. \tag{2.5}$$

The matrix P is then the transition matrix of the Markov chain. As before we denote with p_{eq} the equilibrium probability. The resulting chain is aperiodic and irreducible if and only if there is a k such that every element of G can be written as the product of k elements of $\operatorname{supp}\pi = \{g | \pi(g) > 0\}$, that is $\langle \operatorname{supp}\pi \rangle = G$. In this case it turns out that, with the transition probabilities of a Markov chain given as in (2.5), the matrix P is doubly stochastic, and thus the unique equilibrium distribution is the uniform distribution.

Example 2.12 Let us consider the group $\mathbb{Z}_N$. Let us consider the uniform measure, namely we have that

$$\pi(0) = \pi(1) = \pi(-1) = 1/3$$

The corresponding transition matrix is given by

$$P = \begin{pmatrix} 1/3 & 1/3 & 0 & 0 & \cdots & 0 & 0 & 1/3 \\ 1/3 & 1/3 & 1/3 & 0 & \cdots & 0 & 0 & 0 \\ 0 & 1/3 & 1/3 & 1/3 & \cdots & 0 & 0 & 0 \\ \vdots & \vdots & \vdots & \vdots & \cdots & \vdots & \vdots & \vdots \\ 1/3 & 0 & 0 & 0 & \cdots & 0 & 1/3 & 1/3 \end{pmatrix}.$$

Notice that the transition matrix P is doubly stochastic. $\Diamond$

2.3.2   Bounds on the total variation distance

Given two probability measures on G, π_1 and π_2, we define the *total variation distance* between π_1 and π_2 the following quantity

$$\|\pi_1 - \pi_2\|_{\text{var}} = \max_{A \subset G} \|\pi_1(A) - \pi_2(A)\|.$$

It is possible to show [Behrends 1999] that the total variation can be also written as

$$\|\pi_1 - \pi_2\|_{\text{var}} = \frac{1}{2} \sum_{g \in G} |\pi_1(g) - \pi_2(g)|.$$

The total variation distance is then a measure of how much π_1 is closed to π_2.

We now show that is possible to bound the total variation distance with the L_2-norm of the Fourier transform of the probability measures.

Let π be a probability measure as in (2.5). We can then compute the Fourier transform as in (2.3) obtaining

$$\hat{\pi} : \hat{G} \to \mathbb{C} : \chi \mapsto \sum_{g \in G} \pi(g)\overline{\chi(g)}$$

Proposition 2.3 *Let π, π_1 and π_2 be probability measures on the group G, and let U be the uniform measure.*

(i) *$\pi = U$ if and only $\hat{\pi}(\chi)$ is one for the trivial character and zero otherwise.*

(ii) *The variation distance $\|\pi_1 - \pi_2\|_{\mathrm{var}}$ can be estimated by $(\sum_{\chi \in \hat{G}} |\hat{\pi}_1(\chi) - \hat{\pi}_2(\chi)|^2)^{1/2}/2$ In particular*

$$\|\pi_1 - U\|_{\mathrm{var}} \leq \frac{1}{2} \left(\sum_{\chi \neq \chi_0} |\hat{\pi}_1(\chi)|^2 \right)^{1/2}.$$

Proof. (i) The Fourier transform of U is $\hat{U}(\chi) = \sum_g \chi(g) U(g) = \sum_g \chi(g)/N$, and this sum is 1 if $\chi \neq \chi_0$ and 0 otherwise, by proposition 2.1. Since the map $\pi \mapsto \hat{\pi}$ is bijective then the previous fact happens only for the uniform measure. (ii) For the measure π_1 and π_2 the Plancherel formula has the form

$$\frac{1}{N} \sum_g N^2 |\pi_1(g) - \pi_2(g)|^2 = \sum_\chi |\hat{\pi}_1(\chi) - \hat{\pi}_2(\chi)|^2.$$

Relating the L^1-norm to the L^2-norm we have

$$4\|\pi_1 - \pi_2\|_{\mathrm{var}}^2 = \left(\sum_g |\pi_1(g) - \pi_2(g)| \right)^2 \leq N \sum_g |\pi_1(g) - \pi_2(g)|^2 = \sum_\chi |\hat{\pi}_1(\chi) - \hat{\pi}_2(\chi)|^2$$

where we used the fact that $(\sum_{j=1}^N a_j)^2 \leq N \sum_{j=1}^N a_j^2$ for $a_j \in \mathbb{R}$ to obtain the first inequality, and we used Parseval's formula to obtain the last equality. The second part of (ii) follows from (i) and the first part of (ii). $\qquad\square$

The main result here is that we transformed the problem of determining determining how close a probability measure π_1 is to the uniform measure to the problem of determining how small are the $\hat{\pi}(\chi)$ for all nontrivial characters of the group G.

Let us now do a further step that will be useful in the next section. Let us consider the problem of bounding the total variation distance after k steps, that is $\|\pi^{(k)} - U\|_{\mathrm{var}}$.

We need to study the evolution of the chain. Let, as before, π be the probability measure on G. Assume that we start from the state g. The next state will be $g + h'$ with probability $\pi(h')$, as it follows from (2.5). From $g + h'$ we continue to $(g + h') + h''$ accordingly to π, with h' and h'' chosen independently. We thus have that the of the transition $g + h$, where $h = h' + h''$ is simply $\sum_{h'} \pi(h')\pi(h - h')$. This motivates the following definition.

Definition 2.7 *Let π_1 and π_2 be probability measures on G. We define the convolution as*

$$(\pi_1 * \pi_2)(h) = \sum_{h'} \pi(h')\pi(h - h').$$

Moreover in the special case that $\pi_1 = \pi_2 = \pi$ we define $\pi^{(2)} = \pi * \pi$ and recursively $\pi^{(k)} = \pi^{(k-1)} * \pi$.

Thus now the problem of determining how fast the chain converges to the equilibrium is equivalent to the question of how fast $\pi^{(k)}$ converges to the uniform measure. We have the following result.

Theorem 2.6 *For probability measures π_1 and π_2 on G, the Fourier transform of the convolution $\pi_1 * \pi_2$ is just the product of the functions $\hat{\pi}_1$ and $\hat{\pi}_2$. In particular it follows that, for any probability π the Fourier transform of $\pi^{(k)}$ is the k-th power of $\hat{\pi}$.*

Proof. Let χ be arbitrary then we have that

$$
\widehat{\pi_1 * \pi_2}(\chi) = \sum_{g \in G} (\pi_1 * \pi_2)(g) \overline{\chi(g)} = \sum_{g \in G} \left(\sum_h \pi_1(h) \pi_2(g-h) \right) \overline{\chi(g)}
$$

$$
= \sum_{g,h \in G} \pi_1(h) \pi_2(g-h) \overline{\chi(g+h-h)} = \sum_{h,\ell \in G} \pi_1(h) \overline{\chi(h)} \pi_2(\ell) \overline{\chi(\ell)}
$$

$$
= \hat{\pi}_1(\chi) \hat{\pi}_2(\chi).
$$

where the first equality follows from the definition of Fourier transform, the second from the definition of convolution and the forth from the definition of character. $\square$

We thus have that the size of $\|\pi^{(k)} - U\|_{\mathrm{var}}$ solely depends on the size of the numbers $\hat{\pi}(\chi)$ for the nontrivial characters χ.

2.3.3 Convergence to the equilibrium

We can now relate the total variation distance of a probability measure π from the uniform measure, and the spectral properties of the transition matrix of an irreducible and aperiodic Markov chain defined on Abelian group.

We know that

$$
\|\pi - U\|_{\mathrm{var}} = \frac{1}{2} \sum_{g \in G} \left| \pi(g) - \frac{1}{N} \right|.
$$

From (2.5) we know that $P_{r,s} = \pi(r-s)$, and thus we have that

$$
\frac{1}{2} \sum_{g \in G} \left| \pi(g) - \frac{1}{N} \right| = \frac{1}{2} \sum_{g \in G} \left| \pi(g+h-h) - \frac{1}{N} \right| = \frac{1}{2} \sum_{g \in G} \left| P_{g+h,h} - \frac{1}{N} \right| = \frac{1}{2} \sum_{g \in G} \left| P_{g,h} - \frac{1}{N} \right|,
$$

$\forall h \in G$. Let us denote

$$
\|P - U\|_{\mathrm{var}} = \frac{1}{2} \sum_{g \in G} \left| P_{g,h} - \frac{1}{N} \right|,
$$

then, using Theorem 2.3 and Theorem 2.6, we have that

$$
\|P^k - U\|_{\mathrm{var}}^2 \leqslant \frac{1}{2} \sum_{\chi \neq \chi_0} |\hat{\pi}(\chi)|^{2k}
$$

thus it is clear the role of $\max_{\chi \neq \chi_0} |\hat{\pi}(\chi)|$ that representees the convergence rate of the chain to the equilibrium.

We can relate the numbers $\hat{\pi}(\chi)$ spectral properties of P. Indeed, the transition matrix P can be interpreted as a linear function from $\mathbb{C}^G$ to itself simply considering, for $f \in \mathbb{C}^G$,

$$(Pf)(g) = \sum_{h \in G} P_{g,h} f(h).$$

We then have that for every $\chi \in \hat{G}$

$$(P\chi)(g) = \sum_{h \in G} P_{g,h} \chi(h) = \sum_{h \in G} \pi(g-h)\chi(h) = \sum_{h \in G} \pi(h)\overline{\chi(h)}\chi(g) = \hat{\pi}(\chi)\chi(g),$$

where we used (2.5) and the definition of character. This shows that χ is an eigenfunction of P with eigenvalue $\hat{\pi}(\chi)$. Since the characters form an orthonormal basis, see Theorem 2.3, then P is diagonalizable and its spectrum is given by

$$\sigma(P) = \{\hat{\pi}(\chi) | \chi \in \hat{G}\}.$$

3

CONSENSUS COORDINATION UNDER LIMITED COMMUNICATION

In this chapter we consider a particular class of coordination problems where a team of agents need to reach an agreement over some shared variables. This type of coordination problems arise as a fundamental issue in many applications such as search-and-rescue operations [Vidal et al. 2002; Speranzon and Johansson 2003], collaborative map building and exploration [Fox et al. 2000; Burgard et al. 2005], optimal coverage problems [Cortés et al. 2004c], collaborative flocking and formation maintaining control [Olfati-Saber and Murray 2004; Tanner et al. 2005] and problems of synchronization [Strogatz 2000; Marodi et al. 2002; Lin et al. 2005]. A mathematical formulation of this type of problems was proposed in [Jadbabaie et al. 2003; Olfati-Saber and Murray 2004], and known in the literature as consensus.

In this chapter we are interested to characterize the relationship between the amount of information exchanged by the agents and the achievable control performance. In order to do this we model the communication network by a directed graph, in which each arc represents information transmission from one agent to another one. We then consider the connectivity of each agent with its neighbors as a measure of the amount of information exchanged and relate it to the control performance measured as the convergence speed to the consensus. The main result shows that time-invariant communication networks that exhibit particular symmetries are shown to yield slow convergence if the amount of information exchanged does not scale with the number of agents. On the other randomly time-varying communication networks allow very fast convergence rates, even if the connectivity is very low. The analysis of the problem can be formalized

if we consider a simplified model of the system to be controlled. In particular, as in [Jad-babaie et al. 2003; Olfati-Saber and Murray 2004; Cortés et al. 2004a], we assume that the agents are described by a first order model.

3.1   Outline

The chapter is organized as follows. In Section 3.2 we formally define the consensus problem. In particular we restrict to linear state feedbacks. We then introduce an optimal control problem where the cost function is related to the convergence rate to the barycenter of the initial position of the agents. Under some assumptions, described in Sections 3.2 and 3.3, it turns out that a weighted directed communication graphs, for which the adjacency matrix is doubly stochastic guarantee consensus, with a degree of efficiency that is related to the spectral properties of the matrix. The communication graphs can also be interpreted as Markov chains and thus convergence rate can be related to the mixing rate as we have discussed in Chapter 2. Communication graphs with symmetries impose a structure on the doubly stochastic matrices so that their spectral properties have important characteristics. In particular we will restrict to Cayley graphs defined on Abelian groups. In this case results from Chapter 2 can be applied in order to derive a bound on the convergence rate to the consensus. In Section 3.4, we derive a bound that is a function of the number of agents and the incoming arcs in each vertex. The main result shows that, if we impose symmetries on the communication graph and we keep the number of incoming arcs in each vertex bounded, then the convergence rate degrades as the number of agents increases. Moreover, we derive a bound for the convergence rate and show that the bound is tight. The idea of imposing symmetries on the communication graph is not new [D'Andrea and Dullerud 2003; Recht and D'Andrea 2004; Smith et al. 2005]. In [Smith et al. 2005], for example, the authors show that, for problem similar to consensus, symmetries allow to obtain better performance if the number of incoming arcs on each vertex increases. In this chapter we extend this type of results to a broader class of graphs with symmetries.

In Section 3.5 we consider stochastically time-varying communication graphs. In these strategies the graph is chosen randomly at each time step over a family of graphs with the constraint that the number of incoming arcs in each vertex is constant. A mean square analysis shows that, in this way, we can improve the convergence rate obtained with fixed communication graph. This fact continue to hold true even if the random choice is restricted to families of Cayley graphs. In this case, compared to time-invariant solutions, symmetries yield very good performance.

3.2   Consensus problems

Consider $N > 1$ identical agents whose dynamics are described by the following discrete time state equations

$$x_i^+ = x_i + u_i \qquad i = 1, \ldots, N,$$

where $x_i \in \mathbb{R}$ is the state of the i-th agent, x_i^+ represents the updated state and $u_i \in \mathbb{R}$ is the control input. More compactly we can write

$$x^+ = x + u, \tag{3.1}$$

where $x, u \in \mathbb{R}^N$. The consensus problem is to design a feedback control law

$$u = Kx, \qquad K \in \mathbb{R}^{N \times N}$$

yielding the consensus of the states, namely a control such that all the x_i's become equal asymptotically. More precisely, our objective is to obtain K such that, for any initial condition $x(0) \in \mathbb{R}^N$, the closed loop system

$$x^+ = (I + K)x, \tag{3.2}$$

yields

$$\lim_{t \to \infty} x(t) = \alpha \mathbb{1} \tag{3.3}$$

where $\mathbb{1} = (1, \dots, 1)^T$ and where α is a scalar depending on $x(0)$ and K.

3.2.1 Time-invariant communication graphs

The fact that in the matrix K the element in position i, j is different from zero, means that the agent i needs the state of the agent j in order to compute its feedback action. This implies that we need to communicate the state x_j from the agent j to the agent i. In this context, a good description of the information flow required by a specific feedback K is given by the directed graph $\mathcal{G}_K$ with set of vertices $\{1, \dots, N\}$ in which there is an arc from j to i whenever in the feedback matrix K the element $K_{ij} \neq 0$. The graph $\mathcal{G}_K$ is said to be the *communication graph* associated with K. Conversely, given any directed graph $\mathcal{G}$ with set of vertices $\{1, \dots, N\}$, we say that a feedback K is *compatible* with $\mathcal{G}$ if $\mathcal{G}_K$ is a subgraph of $\mathcal{G}$ (we will use the notation $\mathcal{G}_K \subseteq \mathcal{G}$). We say that the consensus problem is solvable on a graph $\mathcal{G}$ if there exists a feedback K compatible with $\mathcal{G}$ and solving the consensus problem. From now on we assume that $\mathcal{G}$ contains all loops (i, i) meaning that each agent has access to its own state.

Notice that in the model of the communication subsystem, if two agents exchange data from the initial time, they will maintain connectivity for all the successive times. Although this type of assumption could be acceptable in a system where the agents are connected through a wired communication network, one could argue that this is more difficult to realize in a system where agents are mobile robots. To capture more realistic scenarios the communication network could be modelled by proximity graphs [Jaromczyk and Toussaint 1992], where two agents are neighbors if their relative position is less then a given threshold. This approach has been considered in [Jadbabaie et al. 2003; Tanner et al. 2003; Cortés et al. 2004a] where stability is studied, but the overall connectivity of the graph is not clearly addressed. In the following we consider the simplified communication model introduced previously, which allows a formal analysis of the tradeoffs between coordination and connectivity.

3.2.2   Convergence rate to consensus

In order to unveil these tradeoffs we associate to the consensus problem a performance index. The simplest index is the exponential rate of convergence to the agreement. From an intuitive point of view such index is a suitable one since if agents can communicate with many teammates the consensus should be reached faster. For example, if the communication graph is a full graph each agent can move to the consensus point in one step. Notice however that the choice $K = -I$ would yield the fastest convergence rate to the consensus with no communication. In this case, however, the consensus point is always zero. Thus nonzero initial states having equal components, that is, the agents have already reached consensus, would require to steer the agents state to zero. Any effective feedback matrices K must then ensure that nonzero states having equal components correspond to equilibrium points of the closed loop system, because in this case no control action is necessary. This happens if and only if

$$K\mathbb{1} = 0. \tag{3.4}$$

From now on we thus impose this condition on K. Then, it is easy to see that the state agreement problem is solved if and only if all the eigenvalues of $I + K$ are strictly inside the unit circle except for a single eigenvalue in 1. Under this condition the convergence rate can be defined as

$$\rho(I + K) = \max\{|\lambda| : \lambda \in \sigma(I + K) \setminus \{1\}\} \tag{3.5}$$

which is called the essential spectral radius of $I + K$. An interesting particular case that has been considered in the literature corresponds to situation in which we restrict to controllers yielding the agreement at the barycenter of the initial states. We call these control laws barycentric controllers. It is easy to see that K is a barycentric controller if and only if

$$\mathbb{1}^T K = 0. \tag{3.6}$$

Notice that this condition is automatically true for symmetric matrices K satisfying (3.4). From this choice of performance we can formulate the following control problem.

Given N agents communicating over a network modelled by the communication graph $\mathcal{G}$, find a matrix K satisfying (3.4) and (3.6) such that $\mathcal{G}_K \subseteq \mathcal{G}$ and minimizing $\rho(I + K)$.

Remark 3.1
When we are dealing with barycentric controllers it is meaningful to consider the displacement from the barycenter

$$\Delta(t) = x(t) - \left(\frac{1}{N}\mathbb{1}^T x(0)\right)\mathbb{1}. \tag{3.7}$$

It is immediate to check that, if K satisfies condition (3.4) then $\Delta(t)$ satisfies the closed loop equation

$$\Delta^+ = (I + K)\Delta. \tag{3.8}$$

Moreover, if K also satisfies condition (3.6), *then*

$$\Delta(t) = x(t) - \left(\frac{1}{N}\mathbb{1}^T x(t)\right)\mathbb{1}.$$

Notice finally that the initial conditions $\Delta(0)$ *are such that*

$$\mathbb{1}^T \Delta(0) = 0. \qquad (3.9)$$

Hence the asymptotic behavior of our state agreement problem can equivalently be studied by looking at the evolution (3.8) *on the hyperplane characterized by the condition* (3.9). *Thus the index* $\rho(I + K)$ *seems appropriate for analyzing how performance is related to the communication effort associated to a graph.*

3.3 Solvable consensus problems

If we restrict to control laws K making $I + K$ a matrix with all elements nonnegative, condition (3.4) imposes that $I + K$ is a stochastic matrix and conditions (3.4) and (3.6) impose that $I + K$ is doubly stochastic. This means that all the rows and columns sum to one. Since the spectral structure of stochastic and doubly stochastic matrices is well known, this observation allows to understand what conditions on the graph will ensure the solvability of the consensus problem. We need to recall some notation and results on directed graphs [Godsil and Royle 2001; Diestel 2005].

Fix a directed graph $\mathcal{G}$ with set of vertices V and set of arcs $\mathcal{E} \subseteq V \times V$. The adjacency matrix A is a binary square matrix indexed by the elements in V defined by letting $A_{ij} = 1$ if and only $(i, j) \in \mathcal{E}$. Define the in-degree of a vertex j as $\text{indeg}(j) = \sum_i A_{ij}$ and the out-degree of a vertex i as $\text{outdeg}(i) = \sum_j A_{ij}$. Vertices with out-degree equal to 0 are called sinks. A graph is called in-regular (out-regular) of degree k if each vertex has in-degree (out-degree) equal to k. A path in $\mathcal{G}$ consists of a sequence of vertices $i_1 i_2 \ldots \ldots i_r$ such that $(i_\ell, i_{\ell+1}) \in \mathcal{E}$ for every $\ell = 1, \ldots, r-1$; i_1 (i_r) is said to be the initial (terminal) vertex of the path. A cycle is a path in which the initial and the terminal vertices coincide. A vertex i is said to be connected to vertex j if there exists a path with initial vertex i and terminal vertex j. A directed graph is said to be connected if, given any pair of vertices i and j, either i is connected to j or j is connected to i. A directed graph is said to be strongly connected if, given any pair of vertices i and j, i is connected to j.

Given any directed graph $\mathcal{G}$ we can consider its strongly connected components, namely strongly connected subgraphs $\mathcal{G}_k$, $k = 1, \ldots, s$, for a suitable $s \in \mathbb{N}$, with set of vertices $V_k \subseteq V$ and set of arcs $\mathcal{E}_k = \mathcal{E} \cap (V_k \times V_k)$ such that the sets V_k form a partition of V. The various components may have connections among each other. We define another directed graph $T_{\mathcal{G}}$ with set of vertices $\{1, \ldots, s\}$ such that there is an arc from h to k if there is an arc in $\mathcal{G}$ from a vertex in V_k to a vertex in V_h. It can be shown that $T_{\mathcal{G}}$ is a graph without cycles. The following proposition is a straightforward consequence of a standard result on limiting distributions for stochastic matrices [Gantmacher 1959, pages 88, 95].

Proposition 3.1 *Let $\mathcal{G}$ be a directed graph and assume that $\mathcal{G}$ contains all loops (i,i). The following conditions are equivalent:*

  (i) The consensus problem is solvable on $\mathcal{G}$.

  (ii) $T_{\mathcal{G}}$ is connected and has only one sink vertex.

Moreover, if the conditions are satisfied, any K such that

  (a) $I + K$ is stochastic and $K_{ii} \neq -1$ for $i = 1, \ldots, n$,

  (b) $\mathcal{G}_K = \mathcal{G}$,

solves the consensus problem.

When the graph $\mathcal{G}$ satisfies the properties of Proposition 3.1, a particularly simple solution of the consensus problem can be obtained by defining a matrix $P \in \mathbb{R}^{N \times N}$ as follows

$$P_{ij} = \begin{cases} \dfrac{1}{\text{indeg}(i)} & \text{if } i \rightarrow j \\[2ex] 0 & \text{otherwise} \end{cases}$$

and by letting $K = P - I$. In this case the closed loop dynamics have the following form

$$x_i^+ = x_i + \frac{1}{\text{indeg}(i)} \sum_{\substack{j \neq i \\ (j,i) \in \mathcal{E}}} (x_j - x_i). \tag{3.10}$$

Again in case we restrict to K such that $I + K$ is nonnegative, we can relate the existence of barycentric controllers to the structure of the graph by means of a standard result on stochastic matrices.

Proposition 3.2 *Let $\mathcal{G}$ be a directed graph and assume that $\mathcal{G}$ contains all loops (i,i). The following conditions are equivalent:*

  (i) The barycentric consensus problem is solvable on $\mathcal{G}$.

  (ii) $\mathcal{G}$ is strongly connected.

Moreover, if the above conditions are satisfied, any K such that $I + K$ is doubly stochastic, $\mathcal{G}_K = \mathcal{G}$ and $K_{ii} \neq -1$ for every $i = 1, \ldots, n$ solves the barycentric consensus problem.

Notice that in the special case when $(i,j) \in \mathcal{E}$ if and only if $(j,i) \in \mathcal{E}$, it follows that we can find solutions K to the consensus problem that are symmetric and that therefore are automatically doubly stochastic. One example is given by (3.10).

When P is a stochastic matrix, it can be regarded as the transition matrix of a finite Markov chain. The problem of minimizing the essential spectral radius $\rho(P)$ is thus equivalent of maximizing the spectral gap of the Markov chain, $1 - \rho(P)$, which is, for a general Markov chain, a hard problem [Aldous and Fill 200X; Behrends 1999]. Recently some very effective algorithms have been proposed for this maximization limited, however, to the case in which P is a symmetric matrix [Boyd et al. 2004].

3.4 Symmetries in communication graphs

The analysis of the consensus problem and the corresponding controller synthesis becomes more treatable if we limit our search to graphs $\mathcal{G}$ and matrices K that exhibit symmetries. We will show, however, that these symmetries limit the achievable performance in terms of convergence rate.

In order to treat symmetries on a graph $\mathcal{G}$ in a general setting, we introduce the concept of Cayley graph defined on Abelian groups [Babai 1979; Alon and Roichman 1994]. Let G be a finite Abelian group of order $|G| = N$, and let S be a subset of G containing the zero element, see Section 2.2. The Cayley graph $\mathcal{G}(G,S)$ is the directed graph with vertex set G and arc set

$$\mathcal{E} = \big\{ (g,h) : h - g \in S \big\}.$$

Notice that a Cayley graph is always in-regular, namely the in-degree of each vertex is equal to $|S|$. If S is such that $-S = S$ we say that S is inverse-closed. In this case the graph obtained is undirected.

Symmetries can be introduced also on matrices. A matrix $P \in \mathbb{R}^{N \times N}$ is said to be a Cayley matrix over the group G if

$$P_{i,j} = P_{i+h,j+h} \qquad \forall\, i,j,h \in G.$$

It is clear that for a Cayley matrix P there exists a function $\pi : G \to \mathbb{R}$ such that $P_{i,j} = \pi(i - j)$. The function π is called the generator of the Cayley matrix P. Notice that, if π and π' are generators of the Cayley matrices P and P' respectively, then $\pi + \pi'$ is the generator of $P + P'$ and $\pi * \pi'$ is the generator of PP', where $(\pi * \pi')(i) = \sum_{j \in G} \pi(j)\pi'(i-j)$ for all $i \in G$. This shows that P and P' commute. Notice finally that, if P is a Cayley matrix generated by π, then $\mathcal{G}_P$ is a Cayley graph with $S = \{h \in G : \pi(h) \neq 0\}$.

It is clear that the graph $\mathcal{G}_P$ supporting a Cayley matrix P is a Cayley graph with

$$S = \{i : \pi(i) \neq 0\} \cup \{0\}.$$

Since we are interested in doubly stochastic matrices we consider as generator function π a probability measure. This, as we discussed in Section 2.3, is enough to guarantee doubly stochasticity. In the following we will call such P a Cayley stochastic matrix. Notice that the requirement of strong connectivity of the graph, needed to solve the consensus problem (see Proposition 3.2) is fulfilled if $\langle S \rangle = G$, that is, S generates G. Indeed, if this happens then the Markov chain represented by P is aperiodic and irreducible (see Section 2.3.1) and this means that the Cayley graph is strongly connected. We consider some examples.

Example 3.1 Among the multiple possible choices of π there is the uniform probability distribution where $\pi(g) = 1/|S|$ for every $g \in S$. Let us consider again Example 2.12, where we have considered the group $\mathbb{Z}_N$ with the probability distribution

$$\pi(0) = \pi(1) = \pi(-1) = 1/3.$$
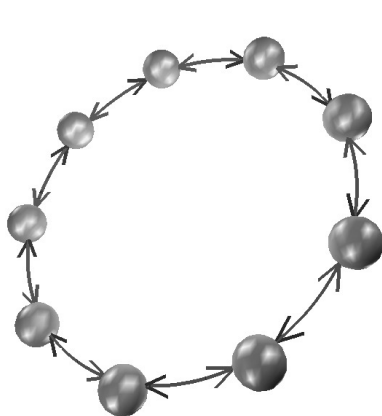
(a) Example of the Cayley graph $\mathcal{G}(\mathbb{Z}_9,\{-1,0,1\})$. Notice that the graph is undirected.
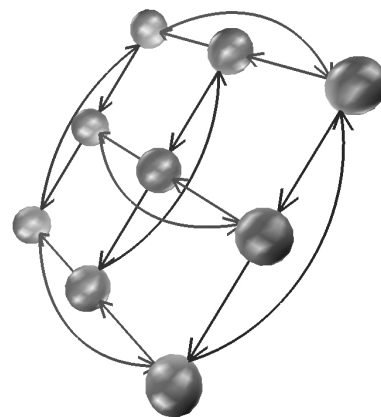
(b) Example of the Cayley graph $\mathcal{G}(\mathbb{Z}_3 \oplus \mathbb{Z}_3,\{(0,0),(0,1),(1,0)\})$. The graph is directed.

Figure 3.1: Some examples of Cayley graphs. For clarity the we did not plot the self-loops. (Pictures produced using "Group Explorer" by N. Charter [Carter 2005]).

The Cayley graph that corresponds to that example is the graph $\mathcal{G}(\mathbb{Z}_N, S)$ where $S = \{-1, 0, 1\}$ and with uniform probability distribution. Notice that in this case S is inverse-closed and thus the corresponding graph is undirected. In the particular case of $N = 9$, we have that the Cayley matrix P is:

$$P = \begin{pmatrix} 1/3 & 1/3 & 0 & 0 & 0 & 0 & 0 & 0 & 0 \\ 0 & 1/3 & 1/3 & 0 & 0 & 0 & 0 & 0 & 0 \\ 0 & 0 & 1/3 & 1/3 & 0 & 0 & 0 & 0 & 0 \\ 0 & 0 & 0 & 1/3 & 1/3 & 0 & 0 & 0 & 0 \\ 0 & 0 & 0 & 0 & 1/3 & 1/3 & 0 & 0 & 0 \\ 0 & 0 & 0 & 0 & 0 & 1/3 & 1/3 & 0 & 0 \\ 0 & 0 & 0 & 0 & 0 & 0 & 1/3 & 1/3 & 0 \\ 0 & 0 & 0 & 0 & 0 & 0 & 0 & 1/3 & 1/3 \\ 1/3 & 0 & 0 & 0 & 0 & 0 & 0 & 0 & 1/3 \end{pmatrix}.$$

Two types of symmetries that can be seen in the structure of P. The first is that the graph is undirected and the second that the graph is circulant. Since $\langle S \rangle = G$ the Cayley graph is strongly connected. This can be clearly seen in Figure 3.1(a) where it is shown the Cayley graph $\mathcal{G} = (\mathbb{Z}_9, \{-1, 0, 1\})$. $\diamond$

Example 3.2 Let us consider the (non-cyclic) group $\mathbb{Z}_3 \oplus \mathbb{Z}_3$ and the subset $S = \{(0,0), (1,0), (0,1)\}$. Notice that in this case the subset S is not inverse-closed and thus the Cay-

ley graph $\mathcal{G}(\mathbb{Z}_3 \oplus \mathbb{Z}_3, S)$ is a directed graph. Let us consider the probability distribution

$$\pi(0,0) = 1/2 \qquad\qquad \pi(1,0) = 1/4 \qquad\qquad \pi(0,1) = 1/4.$$

The corresponding Cayley matrix in this case is given by

$$P = \begin{pmatrix} 1/2 & 0 & 1/4 & 0 & 0 & 0 & 1/4 & 0 & 0 \\ 1/4 & 1/2 & 0 & 0 & 0 & 0 & 0 & 1/4 & 0 \\ 0 & 1/4 & 1/2 & 0 & 0 & 0 & 0 & 0 & 1/4 \\ 1/4 & 0 & 0 & 1/2 & 0 & 1/4 & 0 & 0 & 0 \\ 0 & 1/4 & 0 & 1/4 & 1/2 & 0 & 0 & 0 & 0 \\ 0 & 0 & 1/4 & 0 & 1/4 & 1/2 & 0 & 0 & 0 \\ 0 & 0 & 0 & 1/4 & 0 & 0 & 1/2 & 0 & 1/4 \\ 0 & 0 & 0 & 0 & 1/4 & 0 & 1/4 & 1/2 & 0 \\ 0 & 0 & 0 & 0 & 0 & 1/4 & 0 & 1/4 & 1/2 \end{pmatrix}.$$

Notice that in this case the matrix is not circulant but block circulant. $\diamond$

Given a Cayley graph $\mathcal{G}$ we can define

$$\rho_{\mathcal{G}}^{\text{Cayley}} = \min\{\rho(P) \mid P \text{ Cayley stochastic}, \mathcal{G}_K \subseteq \mathcal{G}\}.$$

We know from Section 3.3.3 that the spectrum of the matrix P is

$$\sigma(P) = \{\hat{\pi}(\chi) \mid \chi \in \hat{G}\}.$$

Thus essential spectral radius is then given by

$$\rho(P) = \min_{\chi \neq \chi_0} \hat{\pi}(\chi), \quad \chi \in \hat{G}.$$

Let us first consider some examples.

Example 3.3 Consider the group $\mathbb{Z}_N$ and the Cayley graph $\mathcal{G}(\mathbb{Z}_N, S)$, where $S = \{0, 1\}$. Consider the probability distribution π on S described by

$$\pi(0) = 1 - k, \ \pi(1) = k.$$

where $k \in [0, 1]$. The Fourier transform of π is

$$\hat{\pi}(\chi_\ell) = \sum_{g \in S} \chi(-g)\pi(g) = 1 - k + k e^{-i\frac{2\pi}{N}\ell}, \qquad \ell = 1, \dots, N - 1.$$

In this case it can be shown that we have consensus if and only if $0 < k < 1$ and that the rate of convergence is

$$\rho(P) = \max_{1 \leq \ell \leq N-1} \left| 1 - k + k e^{-i\frac{2\pi}{N}\ell} \right|.$$

Hence, we have that

$$\rho_{\mathcal{G}}^{\text{Cayley}} = \min_{k} \max_{1 \leq \ell \leq N-1} \left| 1 - k + k e^{-i \frac{2\pi}{N} \ell} \right|.$$

The optimality is obtained when $\ell = 1$ and $k = 1/2$ yielding

$$\rho_{\mathcal{G}}^{\text{Cayley}} = \left(\frac{1}{2} + \frac{1}{2} \cos\left(\frac{2\pi}{N} \right) \right)^{\frac{1}{2}} \simeq 1 - \frac{\pi^2}{2} \frac{1}{N^2}$$

where the last approximation is meant holds for large N. $\diamond$

Example 3.4 Consider the group $\mathbb{Z}_N$ and the Cayley graph $\mathcal{G}(\mathbb{Z}_N, S)$, where $S = \{-1, 0, 1\}$. For the sake of simplicity we assume that N is even; similar results can be obtained for odd N. Consider the probability distribution π on S described by

$$\pi(0) = k_0, \ \ \pi(1) = k_1, \ \ \pi(-1) = k_{-1}.$$

The Fourier transform of π is in this case given by

$$\hat{\pi}(\chi_\ell) = \sum_{g \in S} \chi(-g)\pi(g) = k_0 + k_1 e^{-i \frac{2\pi}{N} \ell} + k_{-1} e^{i \frac{2\pi}{N} \ell}, \qquad \ell = 1, \dots, N-1.$$

We thus have

$$\rho_{\mathcal{G}}^{\text{Cayley}} = \min_{(k_0, k_1, k_{-1})} \max_{1 \leq \ell \leq N-1} \left| k_0 + k_1 e^{-i \frac{2\pi}{N} \ell} + k_{-1} e^{i \frac{2\pi}{N} \ell} \right|.$$

Symmetry and convexity arguments allow to conclude that a minimum is for sure of the type $k_1 = k_{-1}$. The cost function then reduces to

$$\rho(P) = \max_{k_1} \left\{ \left| 1 - 2k_1 \left(1 - \cos\left(\frac{2\pi}{N} \right) \right) \right|, |1 - 4k_1| \right\}.$$

The minimum is achieved for

$$k_0 = \frac{1 - \cos\left(\frac{2\pi}{N} \right)}{3 - \cos\left(\frac{2\pi}{N} \right)}, \quad k_1 = k_{-1} = \frac{1}{3 - \cos\left(\frac{2\pi}{N} \right)}$$

and we have

$$\rho_{\mathcal{G}}^{\text{Cayley}} = \frac{1 + \cos\left(\frac{2\pi}{N} \right)}{3 - \cos\left(\frac{2\pi}{N} \right)} \simeq 1 - 2\pi^2 \frac{1}{N^2} \tag{3.11}$$

where the last approximation is holds for large N. $\diamond$

Notice that in the first example the optimality is obtained when all the nonzero elements of π are equal. This is not a general feature since the same does not happen in the second example in which however, the nonzero elements of π become equal asymptotically as $N \to \infty$. Even this fact is not true in general. To see this it is enough to take the

example in which the group is $\mathbb{Z}_N$ and $S = \{0, \pm 1, \pm 2\}$. Through some rather long and tedious computations it is possible to see that in this case the optimal coefficients are such that $k_{-2} = k_2$, $k_{-1} = k_1$ and for $N \to \infty$ we have that $k_2 \to 1/2$, $k_1 \to 0$ and $k_0 \to 0$.

The case of communication exchange with two neighbors (Example 3.4) offers a better performance compared to the case with one neighbor (Example 3.3). However, in both cases $\rho_{\mathscr{G}}^{\text{Cayley}} \to 1$ for $N \to \infty$. This fact is more general: the essential spectral radius of Abelian stochastic Cayley matrices will always converge to 1 if the in-degree in the Cayley graph, associated to the matrices, is bounded. This is the content of next result.

Theorem 3.1 *Let G be any finite Abelian group of order N and $S \subseteq G$ be a subset containing zero. Let moreover $\mathscr{G}$ be the Cayley graph associated with G and S. If $|S| = v + 1$, then*

$$\rho_{\mathscr{G}}^{\text{Cayley}} \geq 1 - C N^{-2/v}, \tag{3.12}$$

where $C > 0$ is a constant independent of G and S.

Proof. Proof in Appendix 3.A.
□

Theorem 3.1 implies that, if we consider a sequence of Abelian Cayley graphs $\mathscr{G}(G_N, S_N)$ such that $|G_N| = N$ and $|S_N|$ grows slower then logarithmically in N and we consider a sequence of Cayley stochastic matrices P_N compatible with $\mathscr{G}(G_N, S_N)$, then, necessarily, $\rho(P_N)$ converges to 1. This fact was shown using a completely different approach in [Alon and Roichman 1994].

Notice that in Example 3.4 we have that $v = 2$ and we have an asymptotic behavior $\rho_{\mathscr{G}}^{\text{Cayley}} \simeq 1 - 2\pi^2 N^{-2}$, while the lower bound of Theorem 3.1 is, in this case, $1 - 2\pi^2 N^{-1}$. We can wonder whether it is possible to achieve the bound performance. In other words, we would like to understand whether the lower bound we have just found is tight or not. In the following we will show that this is the case.

Consider the group $\mathbb{Z}_N^r$, with $r \in \mathbb{N}$ and $r \geq 1$, and the Cayley graph $\mathscr{G}(\mathbb{Z}_N^r, S)$, where $S = \{0, e_1, \ldots, e_r\}$, where e_j is the j-th vector of the canonical basis of $\mathbb{R}^r$. Consider the probability distribution π on S described by

$$\pi(0) = k_0, \quad \pi(e_j) = k_j, \quad \forall j = 1, \ldots, r$$

with $k_j \geq 0$ and $\sum_{j=0}^r k_j = 1$. The Fourier transform of π is

$$\hat{\pi}(\chi_{\ell_1}, \ldots, \chi_{\ell_r}) = \sum_{g \in S} \chi(-g)\pi(g) = k_0 + \sum_{j=1}^r k_j e^{-i\frac{2\pi}{N}\ell_j}, \qquad \ell_j = 0, 1, \ldots, N-1, \; j = 1, \ldots, r.$$

We thus have

$$\rho_{\mathscr{G}}^{\text{Cayley}} = \min_{\substack{k_j \geq 0 \\ \sum k_j = 1}} \max_{\substack{0 \leq \ell_j \leq N-1 \\ (\ell_1, \ldots, \ell_r) \neq (0, \ldots, 0)}} \left| k_0 + \sum_{j=1}^r k_j e^{-i\frac{2\pi}{N}\ell_j} \right|.$$

Proposition 3.3 *The above min-max is reached either by $(\ell_1, \ldots, \ell_r) = (1, \ldots, 1)$ or by $(\ell_1, \ldots, \ell_r) = (0, \ldots, 1, \ldots, 0)$ and $k_0 = k_1 = \ldots = k_r = 1/(r+1)$, which yield*

$$\rho_{\mathcal{G}}^{Cayley} = \left(1 - \frac{2r}{(r+1)^2}\left(1 - \cos\frac{2\pi}{N}\right)\right)^{\frac{1}{2}} \simeq 1 - \frac{4\pi^2 r}{(r+1)^2}\frac{1}{N^2}$$

Proof. Proof in Appendix 3.B

$\square$

From previous result we see that, by keeping N fixed and by varying r we obtain a sequence of controllers for which the rate of convergence tends to one logarithmically in the number of agents an for which the degree of the associated graph grows logarithmically in the number of agents. The previous result is based on a Cayley graph over the group $\mathbb{Z}_N^r$. The same result can also be obtained considering a Cayley graph over the cyclic group $\mathbb{Z}_N$. Indeed if we take $\mathbb{Z}_{N^r}$ and the subset

$$S = \{0, 1, N, N^2, \ldots, N^{r-1}\},$$

we can construct a Cayley stochastic matrix with a essential spectral radius that is asymptotically equivalent to the one obtained in Proposition 3.3. More in general, it can be proved that, if in the family of groups $\mathbb{Z}_N^r$ we maintain N fixed (prime) and we vary r, there exists a constant $c < 1$ such that for every r there exists $S_r \subseteq \mathbb{Z}_N^r$ such that $|S_r| \simeq cr$ and such that

$$\rho(P_r) \leq d < 1.$$

where $P_r = |S_r|^{-1} A_r$ and where A_r is the adjacency matrices of the corresponding Cayley graph. Such Cayley graphs are constructed using the theory of channel codes over finite fields [Alon and Roichman 1994]. Extensions to non-prime N are likely to be possible considering the theory of group codes.

The question at this point is the following: Is the Cayley structure on the matrix or the Cayley structure on the graph that prevents to obtain good performance? In other words, do there exist stochastic matrices supported by Abelian Cayley graphs that exhibit better performance than what imposed by the bound (3.12)? Notice that, in order to make fair comparisons, we need to limit to doubly stochastic matrices. We conjecture that for doubly stochastic matrices supported on Abelian Cayley graphs the bound (3.12) continues to hold.

What about other graphs? An easy way to restrict to doubly stochastic matrices is by imposing that they are symmetric and so that the corresponding graphs are undirected. If A is the adjacency matrix of a ν-regular undirected graph, then, $P = \nu^{-1} A$ is doubly stochastic. For these graphs, we recall a basic asymptotic lower bound by Alon and Boppana [Alon 1986] on the second eigenvalue

$$\liminf_{N \to +\infty} \rho(P) \geq \frac{2\sqrt{\nu - 1}}{\nu},$$

where the lim inf is intended to be performed along the family of all ν-regular undirected graphs having N vertices.

Ramanujan graphs (see [Murty 2003] and references therein) are those v-regular undirected graphs achieving the previous bound, namely such that $\rho(P) = 2v^{-1}\sqrt{v-1}$. Hence, through these graphs, it would be possible to keep the essential spectral radius bounded away from 1, while keeping the degree fixed. In fact, there are plenty of Ramanujan graphs (for instance any complete graph), but it is still an open problem if for any N and v there exists a Ramanujan graph with N vertices and degree v. There are only partial results in this direction. For example it is possible to prove that, if v is such that $v - 1$ is the power of a prime, then there exist a sequence of Ramanujan graphs with a growing number of vertices and of fixed degree v. Moreover, when available, these constructions are quite complicated and the fact that they strictly depend on the choice of particular number of vertices makes them not so interesting from our point of view. However, it is interesting to notice that graphs behaving similarly to the Ramanujan ones are not so unlikely. Indeed Friedman [Friedman 2004] showed that, by averaging the essential spectral radius of the adjacency matrices A of all undirected v-regular Cayley graphs having N vertices, we obtain for $P = v^{-1}A$

$$\mathbb{E}(\rho(P)) \leqslant \frac{2\sqrt{v-1}}{v}\left(1 + \frac{\ln v/2}{\sqrt{v}} + O\left(\frac{1}{\sqrt{v}}\right)\right) + O\left(\frac{v^{1/2}\ln\ln N}{\ln N}\right).$$

Of course the previous bound has to be interpreted in an asymptotic sense for $N \to +\infty$ and $v \to +\infty$. As a consequence we have in particular that, if we fix v sufficiently large, in the average, $\rho(P)$ will remain bounded away from 1 as $N \to +\infty$.

3.5 Time-varying communication graphs

We noticed in the previous section that controllers with symmetries behave quite poorly. As suggested in the last part of the previous section, a way to overcome this difficulty is to resort to Ramanujan graphs or to undirected regular graphs generated randomly. An alternative way to solve this problem while maintaining the symmetry of the controllers is by a time-varying strategy in which at every time instant the communication graph is chosen randomly in a set of Cayley graphs. Such strategies yield a mean square convergence rate that is higher and, more importantly, independent of the number of agents.

3.5.1 Cayley communication graphs

Fix an Abelian group G and a number $v < |G|$. We consider a sequence of subsets $S_t \subseteq G$ that are randomly generated in the following way.

Let $\alpha_i(t)$, $i = 1,\dots,v$, be v independent sequences of independent random variables taking value on G and uniformly distributed in such a set. We put

$$S_t = \{\alpha_0(t) = 0, \alpha_1(t), \dots, \alpha_v(t)\}.$$

Notice that in S_t there might be repetitions and so its cardinality may be less than $v + 1$.

Fix $k_0, k_1, \ldots, k_v \geq 0$ such that $\sum_j k_j = 1$ consider the sequence of probability distributions π_t on G supported on the sequence of sets S_t defined as

$$\pi_t(g) = \begin{cases} k_j & \text{if } g = \alpha_j(t) \\ 0 & \text{otherwise.} \end{cases}$$

Let P_t be the stochastic Cayley matrix generated with π_t. If we consider the feedback matrix $K_t = I - P_t$, we obtain the closed loop system $x(t+1) = P_t x(t)$, which is a jump Markov linear system [Fang and Loparo 2002; Bolzen et al. 2004]. The state $x(t)$ becomes a random variable that evolves according to

$$x(t) = \prod_{s=1}^{t} P_s x(0) ,$$

where $x(0)$ is a random variable independent of the processes $\alpha_i(t)$.

We want to study the asymptotic behavior of $x(t)$. Since we are interested in consensus, we consider the displacement from the barycenter $\Delta(t) = x(t) - \frac{1}{N}\mathbb{1}\mathbb{1}^T x(0) = (I - \frac{1}{N}\chi_0\chi_0^*)x$, which is governed by

$$\Delta(t) = \prod_{s=1}^{t} P_s \Delta(0) ,$$

where $\Delta(0)$ is now a random variable taking values on $\mathbb{R}^G$ such that $< \Delta(0), \chi_0 >= 0$ and independent of the set of variables $\{\alpha_i(t)\}$. In this probabilistic context it is natural to study the asymptotic behavior of $\mathbb{E}\|\Delta(t)\|^2$. We then obtain the following result.

Proposition 3.4

$$\mathbb{E}\|\Delta(t)\|^2 = \left(\sum_{j=0}^{v} k_j^2\right)^t \mathbb{E}\|\Delta(0)\|^2 .$$

Proof. The element (g, h) of the Cayley stochastic matrix P_t generated by π_t can be written as

$$[P_t]_{g,h} = \pi_t(g - h) = \frac{1}{N} \sum_{\chi \in \hat{G}} \hat{\pi}_t(\chi)\chi(g - h)$$

where we have used the inverse Fourier transform (2.4). Thus

$$\pi_t(g - h) = \frac{1}{N} \sum_{\chi \in \hat{G}} \hat{\pi}_t(\chi)\chi(g)\overline{\chi(h)} .$$

Thus we have that

$$P_t = \sum_{\chi \in \hat{G}} \hat{\pi}_t(\chi)N^{-1}\chi\chi^* .$$

Hence,

$$\prod_{s=1}^{t} P_s = \sum_{\chi \in \hat{G}} \left[\prod_{s=1}^{t} \hat{\pi}_s(\chi) \right] N^{-1} \chi \chi^*.$$

Let us study the average of the squared norm of the various eigenvalues.

$$\mathbb{E}\left[\left| \prod_{s=1}^{t} \hat{\pi}_s(\chi) \right|^2 \right] = \prod_{s=1}^{t} \mathbb{E}\left[|\hat{\pi}_s(\chi)|^2 \right].$$

Since

$$\hat{\pi}_t(\chi) = k_0 + \sum_{j=1}^{v} k_j \chi(-\alpha_j(t)),$$

we obtain

$$\mathbb{E}\left[|\hat{\pi}_t(\chi)|^2 \right] = k_0^2 + \sum_{j=1}^{v} k_0 k_j \left[\mathbb{E}\left[\chi(\alpha_j(t)) \right] + \mathbb{E}\left[\chi(\alpha_j(t))^* \right] \right]$$

$$+ \sum_{j=1}^{v} \sum_{\ell=1}^{v} k_j k_\ell \mathbb{E}\left[\chi(\alpha_j(t)) \chi(\alpha_\ell(t))^* \right]. \tag{3.13}$$

It is immediate to verify that $\mathbb{E}[\chi(\alpha_j(t))] = 0$ when $\chi \neq \chi_0$, $\mathbb{E}[\chi(\alpha_j(t))\chi(\alpha_\ell(t))^*] = 0$ when $j \neq \ell$ and $\mathbb{E}[|\chi(\alpha_j(t))|^2] = 1$. Substituting in (3.13) we then obtain

$$\mathbb{E}\left[|\hat{\pi}_t(\chi)|^2 \right] = k_0^2 + \sum_{j=1}^{v} k_j^2 = \sum_{j=0}^{v} k_j^2, \quad \forall \chi \neq 0.$$

We finally have

$$\mathbb{E}\|\Delta(t)\|^2 = \sum_{\chi \neq \chi_0} \mathbb{E}\left[\left| \prod_{s=1}^{t} \hat{\pi}(\chi) \right|^2 \right] \frac{1}{N} \mathbb{E}| < \Delta(0), \chi >|^2$$

$$= \left(\sum_{j=0}^{v} k_j^2 \right)^t \frac{1}{N} \sum_{\chi \neq \chi_0} \mathbb{E}| < \Delta(0), \chi >|^2 = \left(\sum_{j=0}^{v} k_j^2 \right)^t \mathbb{E}\|\Delta(0)\|^2.$$

$\square$

Notice that

$$\min\left\{ \sum_{j=0}^{v} k_j^2 \,\middle|\, k_j \geq 0, \sum_{j=1}^{v} k_j = 1 \right\} = \frac{1}{v+1}$$

and it is obtained by choosing $k_j = 1/(v+1)$ for all j. With such a choice we have thus obtained the following mean convergence result

$$\mathbb{E}\|\Delta(t)\|^2 = \left(\frac{1}{1+v} \right)^t \mathbb{E}\|\Delta(0)\|^2.$$

This performance is much better than what we had obtained for time-invariant strategies, since in this case the rate of convergence is constant with respect to N.

From an implementation point of view this strategy has an evident drawback: the same random choice done at every time instance has to be done by all agents. This seems to require a supervised communication of this information to every agent. A possible way to overcome this limitation is by imposing that each agent uses the same pseudo-random number generator starting from the same seed.

3.5.2   Bounded in-degree communication graphs

In this section we consider a time-varying strategy similar to the one presented in the previous section. The difference is that here we do not limit the time-varying matrices to be Cayley. We will see that this generalization does not lead to better performance.

In this case we assume that each agent receives the state of v other agents chosen randomly and independently. Because of this it can happen that the resulting communication graph has multiple arcs connecting the same pair of nodes.

Fix $k_0, k_1, \ldots, k_v \geq 0$ such that $\sum_j k_j = 1$. The feedback matrix is in this case

$$K_t = (k_0 - 1)I + \sum_{i=1}^{v} k_i E_i(t)$$

where $E_i(t)$, $i = 1, \ldots, v$, are v independent sequences of independent random variables taking values on the set of matrices

$$\mathcal{M} = \{E \in \{0,1\}^{N \times N} \ : \ E\mathbb{1} = \mathbb{1}\}$$

and uniformly distributed in such a set. The set $\mathcal{M}$ is constituted by all matrices with entries 0 or 1 which have exactly one 1 in each row. The closed loop system becomes $x(t+1) = P_t x(t)$ where

$$P_t = k_0 I + \sum_{i=1}^{v} k_i E_i(t) \tag{3.14}$$

The state $x(t)$ becomes a random variable which evolves according

$$x(t) = \prod_{s=1}^{t} P_s x(0),$$

where $x(0)$ is a random variable independent of the processes $E_i(t)$.

Again, we want to study the asymptotic behavior of $x(t)$. Since the controllers we are using are not necessarily barycentric, we can not longer use the variable $\Delta(t) = x(t) - N^{-1}\mathbb{1}\mathbb{1}^T x(0)$ to study convergence to the consensus point. However we can prove the following result.

Theorem 3.2 *There exists a scalar random variable α^* such that*

$$\mathbb{E}\|x(t) - \alpha^*\mathbb{1}\|^2 \leq C\rho^t \mathbb{E}\|(I - N^{-1}\mathbb{1}\mathbb{1}^T)x(0)\|^2 \tag{3.15}$$

where

$$\rho = k_0^2 + \frac{N-1}{N}\sum_{i=1}^{v} k_i^2, \quad C = \frac{1 - 2k_0 + \sum_{i=1}^{v} k_i^2}{(1 - \rho^{1/2})^2}$$

Proof. Let $Q(t) = \mathbb{E}[x(t)x(t)^T]$. Notice that

$$Q^+ = \mathbb{E}[P_t xx^T P_t^T] = \mathbb{E}[\mathbb{E}[P_t xx^T P_t^T | P_t]]\mathbb{E}[P_t Q P_t^T] =$$

$$= k_0^2 Q + \sum_{i=1}^{v} k_0 k_i (\mathbb{E}[QE_i^T] + \mathbb{E}[E_i Q]) + \sum_{i,j=1}^{v} k_i k_j \mathbb{E}[E_i Q E_j^T]$$

$$= k_0^2 Q + \sum_{i=1}^{v} k_0 k_i (Q\mathbb{E}[E_i^T] + \mathbb{E}[E_i]Q) + \sum_{\substack{i,j=1 \\ i\neq j}}^{v} k_i k_j \mathbb{E}[E_i] Q \mathbb{E}[E_j^T] + \sum_{i=1}^{v} k_i^2 \mathbb{E}[E_i Q E_i^T]$$

Notice that $\mathbb{E}[E_i] = N^{-1}\mathbb{1}\mathbb{1}^T$. Moreover, for any $M \in \mathbb{R}^{N\times N}$ it holds

$$\mathbb{E}[E_i^T M E_i] = \frac{1}{N}\text{tr}\{M\}I + \frac{1}{N^2}\mathbb{1}^T M\mathbb{1}(\mathbb{1}\mathbb{1}^T - I)$$

These relations imply that

$$Q^+ = k_0^2 Q + \sum_{i=1}^{v} k_0 k_i (N^{-1}\mathbb{1}\mathbb{1}^T Q + QN^{-1}\mathbb{1}\mathbb{1}^T) + \sum_{i=1}^{v} k_i^2 \left(N^{-1}\text{tr}(Q)I + N^{-2}\mathbb{1}^T Q\mathbb{1}(\mathbb{1}\mathbb{1}^T - I)\right)$$

$$+ \sum_{\substack{i,j=1 \\ i\neq j}}^{v} k_i k_j N^{-1}\mathbb{1}\mathbb{1}^T QN^{-1}\mathbb{1}\mathbb{1}^T.$$

Let us define $w(t) = \text{tr}(Q(t)) = \mathbb{E}\|x(t)\|^2$ and $s(t) = N^{-1}\mathbb{1}^T Q(t)\mathbb{1}$. Notice that

$$w^+ = k_0^2 w + 2\left(\sum_{i=1}^{v} k_0 k_i\right)s + \left(\sum_{i=1}^{v} k_i^2\right)w + \left(\sum_{\substack{i,j=1 \\ i\neq j}}^{v} k_i k_j\right)s = \left(\sum_{i=0}^{v} k_i^2\right)w + \left(1 - \sum_{i=0}^{v} k_i^2\right)s$$

Moreover we have that

$$s^+ = k_0^2 s + 2\left(\sum_{i=1}^{v} k_0 k_i\right)s + \left(\sum_{i=1}^{v} k_i^2\right)\left(\frac{1}{N}w + \frac{N-1}{N}s\right) + \left(\sum_{\substack{i,j=1 \\ i\neq j}}^{v} k_i k_j\right)s$$

$$= \left(\frac{1}{N}\sum_{i=1}^{v} k_i^2\right)w + \left(1 - \frac{1}{N}\sum_{i=1}^{v} k_i^2\right)s$$

The previous two relations can be summarized as follows

$$\begin{pmatrix} w^+ \\ s^+ \end{pmatrix} = \begin{pmatrix} \sum_{i=0}^{v} k_i^2 & 1 - \sum_{i=0}^{v} k_i^2 \\ \frac{1}{N}\sum_{i=1}^{v} k_i^2 & 1 - \frac{1}{N}\sum_{i=1}^{v} k_i^2 \end{pmatrix}\begin{pmatrix} w \\ s \end{pmatrix}. \tag{3.16}$$

We want now to estimate $\mathbb{E}\|x(t+1) - x(t)\|^2$. Notice that

$$
\begin{aligned}
\mathbb{E}\|x(t+1) - x(t)\|^2 &= \operatorname{tr}\mathbb{E}(x(t+1) - x(t))(x(t+1) - x(t))^T \\
&= \operatorname{tr} Q(t+1) + \operatorname{tr} Q(t) - 2\operatorname{tr}\left[(k_0 I + (1-k_0)\frac{1}{N}\mathbb{1}\mathbb{1}^T) Q(t)\right] \\
&= w(t+1) + w(t) - 2k_0 w(t) - 2(1-k_0) s(t) \\
&= \left(\sum_{i=0}^{v} k_i^2\right) w(t) + \left(1 - \sum_{i=0}^{v} k_i^2\right) s + w(t) - 2k_0 w(t) - 2(1-k_0) s(t) \\
&= \left(1 - 2k_0 + \sum_{i=0}^{v} k_i^2\right)(w(t) - s(t))
\end{aligned}
$$

Notice that, from equation (3.16) we can argue that

$$
(w - s)^+ = \left(k_0^2 + \frac{N-1}{N}\sum_{i=1}^{v} k_i^2\right)(w - s)
$$

which implies that

$$
w(t) - s(t) = \left(k_0^2 + \frac{N-1}{N}\sum_{i=1}^{v} k_i^2\right)^t (w(0) - s(0))
$$

and so

$$
\mathbb{E}\|x(t+1) - x(t)\|^2 = \left(1 - 2k_0 + \sum_{i=0}^{v} k_i^2\right)\rho^t (w(0) - s(0))
$$

where

$$
\rho = k_0^2 + \frac{N-1}{N}\sum_{i=1}^{v} k_i^2
$$

Standard arguments on complete metrics show that the exponential convergence of the previous sequence implies that $x(t)$ must converge to some random variable x^* in the L^2-norm $(\mathbb{E}\|\cdot\|^2)^{1/2}$. Indeed we have that,

$$
\begin{aligned}
(\mathbb{E}\|x(t) - x^*\|^2)^{1/2} &\leq \sum_{s=t}^{+\infty}(\mathbb{E}\|x(s+1) - x(s)\|^2)^{1/2} \\
&= \left(1 - 2k_0 + \sum_{i=0}^{v} k_i^2\right)^{1/2}(w(0) - s(0))^{1/2}\sum_{s=t}^{+\infty}\rho^{s/2} \\
&= \left(\frac{1 - 2k_0 + \sum_{i=0}^{v} k_i^2}{(1-\rho^{1/2})^2}(w(0) - s(0))\right)^{1/2}\rho^{t/2}.
\end{aligned}
$$

If we let $Y = I - \frac{1}{N}\mathbb{1}\mathbb{1}^T$, then $\mathbb{E}\|Y x(t)\|^2 = w(t) - s(t)$ and thus

$$
(\mathbb{E}\|x(t) - x^*\|^2)^{1/2} \leq C^{1/2}\rho^{t/2}(\mathbb{E}\|(I - N^{-1}\mathbb{1}\mathbb{1}^T)x(0)\|^2)^{1/2}.
$$

In order to conclude it remains to show that $x^* = \alpha^*\mathbb{1}$. Notice that since $w(t) - s(t)$ tends to zero, we can argue $Y x^* = 0$ and this implies that there exists a scalar random variable α^* such that $x^* = \alpha^*\mathbb{1}$.

$\square$

Notice that the smallest convergence rate in (3.15) is given by

$$\min\left\{k_0^2 + \frac{N-1}{N}\sum_{i=1}^{\nu} k_i^2 \,\Big|\, k_0, k_1, \dots, k_\nu \geq 0, \, k_0 + \sum_{i=1}^{\nu} k_i = 0\right\} = \frac{N-1}{N(\nu+1)-1},$$

obtained by choosing

$$k_0 = \frac{N-1}{N(\nu+1)-1}, \qquad \text{and} \qquad k_i = \frac{N}{N(\nu+1)-1} \qquad \forall i = 1, \dots, \nu. \qquad (3.17)$$

Notice that this convergence rate is smaller than $1/(\nu+1)$, which is the rate obtained through the time-varying strategy on Cayley graphs discussed before. However, for $N \to +\infty$, the two strategies yield the same rate.

The most important difference between the two random strategies presented here is that the time-varying strategy on Cayley graphs yields convergence to the barycenter of the initial configuration, whereas the one presented in this section will not reach the consensus at the barycenter. Therefore it is interesting to study how far from the barycenter the agents will reach the consensus. We have the following result.

Proposition 3.5

$$\mathbb{E}\|x^* - N^{-1}\mathbb{1}\mathbb{1}^T x(0)\|^2 = \beta \mathbb{E}\|\left(I - N^{-1}\mathbb{1}\mathbb{1}^T\right) x(0)\|^2,$$

where

$$\beta = \frac{\sum_{i=1}^{\nu} k_i^2}{N[N(1-k_0^2) + (1-N)\sum_{i=1}^{\nu} k_i^2]}.$$

Proof. Consider $\Delta(t) = x(t) - N^{-1}\mathbb{1}\mathbb{1}^T x(0)$. We know from (3.8) that the dynamics of $\Delta(t)$ is described by the equation $\Delta^+ = P_t \Delta$ where P_t is given in (3.14). For this reason, by denoting $Q(t) := \mathbb{E}[\Delta(t)\Delta(t)^T]$, $w(t) = \text{tr}(Q(t)) = \mathbb{E}\|\Delta(t)\|^2$ and $s(t) = N^{-1}\mathbb{1}^T Q(t)\mathbb{1}$, exactly the same computation done in the proof of the previous result show that equation (3.16) still holds true. The transition matrix has eigenvalues $\lambda_1 = 1$, and $\lambda_2 = k_0^2 + \frac{N-1}{N}\sum_{i=1}^{\nu} k_i^2$. The second eigenvalue coincides with the convergence rate ρ computed before. The time evolution of $w(t)$ and $s(t)$ is thus given by

$$\begin{pmatrix} w(t) \\ s(t) \end{pmatrix} = c_1 \lambda_1^t a_1 + c_2 \lambda_2^t a_2$$

where c_1, c_2 are constants and a_1, a_2 are the eigenvectors associated to λ_1 and λ_2. Notice that $a_1 = (1\ 1)^T$. At steady state the vector $(w(\infty), s(\infty))^T$ is aligned to the dominant eigenvector a_1 and thus $w(\infty) = c_1$. Simple calculations yield

$$w(\infty) = \beta \mathbb{E}\|\left(I - N^{-1}\mathbb{1}\mathbb{1}^T\right) x(0)\|^2,$$

where

$$\beta = \frac{\sum_{i=1}^{\nu} k_i^2}{N[N(1-k_0^2) + (1-N)\sum_{i=1}^{\nu} k_i^2]}.$$

$\square$

If we use the control gains $k_0, k_1, \ldots, k_v$ as in (3.17), which yield the fastest convergence rate, then we have

$$\mathbb{E}\|x^* - N^{-1}\mathbb{1}\mathbb{1}^T x(0)\|^2 = \frac{1}{N(N(1+v)-1)}\mathbb{E}\|\left(I - N^{-1}\mathbb{1}\mathbb{1}^T\right)x(0)\|^2.$$

Notice that, if the initial states $x_i(0)$ of the agents are independent and $\mathbb{E}\left(x_i(0)^2\right)$ is the same for all i, then as $N \to \infty$ the mean square distance to the barycenter tends to zero.

3.6   Summary

In this chapter we have analyzed the tradeoffs between how fast agents can coordinate and the amount of information that need to be exchanged. In particular we have modelled the coordination problem as a consensus problem. Under the assumption that the communication network can be described by a Cayley graph defined on Abelian groups, that is a graph with symmetries, we have been able to bound the convergence rate to the consensus. Furthermore, we have proved that the convergence rate to the barycenter of the initial configuration decreases as the number of agents increases, if the amount of information received by each agent remain constant. We have also considered some particular random strategies that consist in choosing randomly a communication graph from a predefined family of graphs. In particular we have considered stochastically time-varying Cayley graphs and graphs with bounded in-degree. It turns out that choosing randomly over such family of graphs yield a significant improvement of the performance compare to time-invariant communication graphs.

3.A   Proof Theorem 3.1

In order to prove Theorem 3.1 we need the following technical lemma.

Lemma 3.1   *Let* $\mathbb{T} = \mathbb{R}/\mathbb{Z} \cong [-1/2, 1/2[$. *Let* $0 \leq \delta < 1/2$ *and consider the hypercube* $V = [-\delta, \delta]^k \subseteq \mathbb{T}^k$. *For every finite set* $\Lambda \subseteq \mathbb{T}^k$ *such that* $|\Lambda| \geq \delta^{-k}$, *there exist* $\bar{x}_1, \bar{x}_2 \in \Lambda$ *with* $\bar{x}_1 \neq \bar{x}_2$ *such that* $\bar{x}_1 - \bar{x}_2 \in V$.

   Proof. For any $x \in \mathbb{T}$ and $\delta > 0$, define the following set

$$L(x, \delta) = [x, x+\delta] + \mathbb{Z} \subseteq \mathbb{T}.$$

Observe that for all $y \in \mathbb{T}$, $L(x, \delta) + y = L(x+y, \delta)$. Now let $\bar{x} = (\bar{x}_1, \ldots, \bar{x}_k) \in \mathbb{T}^k$ and define

$$L(\bar{x}, \delta) = \prod_{i=1}^{k} L(\bar{x}_i, \delta).$$

   Also in this case we observe that $L(\bar{x}, \delta) + \bar{y} = L(\bar{x} + \bar{y}, \delta)$ for every $\bar{y} \in \mathbb{T}^k$. Consider now the family of subsets

$$\{L(\bar{x}, \delta), \ \bar{x} \in \Lambda\}.$$

We claim that there exist $\bar{x}_1$ and $\bar{x}_2$ in Λ such that $\bar{x}_1 \neq \bar{x}_2$ and such that $L(\bar{x}_1, \delta) \cap L(\bar{x}_2, \delta) \neq \emptyset$. Indeed, if not, we would have that

$$1 \geq m\left(\bigcup_{\bar{x} \in \Lambda} L(\bar{x}, \delta)\right) = \sum_{\bar{x} \in \Lambda} m\left(L(\bar{x}, \delta)\right) = |\Lambda| \delta^k \geq 1$$

where $m(\cdot)$ is the Lebesgue measure on $\mathbb{T}^k$ and where we used the hypothesis $|\Lambda| \geq \delta^{-k}$. However, since all $L(\bar{x}_1, \delta)$ are closed, it is not possible that $m\left(\bigcup_{\bar{x} \in \Lambda} L(\bar{x}_1, \delta)\right) = 1$. Notice finally that

$$L(\bar{x}_1, \delta) \cap L(\bar{x}_2, \delta) \neq \emptyset \iff L(0, \delta) \cap L(\bar{x}_2 - \bar{x}_1, \delta) \neq \emptyset \iff \bar{x}_2 - \bar{x}_1 \in V.$$

$\square$

We can now prove Theorem 3.1.

Proof. With no loss of generality we can assume that

$$G = \mathbb{Z}_{N_1} \oplus \ldots \oplus \mathbb{Z}_{N_r}.$$

Assume we have fixed a probability distribution π supported on S. Let P be the corresponding stochastic Cayley matrix. Since, as we already said

$$\rho(P) = \{\hat{\pi}(\chi) | \chi \in \hat{G}\}.$$

Since the characters are the N-th roots of the unity as we showed in Chapter 2 then we can explicitly write

$$\sigma(P) = \left\{ \sum_{k_1=0}^{N_1-1} \sum_{k_2=0}^{N_2-1} \ldots \sum_{k_r=0}^{N_r-1} \pi(k_1, \ldots, k_r) e^{i\frac{2\pi}{N_1}k_1\ell_1} e^{i\frac{2\pi}{N_2}k_2\ell_2} \cdots e^{i\frac{2\pi}{N_r}k_r\ell_r} : \ell_1 \in \mathbb{Z}_{N_1}, \ldots, \ell_r \in \mathbb{Z}_{N_r} \right\}$$

Denote by $\bar{k}^j = (k_1^j, \ldots, k_r^j)$, for $j = 1, \ldots, \nu$, the non-zero elements in S, and consider the subset

$$\Lambda = \left\{ \left(\sum_{i=1}^{r} \frac{k_i^1 \ell_i}{N_i}, \ldots, \sum_{i=1}^{r} \frac{k_i^\nu \ell_i}{N_i} \right) + \mathbb{Z}^\nu : \ell_1 \in \mathbb{Z}_{N_1}, \ldots, \ell_r \in \mathbb{Z}_{N_r} \right\} \subseteq \mathbb{T}^\nu.$$

Let $\delta = (\prod_i N_i)^{-1/\nu}$ and let V be the corresponding hypercube in $\mathbb{T}^\nu$ defined as in Lemma 3.1. We want to show that there exists $\bar{\ell} = (\ell_1, \ldots \ell_r) \in \mathbb{Z}_{N_1} \times \cdots \times \mathbb{Z}_{N_r}$, $\bar{\ell} \neq 0$ such that

$$\left(\sum_{i=1}^{r} \frac{k_i^1 \ell_i}{N_i}, \ldots, \sum_{i=1}^{r} \frac{k_i^\nu \ell_i}{N_i} \right) + \mathbb{Z}^\nu \in V.$$

We consider two cases.

1. If there exists $\bar{\ell} = (\ell_1, \ldots \ell_r) \in \mathbb{Z}_{N_1} \times \cdots \times \mathbb{Z}_{N_r}$, $\bar{\ell} \neq 0$ such that

$$\left(\sum_{i=1}^{r} \frac{k_i^1 \ell_i}{N_i}, \ldots, \sum_{i=1}^{r} \frac{k_i^\nu \ell_i}{N_i} \right) + \mathbb{Z}^\nu = 0 \in V \tag{3.18}$$

then clearly we are done.

2. Assume now there are no $\bar{\ell} = (\ell_1, \dots \ell_r) \in \mathbb{Z}_{N_1} \times \cdots \times \mathbb{Z}_{N_r}$, $\bar{\ell} \neq 0$ satisfying condition (3.18). In this case it can be shown that two different $\bar{\ell}', \bar{\ell}'' \in \mathbb{Z}_{N_1} \times \cdots \times \mathbb{Z}_{N_r}$ yield

$$\left(\sum_{i=1}^{r} \frac{k_i^1 \ell_i'}{N_i}, \dots, \sum_{i=1}^{r} \frac{k_i^\nu \ell_i'}{N_i} \right) + \mathbb{Z}^\nu \neq \left(\sum_{i=1}^{r} \frac{k_i^1 \ell_i''}{N_i}, \dots, \sum_{i=1}^{r} \frac{k_i^\nu \ell_i''}{N_i} \right) + \mathbb{Z}^\nu,$$

namely different elements in $\mathbb{Z}_{N_1} \times \cdots \times \mathbb{Z}_{N_r}$ always lead do distinct elements in Λ. This implies that $|\Lambda| = \prod_i N_i = \delta^{-\nu}$ and so we are in a position to apply Lemma 3.1 and conclude that there exist two different $\bar{\ell}', \bar{\ell}'' \in \mathbb{Z}_{N_1} \times \cdots \times \mathbb{Z}_{N_r}$ such that

$$\left[\left(\sum_{i=1}^{r} \frac{k_i^1 \ell_i'}{N_i}, \dots, \sum_{i=1}^{r} \frac{k_i^\nu \ell_i'}{N_i} \right) + \mathbb{Z}^\nu \right] - \left[\left(\sum_{i=1}^{r} \frac{k_i^1 \ell_i''}{N_i}, \dots, \sum_{i=1}^{r} \frac{k_i^\nu \ell_i''}{N_i} \right) + \mathbb{Z}^\nu \right] \in V$$

and hence

$$\left(\sum_{i=1}^{r} \frac{k_i^1 \ell_i}{N_i}, \dots, \sum_{i=1}^{r} \frac{k_i^\nu \ell_i}{N_i} \right) + \mathbb{Z}^\nu \in V,$$

where $\bar{\ell} = \bar{\ell}' - \bar{\ell}'' \neq 0$.

Consider now the eigenvalue

$$\lambda = \sum_{k_1=0}^{N_1-1} \sum_{k_2=0}^{N_2-1} \dots \sum_{k_r=0}^{N_r-1} \pi(k_1, \dots, k_r) e^{i\left(\frac{2\pi}{N_1} k_1 \ell_1 + \frac{2\pi}{N_2} k_2 \ell_2 + \dots + \frac{2\pi}{N_r} k_r \ell_r \right)}$$

$$= \pi(0, \dots 0) + \sum_{j=1}^{\nu} \pi(k_1^j, \dots, k_r^j) e^{i\left(\frac{2\pi}{N_1} k_1^j \ell_1 + \frac{2\pi}{N_2} k_2^j \ell_2 + \dots + \frac{2\pi}{N_r} k_r^j \ell_r \right)}.$$

Its norm can be estimated as follows

$$|\lambda| \geq \pi(0, \dots 0) + \sum_{j=1}^{\nu} \pi(k_1^j, \dots, k_r^j) \cos\left(\frac{2\pi}{N_1} k_1^j \ell_1 + \frac{2\pi}{N_2} k_2^j \ell_2 + \dots + \frac{2\pi}{N_r} k_r^j \ell_r \right)$$

$$\geq \pi(0, \dots 0) + \sum_{j=1}^{\nu} \pi(k_1^j, \dots, k_r^j) \left(1 - 2\pi^2 \left(\frac{k_1^j}{N_1} \ell_1 + \frac{k_2^j}{N_2} \ell_2 + \dots + \frac{k_r^j}{N_r} \ell_r \right)^2 \right)$$

$$\geq \pi(0, \dots 0) + \sum_{j=1}^{\nu} \pi(k_1^j, \dots, k_r^j) - \sum_{j=1}^{\nu} \pi(k_1^j, \dots, k_r^j) 2\pi^2 \frac{1}{N^{2/\nu}}$$

$$\geq 1 - 2\pi^2 \frac{1}{N^{2/\nu}}$$

and so we can conclude. $\square$

3.B   Proof Proposition 3.3

We first need the following technical lemma to prove the result.

Lemma 3.2

$$\max_{\substack{0 \le \ell_j \le N-1 \\ (\ell_1,\ldots,\ell_r) \ne (0,\ldots,0)}} \left| k_0 + \sum_{j=1}^{r} k_j e^{-i\frac{2\pi}{N}\ell_j} \right| = \max_{\substack{\ell_j \in \{0,1\} \\ (\ell_1,\ldots,\ell_r) \ne (0,\ldots,0)}} \left| k_0 + \sum_{j=1}^{r} k_j e^{-i\frac{2\pi}{N}\ell_j} \right|$$

Proof. consider a r-tuple $(\ell_1,\ldots,\ell_r) \ne (0,\ldots,0)$ and let $\ell \ne 0$ be a value taken by some of the ℓ_j. Let $J \subseteq \{1,\ldots,r\}$ be the nonempty index set such that $\ell_j = \ell$ if and only if $j \in J$. Consider the new r-tuple $(\ell'_1,\ldots,\ell'_r)$ defined as follows

$$\ell'_j = \begin{cases} 1 & \text{if } j \in J \\ 0 & \text{otherwise} \end{cases}$$

We want to show that

$$\left| k_0 + \sum_{j=1}^{r} k_j e^{-i\frac{2\pi}{N}\ell_j} \right| \le \left| k_0 + \sum_{j=1}^{r} k_j e^{-i\frac{2\pi}{N}\ell'_j} \right| \tag{3.19}$$

Indeed, we have that

$$\left| k_0 + \sum_{j=1}^{r} k_j e^{-i\frac{2\pi\ell_j}{N}} \right|^2 = \left| k_0 + \sum_{j=1}^{r} k_j \cos\frac{2\pi\ell_j}{N} - i\left(\sum_{j=1}^{r} k_j \sin\frac{2\pi\ell_j}{N}\right) \right|^2$$

$$= \left(k_0 + \sum_{j=1}^{r} k_j \cos\frac{2\pi\ell_j}{N} \right)^2 + \left(\sum_{j=1}^{r} k_j \sin\frac{2\pi\ell_j}{N} \right)^2$$

$$= \sum_{j=0}^{r} k_j^2 + 2k_0 \sum_{j=1}^{r} k_j \cos\left(\frac{2\pi\ell_i}{N}\right) + 2\sum_{i=1}^{r-1}\sum_{j=i+1}^{r} k_i k_j \cos\left(\frac{2\pi\ell_i}{N}\right) \cdot$$

$$\cdot \cos\left(\frac{2\pi\ell_j}{N}\right) + 2\sum_{i=1}^{r-1}\sum_{j=i+1}^{r} k_i k_j \sin\left(\frac{2\pi\ell_i}{N}\right) \sin\left(\frac{2\pi\ell_j}{N}\right)$$

$$= \sum_{j=0}^{r} k_j^2 + 2k_0 \sum_{j=1}^{r} k_j \cos\left(\frac{2\pi\ell_i}{N}\right) + 2\sum_{i=1}^{r-1}\sum_{j=i+1}^{r} k_i k_j \cos\left(\frac{2\pi(\ell_j - \ell_i)}{N}\right)$$

Observe now that

$$\cos\left(\frac{2\pi\ell_i}{N}\right) \le \cos\left(\frac{2\pi\ell'_i}{N}\right)$$

for all j, and that

$$\cos\left(\frac{2\pi(\ell_j - \ell_i)}{N}\right) \le \cos\left(\frac{2\pi(\ell'_j - \ell'_i)}{N}\right)$$

for all i, j. This yields (3.19) and proves the lemma. $\square$

We can now prove the Proposition 3.3.

Proof. Suppose that $k_0,\ldots,k_r$ are fixed. We are interested in determining

$$\max_{\substack{0 \le \ell_j \le N-1 \\ (\ell_1,\ldots,\ell_r) \ne (0,\ldots,0)}} \left| k_0 + \sum_{j=1}^{r} k_j e^{-i\frac{2\pi}{N}\ell_j} \right|$$

Using the previous Lemma, if $\ell_j \in \{0,1\}$, then

$$\left| k_0 + \sum_{j=1}^{r} k_j e^{-i \frac{2\pi}{N} \ell_j} \right|^2 = 1 - 2 \left(\sum_{j \in J} k_j \right) \left(1 - \sum_{j \in J} k_j \right) \left(1 - \cos \frac{2\pi}{N} \right)$$

where $J \subseteq \{1, \dots, r\}$ is such that $j \in J$ if and only if $\ell_j = 1$. Maximizing this quantity over the non identically zero vectors $(\ell_1, \dots, \ell_r) \in \{0,1\}^r$ is equivalent to maximize over all the possible nonempty sets J. From this it is not difficult to see that

$$\max_{\substack{0 \leq \ell_j \leq N-1 \\ (\ell_1, \dots, \ell_r) \neq (0, \dots, 0)}} \left| k_0 + \sum_{j=1}^{r} k_j e^{-i \frac{2\pi}{N} \ell_j} \right|^2 = 1 - 2m(1-m) \left(1 - \cos \frac{2\pi}{N} \right)$$

where $m := \min\{k_0, k_1, \dots, k_r\}$. Since $m \leq 1/2$, then in order to minimize $1 - 2m(1-m)\left(1 - \cos \frac{2\pi}{N}\right)$ over the possible $k_0, k_1, \dots, k_r$, we need to maximize m. This is obtained by choosing $k_0 = k_1 = \dots = k_r = 1/(r+1)$, which yield $m = 1/(r+1)$ and

$$\rho_{\mathscr{G}}^{\text{Cayley}} = \left(1 - \frac{2r}{(r+1)^2} \left(1 - \cos \frac{2\pi}{N} \right) \right)^{\frac{1}{2}} \simeq 1 - \frac{4\pi^2 r}{(r+1)^2} \frac{1}{N^2} .$$

$\square$

QUANTIZATION IN CONSENSUS COORDINATION

When we consider the problem of coordinating the communication bandwidth limitation imposes a threshold on the overall system performance. Agents cannot exchange data with infinite precision, so data need to be quantized and converted into symbols. of finite length in order to cope with bandwidth limitations. When agents need to base their actions upon such distorted information, many important questions arise: Is a team able to accomplish a task, and if so when will the task be completed? How does this depend on the distortion introduced? In general a weaker concept of accomplished task need to be considered, which depends on the accuracy of the information received. Answers to these questions become even more important to be found when the number of agents is large. In this case, the bandwidth needs to be shared and thus the agents should communicate symbols that can be encoded with few bits.

The contributions of the chapter are some partial answers to the previous questions in the context of consensus problems. The main results can be summarized in two points: the design of control strategies that solve the consensus problem in presence of uniform and logarithmic quantizers and the study of the corresponding control performance for communication networks that presents symmetries. Results in this chapter can be considered as a first step towards the characterization of bandwidth constraints in multi-agent systems. This topic has not been very much investigated even if quantization in control loops has been studied for some time, e.g., [Curry 1970; Delchamps 1990; Wong and Brockett 1997; Mitter 2000; Brockett and Liberzon 2000; Elia and Mitter 2001; Tatikonda and Mitter 2004; Fagnani and Zampieri 2004; De Persis 2004]. Some of the results of this chapter are built on tools developed for quantized control systems

4.1 Outline

We start defining, in the next section, a weak concept of consensus among agents, which is needed since asymptotic convergence is not possible in presence of quantization [Delchamps 1990]. We also recall the model of two particular quantizers: the uniform and the logarithmic. The second one is preferable because it is possible to stabilize a system with fewer symbols [Elia and Mitter 2001; Fagnani and Zampieri 2004]. In Section 4.3 we formalize an optimal control problem, in a similar fashion as in Chapter 4, for the case of perfect information. This will be instrumental for the results in Section 4.4 and Section 4.5. In these two sections we propose a control design method, which is based on the optimal controller derived in Section 4.3, that solve the consensus problem with uniformly and a combination of uniformly and logarithmically quantized data. We also show that the exchange of only logarithmically quantized information does not yield consensus, in general. Section 4.6 is devoted to the study of the effect of quantization in communication networks that can be modelled as Cayley graphs defined on Abelian groups. We show that it is possible to design controllers that solve the consensus problem. Control performance is also discussed. In this context we show that for a particular Cayley graph adding extra logarithmically quantized data exchange improve the performance with little growth of the needed bandwidth.

4.2 Problem formulation

We recapture here the mathematical formulation of the consensus problem we have introduced in Chapter 3 and extend it to the case of quantized information. Consider $N > 1$ identical agents whose dynamics are described by first order discrete time equations. Let $x_i \in \mathbb{R}$ be the state of each agent and the $u_i \in \mathbb{R}$ control input. Each agent is modelled by a first order system

$$x_i^+ = x_i + u_i \qquad i = 1, \dots, N.$$

In matrix form we have

$$x^+ = x + u,$$

where $x, u \in \mathbb{R}^N$. We assume that the feedback control law is a linear state feedback

$$u = Kx, \qquad K \in \mathbb{R}^{N \times N}.$$

When agents exchange quantized data, we cannot require global asymptotic convergence to the point $\alpha \mathbb{1}$, with $\mathbb{1} = (1, \dots, 1)^T$ as in Chapter 4. Indeed, it is well known that a feedback law which guarantees globally asymptotically convergence of given system in the absence of quantization will in general fail to provide it for the closed-loop system that arises in the presence of a quantizer with a finite number of values. One reason is the saturation of the quantized signal when it is outside the range of the quantizer. In this case the quantization error is large and the control law designed for the ideal case of no quantization may lead to instability. Another reason is deterioration of performance

near the equilibrium. Indeed, as the difference between the current and the desired values of the state becomes small, higher precision is required, and so in the presence of quantization errors asymptotic convergence is typically lost. Due to these phenomena, instead of seeking for global asymptotic convergence results, it is more reasonable to expect that the state starting from a given region remains bounded and approaches a smaller region. Such weaker concept of convergence was introduced in [Delchamps 1990].

We state the consensus problem in presence of quantized data as follows. Let us fix two positive scalar M and ϵ, with $\epsilon < M$, we want to design a matrix K such that, for any initial condition $x(0) \in [-M, M]^N$, the closed loop system

$$x^+ = (I + K)x, \tag{4.1}$$

yields

$$\lim_{t \to \infty} x(t) \in [-\epsilon + \alpha, \epsilon + \alpha]^N \tag{4.2}$$

for any scalar α. We say that the control law $u = Kx$ solves the consensus problem under quantized communication if (4.2) holds.

4.2.1   Quantized communication

In this chapter we assume that the communication is over communication channels with bit rate limitations and thus quantization is needed in order to cope with the limitation. A quantizer can be mathematically described as follows. Let $\mathscr{I}$ be an index set and $\mathscr{Q} = \{q_i\}_{i \in \mathscr{I}}$ a subset of $\mathbb{R}^n$. A quantizer is then modelled as a piecewise constant function

$$q : \mathbb{R}^n \to \mathscr{Q}.$$

To each point $q_i \in \mathscr{Q}$ we can associate a quantization region $V_i = \text{cl}\{x \in \mathbb{R}^n | q(x) = q_i\}$, where cl{.} is the closure. In Figure 4.1(a) is shown a two dimensional function $f(x_1, x_2)$ and in Figure 4.1(b) the quantized version of it, $q(f(x_1, x_2))$. As shown in the figures, the function q maps V_i to a single value q_i.

Depending on the quantization map q, we can divide the quantizers in two classes: uniform quantizers and nonuniform quantizers. The first class is characterized by the fact that the quantization regions are of equal size, see Figure 4.2(a). The nonuniform quantizers have quantization regions that need not to be equal. Figure 4.2(b) shows an example of a scalar logarithmic quantizer. In this chapter we discuss the application of uniform and logarithmic quantizers. We recall here how these maps are defined. Let $\delta > 0$ be the quantization step. A scalar uniform quantizer is a map $q_u : \mathbb{R} \to \mathscr{Q}$ such that

$$q_u(x) = \delta \left\lfloor \frac{x}{\delta} \right\rfloor.$$

The quantization regions for a scalar uniform quantizer are the intervals

$$V_i = [-\delta/2 + i\delta, \delta/2 + i\delta], \quad i \in \mathscr{I}.$$

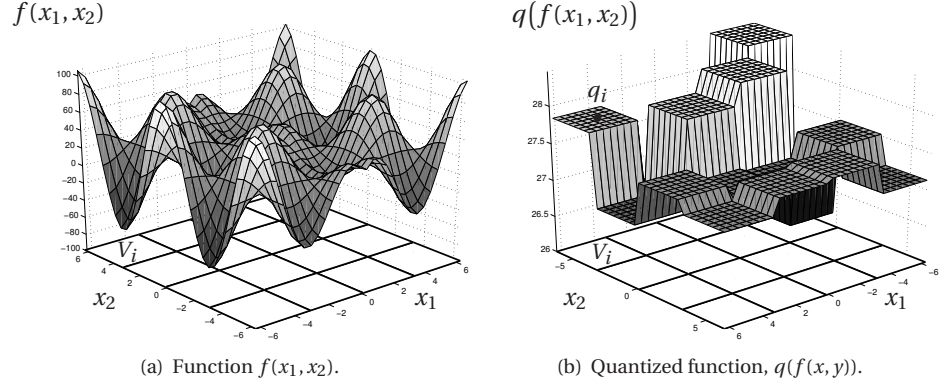(a) Function $f(x_1, x_2)$.   (b) Quantized function, $q(f(x, y))$.

Figure 4.1: A 2D quantizer. V_i represents a quantization region and q_i is the quantized value associated to the quantization region V_i.

The error due to quantization can be bounded as

$$|q_u(x) - x| \leqslant \delta. \tag{4.3}$$

A logarithmic quantizer is a map $q_\ell : \mathbb{R} \to \mathcal{Q}$ such that

$$q_\ell(x) = \exp(q_u(\ln x)). \tag{4.4}$$

The quantization regions for a scalar logarithmic quantizer are the intervals

$$V_i = [\exp(-\delta/2 + i\delta), \exp(\delta/2 + i\delta)], \quad i \in \mathscr{I}.$$

The quantization error for a logarithmic quantizer can be bounded as follow

$$|q_\ell(x) - x| \leqslant \delta_\ell |x|, \qquad \delta_\ell = 1 - e^{-\delta_u}. \tag{4.5}$$

Notice the smaller x gets the finer the quantizer becomes. For a realistic logarithmic quantizer clearly this cannot be true. Generally around the origin the logarithmic quantizer is substituted with a uniform one, as shown in Figure 4.2(b). More precisely

$$q_\ell(x) = \begin{cases} \exp(q_u(\ln x)) & \text{if } |x| > \gamma \\ q_u(x) & \text{otherwise} \end{cases}$$

where γ is a scalar.

4.3   Consensus with perfect data

Let us consider the centralized case with perfect information. In this case the communication network can be modelled as a complete graph, which we denote with $\mathscr{K}_N$. Notice

(a) Uniform quantizer. The scalar case.
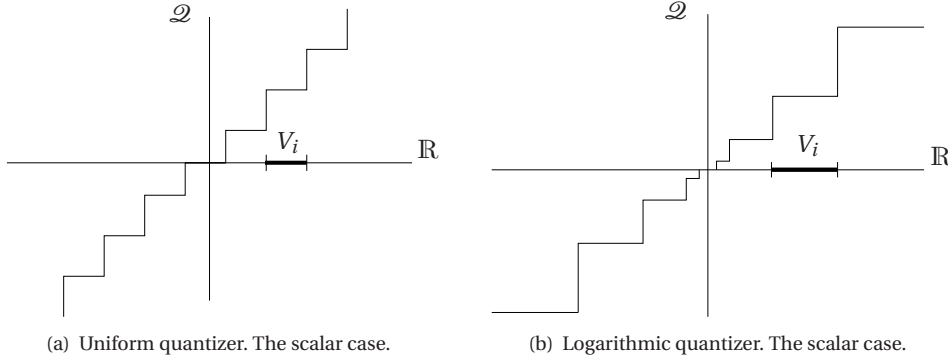
(b) Logarithmic quantizer. The scalar case.

Figure 4.2: Two different types of quantizers: uniform and logarithmic.

that he graph $\mathcal{K}_N$ is an undirected graph. In this particular case equation (4.2) becomes simply

$$\lim_{t \to \infty} x(t) = \alpha \mathbb{1} . \tag{4.6}$$

Let us now consider a vector

$$z = Zx, \qquad Z \in \mathbb{R}^{N-1 \times N} \tag{4.7}$$

such that the vector z are $N-1$ differences of the type $x_i - x_j$ with $i < j$. In other words the matrix Z represents the incident matrix of a directed tree, which is a subset of the complete graph $\mathcal{K}_N$.

Example 4.1 Let us consider the complete graph $\mathcal{K}_3$. Then we can choose

$$Z = \begin{pmatrix} 1 & 0 & -1 \\ 1 & -1 & 0 \end{pmatrix}$$

corresponding to a directed tree with arcs $(1,3)$ and $(1,2)$. Thus we have that

$$z = \begin{pmatrix} 1 & 0 & -1 \\ 1 & -1 & 0 \end{pmatrix} x = \begin{pmatrix} x_1 - x_3 \\ x_1 - x_2 \end{pmatrix} .$$

$\Diamond$

Notice that the condition (4.6) is equivalent to

$$\lim_{t \to +\infty} z(t) = 0, \tag{4.8}$$

since $\ker Z = \langle \mathbb{1} \rangle$. We then have the following difference equation
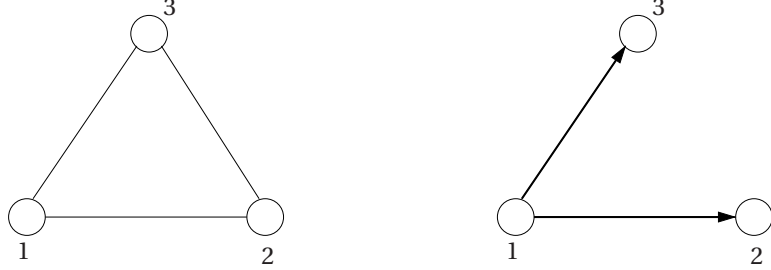
$$z^+ = z + Zu, \tag{4.9}$$

Figure 4.3: On the left the complete graph $\mathcal{K}_3$ and on the right the directed tree described by the incident matrix Z of Example 4.1.

describing the differences between the states of the agents. Thus in $z(t)$ the consensus problem becomes a problem of asymptotic stability.

In order to exclude simple solutions, such as dead-beat controllers, but that requires large input signals and thus are energy inefficient, we consider an optimal control problem. Since for any $\alpha \in \mathbb{R}$ we need to have $\lim_{t\to\infty} x(t) = \alpha \mathbb{1}$, we consider the following optimal control problem

$$\text{minimize}_u \quad \sum_{t=0}^{\infty} (x(t) - \alpha\mathbb{1})^T Q(x(t) - \alpha\mathbb{1}) + u(t)^T R u(t) \qquad (4.10)$$
$$\text{s.t.} \quad x^+ = x + u$$
$$\lim_{t\to\infty} x(t) = \alpha\mathbb{1}, \quad \alpha \in \mathbb{R}.$$

where we assume that full information is available at each vehicle. Clearly we do not know the value of α a-priori and thus we cannot solve the previous problem. A possible way is that of optimizing over α as well, as we considered in Chapter 5. Since we want to keep α as free variable, we can transform the problem considering a weighting matrix Q the Laplacian of $\mathcal{K}_N$. This is a semi-definite matrix such that

$$Q_{ij} = \begin{cases} \deg(i) & \text{if } i = j \\ -1 & \text{if } i \sim j \\ 0 & \text{otherwise}, \end{cases}$$

where $i \sim j$ denotes that the vertexes i and j are neighbors and $\deg(i)$ is the number of edges that are incident to i. There always exists a matrix L such that $(I, L^T)Z$ is the incident matrix of the complete graph, so we can rewrite Q as

$$Q = Z^T (I + L^T L) Z.$$

With this choice of Q we can rewrite the previous optimal control problem as a classical LQ problem

$$\min_u \quad \sum_{t=0}^{\infty} z(t)^T (I + L^T L) z(t) + u(t)^T R u(t) \tag{4.11}$$
$$\text{s.t.} \quad z^+ = z + Zu$$

where we used equation (4.7). The solution of the previous problem can be computed in closed form.

Proposition 4.1 *The state feedback that solves the problem* (4.11) *with $R = I$ is $u = Fz$ with*

$$F = -kZ^T (I + L^T L), \qquad k = \frac{N + \sqrt{N^2 + 4N}}{N^2 + N\sqrt{N^2 + 4N} + 2N}.$$

Proof. We first show that we can find $\alpha > 0$ such that $S = \alpha(I + L^T L)$ is a solution of the Riccati equation associated to the optimal control problem (4.11). The Riccati equation is

$$SZ(R + Z^T SZ)^{-1} Z^T S = I + L^T L.$$

If we substitute we get that

$$\alpha(I + L^T L) Z (R + \alpha Z^T (I + L^T L) Z)^{-1} Z^T \alpha (I + L^T L) = I + L^T L.$$

Let us multiply on the left and the right with Z^T and Z respectively. The matrix $Z^T (I + L^T L) Z$ is the Laplacian of a complete graph and thus we have that $Z^T (I + L^T L) Z = NI - \mathbb{1}\mathbb{1}^T$. Substituting we obtain

$$\alpha(NI - \mathbb{1}\mathbb{1}^T) \underbrace{\left(I + \alpha(NI - \mathbb{1}\mathbb{1}^T)\right)^{-1}}_{\Gamma} \alpha(NI - \mathbb{1}\mathbb{1}^T) = NI - \mathbb{1}\mathbb{1}^T. \tag{4.12}$$

Notice that Γ can be written as

$$\Gamma = \left((1 + \alpha N)I - \alpha\mathbb{1}\mathbb{1}^T\right)^{-1} = \frac{1}{1 + \alpha N}\left(I + \sum_{i=1}^{\infty}\left(\frac{\alpha N}{1 + \alpha N}\right)^i (\mathbb{1}\mathbb{1}^T)^i\right).$$

Since $(\mathbb{1}\mathbb{1}^T)^i = N^{i-1}\mathbb{1}\mathbb{1}^T$, we can compute the previous sum, we have that

$$\Gamma = \gamma(\alpha)\left(I + \beta(\alpha)\mathbb{1}\mathbb{1}^T\right)$$

with

$$\gamma(\alpha) = \frac{1}{1 + \alpha N}, \quad \beta(\alpha) = \frac{\alpha N}{\left(-N^2 + N\right)\alpha + 1}.$$

Equation (4.12) becomes

$$\alpha^2 \gamma(\alpha) N\left(NI - \mathbb{1}\mathbb{1}^T\right) = NI - \mathbb{1}\mathbb{1}^T$$

from which we can compute

$$\alpha = \frac{1}{2} + \frac{1}{2N}\sqrt{N^2 + 4N}. \qquad (4.13)$$

The feedback F is then given by

$$F = -(I + Z^T S Z)^{-1} Z^T S.$$

Notice that $(I + Z^T S Z)^{-1} = \Gamma$ and since $S = \alpha(I + L^T L)$ we have

$$F = -\alpha\gamma(\alpha)(I + \beta(\alpha)\mathbb{1}\mathbb{1}^T)Z^T(I + L^T L).$$

Using the fact that $Z\mathbb{1} = 0$ we obtain

$$F = -\alpha\gamma(\alpha)Z^T(I + L^T L) = -kZ^T(I + L^T L)$$

with

$$k = \alpha\gamma(\alpha) = \frac{N + \sqrt{N^2 + 4N}}{2N + N^2 + N\sqrt{N^2 + 4N}},$$

and this concludes the proof. $\square$

Corollary 4.1 *The optimal control strategy $u = Kx$ solves* (4.10) *for some $\alpha \in \mathbb{R}$, with Q Laplacian of the graph $\mathcal{K}_N$ and $R = I$. The feedback matrix is*

$$K = -k(NI + L^T L), \qquad k = \frac{N + \sqrt{N^2 + 4N}}{N^2 + N\sqrt{N^2 + 4N} + 2N}.$$

Proof. Using the result of the previous proposition we have that the optimal control for the problem (4.10) is

$$u = Fz = FZx = -kZ^T(I + L^T L)Z = -k(NI - \mathbb{1}\mathbb{1}^T).$$

$\square$

Notice that $(I + K)\mathbb{1} = 1$, $\mathbb{1}^T(K + I) = \mathbb{1}^T$ and $I + K$ is non-negative. Thus the optimal feedback matrix is doubly stochastic. From the discussion we had in Chapter 3 this implies the agents converge to the barycenter of the initial condition.

4.4   Consensus with uniformly quantized data

Let us now assume that the agents can communicate over a communication network that is modelled as a complete graph but with uniformly quantized information. This implies the agent i has available its own state and quantized states of the teammates. The transmission of quantized data allows us to cope with bandwidth constraints. Let us define, as in [Fagnani and Zampieri 2004], the contraction rate as $C = M/\epsilon$, where

M is the half the size of the hypercube in which the initial condition lies, and ϵ is half the size of the hypercube where the state converges. It is possible to show [Fagnani and Zampieri 2004] that using uniform quantizers one needs at least C different levels, and thus an alphabet of C different symbols, to drive the state inside the hypercube of size 2ϵ. Thus, if the agents exchange uniformly quantized data, the total number of symbols that are sent over the network, in order to solve the consensus problem, are

$$L_u = \frac{N(N-1)}{2}C,$$

which thus grows linearly with C.

Using as feedback gains the optimal one we compute previously, the feedback control law for the overall system becomes

$$u_i = -k(N-1)x_i + k\sum_{j\neq i}q_u(x_j), \qquad i = 1,\dots,N. \tag{4.14}$$

We have the following result.

Proposition 4.2 *The feedback control law* (4.14) *solves the consensus problem under uniformly quantized communication.*

Proof. Let us consider a component $z_i = x_i - x_j$ with $i < j$. Then we have that the closed loop system becomes

$$z_i^+ = (1 - k(n-1))z_i + k\left(\sum_{s\neq i}q_u(x_i) - \sum_{r\neq j}q_u(x_r)\right).$$

Let us consider the function $V(z_i) = |z_i|$. Then we have that

$$\Delta(V(z_i)) = V(z_i^+) - V(z_i) = \left|(1 - kN)z_i + k\sum_{s\neq i}q_u(x_i) - k\sum_{r\neq j}q_u(x_r)\right| - |z_i|$$

$$\leqslant (|1 - kN| - 1)|z_i| + k|q_u(x_i) - x_i| + k|q_u(x_j) - x_j|$$

$$\leqslant (|1 - kN| - 1)|z_i| + 2k\delta.$$

Since

$$kN = \frac{N^2 + N\sqrt{N^2 + 4N}}{N^2 + N\sqrt{N^2 + 4N} + 2N} \leqslant 1$$

we have that $\Delta V(z_i) < 0$ if $|z_i| > 2\delta/N$. We can then consider the following Lyapunov function

$$\mathcal{V}(z_1,\dots,z_{N-1}) = V(z_1) + \dots + V(z_{N-1}).$$

We have that $\Delta\mathcal{V} < 0$ for

$$|z_1| + \dots + |z_{N-1}| > \frac{2(N-1)\delta}{N}.$$

Figure 4.4: Figure showing the situation discussed in the proof of Proposition 4.2.

If $|z_i| \in [-2\delta/N, 2\delta/N]$ then the previous equation is satisfied. Thus $\Delta\mathcal{V} < 0$ if $|x_i - x_j| > \frac{2\delta}{N}$ for all i and j such that $i < j$.

We now need to show that the $\lim_{t\to+\infty} x(t) \in [\alpha-\epsilon, \alpha+\epsilon]$. We limit here the proof to the case when $N = 2$, the general case can then be proved in a similar way.

The condition $\Delta\mathcal{V} < 0$ holds true in this case if $|z_1| = |x_1 - x_2| > \delta$. This implies that the Lyapunov function is negative outside the region delimited by the two lines $x_2 = x_1 + \delta$ and $x_2 = x_1 - \delta$ showed in Figure 4.4. Thus for $t \to +\infty$ the state will be confined inside that region. We now have two possible situation that can occur

(i) The state enters in one of the shaded regions shown in Figure 4.4. We have indicated in dashed line the boundaries of the areas where $q_u(x_1)$ is constant and with dotted lines the areas where $q_u(x_2)$ constant. Thus each of the shaded areas represents the intersection between areas of the state space where $q_u(x_1) = q_u(x_2) = \xi$ and the region delimited by the two lines described by $|x_1 - x_2| = \delta$. In this case we have that the system dynamics reduce to

$$x_1^+ = (1-k)^2 x_1 + k\xi$$
$$x_2^+ = (1-k)^2 x_2 + k\xi$$

and we have that the steady state is given by $x_1 = x_2 = \xi$. Thus this means that the state converges asymptotically to the center of the cell delimited by the dashed

and dotted lines. We have

$$\lim_{t \to +\infty} x(t) = \xi,$$

and thus (4.2) is fulfilled.

(ii) The state enters the region delimited by solid bold lines in Figure 4.4 in the white area, between the two shaded one. Assume that the state is at the point P, denoted by the cross in the figure. In this case we have that two possibilities: the first the system dynamics evolves so that the trajectory enters the shaded area, and we thus obtain a behavior as described in point (i), otherwise the trajectories remain confined in that white area. In this case anyway, it is clear that

$$\lim_{t \to +\infty} x(t) \in [\alpha - \delta, \alpha + \delta],$$

where (α, α) is the coordinate of the point Q in the Figure.

This concludes the proof. □

Remark 4.1
Notice that any trajectory of the system

$$x_1^+ = (1 - k)x_1 + kq_u(x_2)$$
$$x_2^+ = (1 - k)x_2 + kq_u(x_1)$$

either converges to a point such that $q_u(x_1) = q_u(x_2)$ or to a limit cycle of period 2.

The first statement follows directly from the previous proposition. We show that a trajectory can converge to a limit cycle. Let us assume, without loss of generality, that the initial condition is a point P as in Figure 4.4, which can be reached by the argument in the previous proposition. Let $P = (\bar{x}_1, \bar{x}_2)$. Then we have that after two time steps the state reaches

$$x_1^{(2)} = (1 - k)^2 \bar{x}_1 + k(2 - k)\xi_2$$
$$x_2^{(2)} = (1 - k)^2 \bar{x}_2 + k(2 - k)(\xi_2 - \delta)$$

where the difference in quantization level is only δ since $\bar{x}_1$ and $\bar{x}_2$ belong to neighbor cells. Straightforward calculations show that $(x_1^{(2)}, x_2^{(2)}) = P$ if $\bar{x}_1(0) = \xi_2$ and $\bar{x}_2(0) = \xi_2 - \delta$. In this case then we obtain the following system

$$\begin{pmatrix} x_1^{(2)} \\ x_2^{(2)} \end{pmatrix} = \begin{pmatrix} (1 - k)^2 & k(2 - k) \\ k(2 - k) & (1 - k)^2 \end{pmatrix} \begin{pmatrix} \bar{x}_1 \\ \bar{x}_2 \end{pmatrix}$$

where the state transition matrix has eigenvalues $\lambda_1 = 1$ and $\lambda_2 = 1 - 4k + 2k^2$ with eigenvectors $(1, 1)^T$ and $(1, -1)^T$, respectively. Thus P is close to the line passing through Q with angle $-45°$ then the system enters in a limit cycle of period 2, whereas if the point lies close the the $45°$ line then the trajectory converges.

4.5 Consensus with uniformly and logarithmically quantized data

Although the uniform quantization of the information allows to cope with limited bandwidth channels, the number of bits that needs to be transmitted is rather large. In this section we study some alternatives where data is logarithmically quantized.

4.5.1 Logarithmic-logarithmic quantization

In the case when only logarithmic quantizers are used, using results from [Fagnani and Zampieri 2004], the total number of symbols on the network is

$$L_\ell = \frac{N(N-1)}{\log \frac{1+\delta_\ell}{1-\delta_\ell}} \log C,$$

where $\delta_\ell \in (0,1)$ is the quantization level of the logarithmic quantizer. Notice that now the number of symbols grows only logarithmically with C. Thus it would be convenient from a bandwidth point of view to use as many logarithmic quantizers as possible. However, we show in the following that it is not possible to substitute all the uniform quantizers with logarithmic one.

In order to carry out the analysis, we approximate the quantization error for a logarithmic quantizer as multiplicative noise

$$q_\ell(x) \approx x(1+e) \tag{4.15}$$

where $e \sim \mathcal{U}(-\delta_u, +\delta_u)$. Since a uniform quantizer can be approximated as additive noise [Widrow et al. 1995], then from (4.4) we have that

$$q_\ell(x) = \exp(q_u(\log(x))) \approx \exp(log(x) + e) = x + \exp(e)$$

with $e \sim \mathcal{U}(-\delta_u, +\delta_u)$. For small e we have that $\exp(e) \approx (1+e)$ and thus we obtain (4.15).

Under this assumption we state a stochastic consensus problem where the state x is now a random variable. We will say that a feedback law $u = g(x)$ solves the consensus problem for the system $x^+ = x + u$, if

$$\lim_{t \to +\infty} \mathbb{E}x(t) = \alpha \mathbb{1},$$

and the variance of x is bounded. We have the following result.

Proposition 4.3 *The feedback control law, for a system with $N = 2$ agents,*

$$u_1 = -kq_\ell(q_\ell(x_1) - x_2)$$
$$u_2 = -k(x_2 - q_\ell(x_1)).$$

with k given as in Corollary 4.1, does not solve the stochastic consensus problem.

Proof. Modelling the quantization as multiplicative noise we have

$$x^+ = \begin{pmatrix} 1-k & k \\ k & 1-k \end{pmatrix} x + e_1 \begin{pmatrix} -k & 0 \\ k & 0 \end{pmatrix} x$$

$$+ e_2 \begin{pmatrix} -k & k \\ 0 & 0 \end{pmatrix} x + e_1 e_2 \begin{pmatrix} -k & 0 \\ 0 & 0 \end{pmatrix} x$$

$$= (A + e_1 B + e_2 C + e_1 e_2 D) x,$$

where we assume that e_1 and e_2 are random variables uniformly distributed in $[-\delta_u, \delta_u]$ and independent. In order to prove that the consensus is not solved we show that variance is unbounded. Let us consider $z = x_1 - x_2$, we show that $\mathbb{E} z^2$ is unbounded when $t \to +\infty$. We can write

$$\mathbb{E} z^2 = \mathbb{E}(x_1^2 + x_2^2 - 2x_1 x_2) = \begin{pmatrix} 1 & -1 \end{pmatrix} \mathbb{E}(xx^T) \begin{pmatrix} 1 \\ -1 \end{pmatrix}. \tag{4.16}$$

Let us define $Q = \mathbb{E} xx^T$. Then we have, after some cumbersome calculations, that

$$Q^+ = AQA^T + \sigma^2 BQB^T + \sigma^2 CQC^T + \sigma^4 DQD^T = \begin{pmatrix} Q_{11} & Q_{12} \\ Q_{12} & Q_{22} \end{pmatrix}, \tag{4.17}$$

where $\sigma^2 = \mathbb{E} e_1^2 = \mathbb{E} e_2^2 = \delta_u^2/6$. Let $P = \text{vec}(Q) = [Q_{11}, Q_{12}, Q_{12}, Q_{22}]^T$ then we obtain

$$P^+ = \underbrace{(A \otimes A + \sigma^2 B \otimes B + \sigma^2 C \otimes C + \sigma^4 D \otimes D)}_{=\Omega} P. \tag{4.18}$$

Let us consider $\overline{\Omega}$ the matrix Ω where the third row and column, corresponding to the repeated state Q_{12}, has been removed. We compute the polynomial characteristic $q(z) = \det(zI - \overline{\Omega})$ and we obtain that

$$q(0) = 1 - \frac{1}{324} \delta^8 k^5 + \left(16 + \frac{5}{648} \delta^8 + 2/9 \delta^4\right) k^4 + \left(-32 - 2/9 \delta^4 - \frac{1}{216} \delta^8\right) k^3 +$$

$$\left(24 + \frac{1}{1296} \delta^8 + 1/18 \delta^4\right) k^2 - 8 k$$

Substituting $k = (1 + \sqrt{3})/(2(2 + \sqrt{3}))$ we obtain that $q(0) < 0$ for any δ_u. From Jury's stability criterion [Åström and Witternmark 1997, page 81] we can conclude that the matrix $\overline{\Omega}$ has at least one eigenvalue outside the unit circle. This implies that the system (4.18) is unstable. But since $\mathbb{E} z^2$ is a linear combination of the elements of P, then (4.16) also diverges. □

Remark 4.2

The intuitive explanation of why the previous strategy does not yield consensus is that we quantize logarithmically the state and not a difference. Indeed the quantization error of a logarithmic quantizer is small around the origin (see Figure 4.2(b)). However in the consensus problem we want small errors around the equilibrium $\alpha \mathbb{1}$. Clearly if we consider the quantization of the differences, such as z, then the equilibrium point is the origin, see equation 4.9.

4.5.2   Uniform-logarithmic quantization

The previous negative result forces the design of control laws where data are both uniformly and logarithmically quantized.

Let us then consider the case where only some of the uniform quantizers are substituted by logarithmic quantizers. We consider topologies where the complete graph is divided in two subgraphs: a tree, modelling data that is uniformly quantized, and the remaining graph modelling logarithmically quantized data exchange. We have that for a system of N agents the total amount of symbols is

$$L_{u,\ell} = (N-1)C + \frac{N^2 - 3N + 2}{2\log\frac{1+\delta_\ell}{1-\delta_\ell}}\log C.$$

Let us consider two instrumental cases, that is the two- and three-agent system.

Proposition 4.4   *The feedback control law*

$$u_1 = -k\,q_\ell\big(q_u(x_1) - x_2\big)$$
$$u_2 = -k\big(x_2 - q_u(x_1)\big)$$

with k given as in Corollary 4.1, solves the consensus problem.

Proof. Let us consider the difference $z = x_1 - x_2$. Let us consider the Lyapunov function candidate $V = |z|$. Using the bounds on the quantization errors, we have that

$$\Delta V(z) = |z - k(q_\ell(q_u(x_1) - x_2) - x_2 + q_u(x_1))| - |z|$$
$$\leq -2k|z| + k|z|\delta_\ell + 2k\delta + k\delta\delta_\ell.$$

Thus it follows that $\Delta V(z) < 0$ if

$$|z| > \frac{\delta(2 + \delta_\ell)}{2 - \delta_\ell}.$$

Then we have an analogous situation to that the proof of Proposition 4.2. The state enters the region limited by the solid lines shown in Figure 4.5. In this case the shaded regions are of different shape, but similar arguments as in the proof of Proposition 4.2 conclude the proof.

□

When the number of agents is $N = 3$, then there are three different topologies, depending on how we chose the tree in the complete graph. In Figure 4.6 the tree possible topologies are shown (up to a relabelling of the agents).

We can prove a result similar to the case $N = 2$.

Proposition 4.5   *Let us define the following feedback control laws for the three different topologies shown in Figure 4.6*
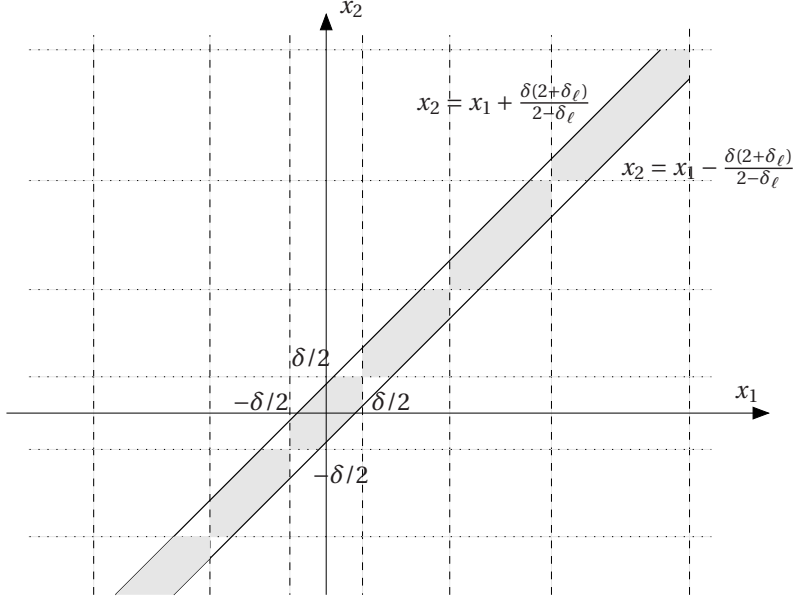
Figure 4.5: Figure showing the situation discussed in the proof of Proposition 4.4.

- *Topology 1*

$$u_1 = -kq_\ell(q_u(x_1) - x_3) - kq_\ell(q_u(x_2) - x_3)$$
$$u_2 = kq_\ell(q_u(x_1) - x_3) - 2kq_\ell(q_u(x_2) - x_3)$$
$$u_3 = -k(q_u(x_1) - x_3) - k(q_u(x_2) - x_3).$$

- *Topology 2*

$$u_1 = -kq_\ell(q_u(x_1) - x_2) - kq_\ell(q_u(x_1) - x_3)$$
$$u_2 = -kq_u(x_1) - x_2) - kq_\ell(q_u(x_1) - x_3))$$
$$u_3 = -2kq_u(x_1) - 2kq_\ell(q_u(x_1) - x_2).$$

- *Topology 3*

$$u_1 = 2kq_\ell(q_u(x_1) - x_2) - kq_\ell(q_u(x_2) - x_3)$$
$$u_2 = k(q_u(x_1) - x_2) - kq_\ell(q_u(x_2) - x_3)$$
$$u_3 = kq_\ell(q_u(x_1) - x_3)kq_u(x_2) - x_3).$$

with k given as in Corollary 4.1 These control law solve the consensus problem.
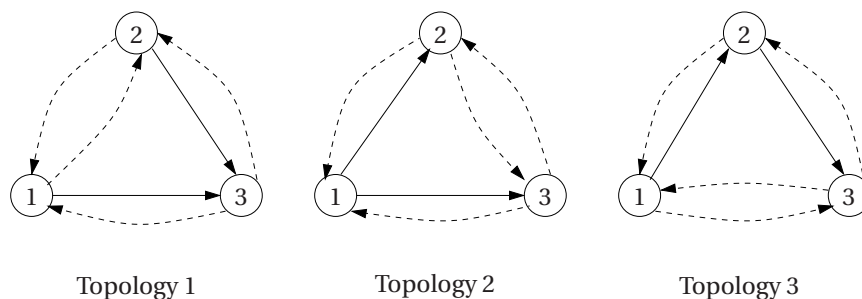
Proof. Similar to the proof of Proposition 4.4.

Figure 4.6: Three different communication topologies for $N = 3$. Solid lines denote uniformly quantized data exchange, and dashed lines logarithmically quantized data exchange.

$\square$

This methodology can be carried on for any given number of agents. However, it is rather complicated to characterize the feedback laws for all the topologies corresponding to a particular N. In the next section we consider the class of Cayley graphs.

4.6   Consensus over Cayley graphs with logarithmically quantized data

Let us assume we have fixed an Abelian group G having N elements and a subset $S \subseteq G$ such that $0 \in S$. Consider the Cayley graph $\mathcal{G}$ associated with G and S, as we discussed in Section 3.4. We will assume that the Cayley graph represents almost perfect data exchange (namely a uniform quantization with very small quantization error). Let P_0 be a Cayley stochastic matrix compatible with $\mathcal{G}$. We now consider the possibility that each agent i can transmit functions of the exact information it has available to some other agent. We assume that such transmissions are logarithmically quantized and that the symmetry of the overall structure, imposed by the Cayley graph, is maintained. In order to achieve this, we define q outputs

$$z_s = H_s x, \quad s = 1, \ldots, q \tag{4.19}$$

where H_s are Cayley matrices compatible with $\mathcal{G}$. Thus the i-th component of outputs $z_1, \ldots, z_q$ represents the information the i-th agent transmits to the other agents. In this way every agent transmits q scalar messages. We assume that logarithmically quantized data are modelled as a multiplicative noise distortion, in particular we have that each component of the output z_s is distorted by the multiplicative noise $1 + e_{s,i}$. To complete the model we have to specify which systems receive this information and how this information is used for control.

We assume that each agent weights the output data from the other agents through Cayley matrices P_s, compatible with $\mathcal{G}$, such that the closed loop dynamics can be de-

scribed as

$$x^+ = P_0 x + \sum_{s=1}^{q} P_s (I + E_s) H_s x, \tag{4.20}$$

where E_s is the matrix

$$E_s = \begin{pmatrix} e_{s,1} & & \\ & \ddots & \\ & & e_{s,N} \end{pmatrix}.$$

All noises $e_{s,i}$ are assumed to be independent, having zero mean and finite variance δ_s^2. Notice that the nonzero elements of the matrix P_s specify which logarithmic link is active. More precisely, $(P_s)_{ij} \neq 0$ means that the signal $(H_s x)_j$ is transmitted to i after being logarithmically quantized.

Let us impose, as in Chapter 4, that the configurations $x = \alpha \mathbb{1} = \alpha \chi_0$ are equilibrium points, with χ_0 the trivial character of the group G and $\alpha \in \mathbb{R}$. Thus we impose that $\mathbb{E}x^+ = \mathbb{E}x$ where the expected value is taken with respect to all $e_{s,i}$. This happens if

$$P_0 \chi_0 = \chi_0,$$
$$H_s \chi_0 = 0, \quad s = 1, \ldots, q.$$

The asymptotic behavior of the dynamical system (4.20) can be studied in a similar way to the random case treated in Section 3.5.2 by considering $Q = \mathbb{E}[xx^T]$. Let $P = P_0 + \sum_s P_s H_s$. The evolution for Q can be described as follows

$$Q^+ = PQP^T + \sum_{s=1}^{q} P_s \mathbb{E}\left(E_s H_s Q H_s^T E_s\right) P_s^T.$$

Observe that, if M is any square matrix, then

$$\mathbb{E}(E_s M E_s)_{ij} = \mathbb{E}(e_{si} M_{ij} e_{sj}) = \begin{cases} M_{ii} \mathbb{E}(e_{si}^2) & \text{if } i = j. \\ 0 & \text{if } i \neq j \end{cases}$$

This implies that

$$Q^+ = PQP^T + \sum_{s=1}^{q} \delta_s^2 P_s \text{diag}(H_s Q H_s^T) P_s^T, \tag{4.21}$$

where we use the notation

$$\text{diag}(M) = \text{diag}(M_{1,1}, \ldots, M_{N,N}).$$

Let $Y = I - N^{-1} \chi_0 \chi_0^*$ and define the signals $y(t) = Y x(t)$ and $x_B(t) = N^{-1} \chi_0 \chi_0^* x(t)$. Let moreover

$$w(t) = \mathbb{E}[||y(t)||^2] = \text{tr}\,\mathbb{E}[y(t)y(t)^T] = \text{tr}\,(YQ(t)Y^T)$$
$$w_s(t) = \mathbb{E}[||z_s(t)||^2] = \text{tr}\,(H_s Q(t) H_s^T)$$
$$s(t) = \mathbb{E}[||x_B(t)||^2] = \text{tr}\,(N^{-1} \chi_0 \chi_0^* Q(t) N^{-1} \chi_0 \chi_0^*) = N^{-1} \chi_0^* Q(t) \chi_0,.$$

where the signals $z_s(t)$ are defined in (4.19).

In order to study the evolution of the above quantities, we need a technical result on the trace operator for Cayley matrices. Assume P is a Cayley matrix. We know that P can be written as

$$P = \sum_{\chi \in \hat{G}} \theta(\chi) N^{-1} \chi \chi^*. \tag{4.22}$$

Consider now the norm $||P||^2 = \sum_{\chi \in \hat{G}} |\theta(\chi)|^2$. Notice that, if π is the generator of P, then $\theta(\chi) = \hat{\pi}(\chi)$ for all $\chi \in \hat{G}$, where $\hat{\pi}$ is the Fourier transform of π. Moreover by Parseval theorem we have that $||P||^2 = \sum_{\chi \in \hat{G}} |\hat{\pi}(\chi)|^2 = N \sum_{g \in G} |\pi(g)|^2$. We have the following result.

Lemma 4.1 *Assume that P is a Cayley matrix and D is a diagonal matrix. Then,*

$$\mathrm{tr}(PDP^*) = N^{-1} ||P||^2 \mathrm{tr}(D).$$

Proof. Assume that P is represented as in (4.22). We can write

$$PDP^* = \sum_{\chi, \bar{\chi}} \theta(\chi) \theta(\bar{\chi}) N^{-1} \chi \chi^* D N^{-1} \bar{\chi} \bar{\chi}^* = N^{-1} \sum_{\chi, \bar{\chi}} \theta(\chi) \theta(\bar{\chi}) (\chi^* D \bar{\chi}) N^{-1} \chi \bar{\chi}^*.$$

Hence,

$$\mathrm{tr}(PDP^*) = N^{-1} \sum_{\chi, \bar{\chi}} \theta(\chi) \theta(\bar{\chi}) (\chi^* D \bar{\chi}) \mathrm{tr}(N^{-1} \chi \bar{\chi}^*).$$

It is immediate to verify that

$$\mathrm{tr}(N^{-1} \chi \bar{\chi}^*) = \begin{cases} 0 & \text{if } \chi \neq \bar{\chi} \\ 1 & \text{if } \chi = \bar{\chi} \end{cases}$$

Moreover, we have that

$$\chi^* D \chi = \sum_{g \in G} \chi(g)^* D_{gg} \chi(g) = \sum_{g \in G} D_{gg} = \mathrm{tr}(D).$$

Substituting in the expression above we finally obtain

$$\mathrm{tr}(PDP^*) = N^{-1} \sum_{\chi} |\theta(\chi)|^2 \mathrm{tr}(D) = N^{-1} ||P||^2 \mathrm{tr}(D).$$

$$\square$$

Using the above lemma, we obtain from (4.21) that

$$w^+ = \mathrm{tr}(YPQP^TY^T) + N^{-1} \sum_{s=1}^q \delta_s^2 ||YP_s||^2 w_s$$

$$w_r^+ = \mathrm{tr}(H_r PQP^T H_r^T) + N^{-1} \sum_{s=1}^q \delta_s^2 ||H_r P_s||^2 w_s \tag{4.23}$$

$$s^+ = s + N^{-1} \sum_{s=1}^q \delta_s^2 |\lambda_s|^2 w_s$$

where λ_s is defined by $P_s\chi_0 = \lambda_s\chi_0$ (equivalently, $\lambda_s = \hat{\pi}_{P_s}(\chi_0)$).

Define $\zeta(t)$ to be the q-dimensional vector with $w_s(t)$ at position s and L the $q \times q$-matrix with $L_{rs} = N^{-1}\delta_s^2||H_r P_s||^2$. We have the following result.

Lemma 4.2 *We have*

$$\zeta(t) \leq (\rho^2 I + L)^t \zeta(0)$$

where the inequality is meant componentwise and where $\rho = \rho(P)$ is the essential spectral radius of P as defined in Section 3.5.

Proof. Since P is a Cayley matrix, it can be written as in (4.22). Then

$$\text{tr}(H_r P Q P^T H_r^T) = \frac{1}{N} \sum_{\chi \neq \chi_0} |\theta(\chi)|^2 \text{tr}(H_r Q H_r^T \chi\chi^*)$$

$$\leq \frac{1}{N} \max\{|\theta(\chi)|^2 : \chi \neq \chi_0\} \sum_{\chi \neq \chi_0} \text{tr}(H_r Q H_r^T \chi\chi^*)$$

$$= \rho^2 \text{tr}\left(H_r Q H_r^T \frac{1}{N} \sum_{\chi} \chi\chi^*\right) = \rho^2 \text{tr}\left(H_r Q H_r^T\right) = \rho^2 w_r$$

Define now a sequence of q dimensional vectors $\bar{\zeta}(t)$ as follows. Let $\bar{\zeta}(0) = \zeta(0)$ and let

$$\bar{\zeta}^+ = (\rho^2 I + L)\bar{\zeta}$$

By induction it can be proved that $\zeta(t) \leq \bar{\zeta}(t)$ for all t and this proves the inequality. $\square$

Define the q-dimensional column vectors a, b defined by $a_s = N^{-1}\delta_s^2||YP_s||^2$ and $b_s = N^{-1}\delta_s^2|\lambda_s|^2$ respectively. We can state and prove a general convergence result.

Theorem 4.1 *Let $\rho = \rho(P)$ and let $\bar{\rho}^2$ be the induced 2-norm of the matrix $\rho^2 I + L$. Assume that $L \neq 0$ and that $\bar{\rho}^2 < 1$. Then, there exists a scalar random variable α^* such that*

$$\mathbb{E}||\alpha^*\chi_0 - x(t)||^2 \leq A\rho^{2t} + B\bar{\rho}^{2t} \qquad (4.24)$$

where

$$A = \mathbb{E}||Yx(0)||^2 - \frac{||a||}{\bar{\rho}^2 - \rho^2}(\mathbb{E}||Hx(0)||^2)^{1/2}$$

$$B = \left(\frac{||a||}{\bar{\rho}^2 - \rho^2} + \frac{||b||}{(1-\bar{\rho})^2}\right)(\mathbb{E}||Hx(0)||^2)^{1/2}$$

and where $Y = I - \frac{1}{N}\chi_0\chi_0^*$ and

$$H = \begin{bmatrix} H_1 \\ \vdots \\ H_q \end{bmatrix}$$

Proof. Notice that, as showed in the proof of Lemma 4.2, we have

$$\mathrm{tr}(YPQP^TY^T) \le \rho^2 w.$$

Define the sequence $\bar{w}(t)$ as follows. Let $\bar{w}(0) = w(0)$ and let

$$\bar{w}^+ = \rho^2 \bar{w} + ||a||\,||\bar{\zeta}||$$

By induction it can be proved that $w(t) \le \bar{w}(t)$ for all t. Notice moreover that

$$
\begin{aligned}
\bar{w}(t) &= \rho^{2t} w(0) + ||a|| \sum_{i=0}^{t-1} \rho^{2(t-1-i)} ||(\rho^2 I + L)^i \zeta(0)|| \le \\
&\le \rho^{2t} w(0) + ||a|| \sum_{i=0}^{t-1} \rho^{2(t-1-i)} \bar{\rho}^{2i} ||\zeta(0)|| = \\
&= \left(w(0) - \frac{||a||\,||\zeta(0)||}{\bar{\rho}^2 - \rho^2} \right) \rho^{2t} + \left(\frac{||a||\,||\zeta(0)||}{\bar{\rho}^2 - \rho^2} \right) \bar{\rho}^{2t}
\end{aligned}
$$

Since $L \ne 0$, we have that $\bar{\rho}^2 > \rho^2$.

Notice now that

$$\mathbb{E}[||x_B(t+1) - x_B(t)||^2] = \mathbb{E}[||x_B(t+1)||^2] + \mathbb{E}[||x_B(t)||^2] - 2\mathrm{tr}\,\mathbb{E}[x_B(t+1)x_B(t)^T].$$

On the other hand, since

$$x_B^+ = x_B + N^{-1} \sum_{s=1}^{q} \chi_0 \chi_0^* P_s E_s H_s x$$

we have that

$$\mathrm{tr}\,\mathbb{E}[x_B(t+1)x_B(t)^T] = \mathrm{tr}\,\mathbb{E}[x_B(t)x_B(t)^T] + N^{-1} \sum_{s=1}^{q} \mathrm{tr}\,[\chi_0 \chi_0^* P_s \mathbb{E}(E_s) H_s \mathbb{E}(x(t)x_B(t)^T)] = s(t).$$

Using Lemma 4.2 we can then estimate as follows

$$\mathbb{E}[||x_B(t+1) - x_B(t)||^2] = s(t+1) - s(t) = b^T \zeta(t) \le b^T (\rho^2 I + L)^t \zeta(0) \le \bar{\rho}^{2t} ||b||\,||\zeta(0)||. \tag{4.25}$$

This shows that $x_B(t)$ converges in mean square sense to a random variable $\alpha^* \chi_0$ and that

$$(\mathbb{E}||\alpha^* \chi_0 - x_B(t)||^2)^{1/2} \le \sum_{s=t}^{\infty} (\mathbb{E}||x_B(s+1) - x_B(s)||^2)^{1/2} \le \frac{||b||^{1/2}\,||\zeta(0)||^{1/2}}{1 - \bar{\rho}} \bar{\rho}^t. \tag{4.26}$$

The bound (4.24) now follows from

$$\mathbb{E}||\alpha^* \chi_0 - x(t)||^2 = \mathbb{E}||\alpha^* \chi_0 - x_B(t)||^2 + \mathbb{E}||y(t)||^2 \tag{4.27}$$

and from the fact that $w(0) = \mathbb{E}||Yx(t)||^2$ and $\zeta(0) = \mathbb{E}||Hx(t)||^2$.

$\square$

Notice that, since $\bar{\rho} > \rho$, then the rate of convergence is determined by the parameter $\bar{\rho}$, namely by the induced 2-norm of the matrix $\rho^2 I + L$. In the sequel we will apply previous results to analyze a particular but significant example.

We assume the same communication graph of Example 3.3, namely, the Cayley graph $\mathcal{G}(\mathbb{Z}_N, S)$, where $S = \{0, 1\}$. We assume that P_0 is the stochastic Cayley matrix generated by the distribution

$$\pi_{P_0}(0) = 1 - k, \quad \pi_{P_0}(1) = k.$$

where $k \in [0, 1]$. Assume moreover $q = 1$, namely that each agent transmits just one scalar signal. Precisely, define H_1 to be the Cayley matrix generated by the distribution

$$\pi_{H_1}(0) = 1, \quad \pi_{H_1}(1) = -1.$$

This means that each agent i transmits the difference between its own state x_i and the the state x_{i-1} which is known exactly by the agent i. It remains to choose the matrix P_1. Our objective is to choose P_1 in such a way that $P = P_0 + P_1 H_1 = N^{-1} \chi_0 \chi_0^*$. This can be done by letting

$$\pi_{P_1}(0) = \pi_{P_1}(N-1) = 0, \qquad \pi_{P_1}(g) = \frac{g+1-N}{N} \quad g = 1, \ldots, N-2$$

and $k = \frac{N-1}{N}$. Indeed, noticing that $\pi_{P_1 H_1}(g) = \pi_{P_1}(g) - \pi_{P_1}(g-1)$, this definitions yield $P_1 H_1$ with the following generator

$$\pi_{P_1 H_1}(0) = 0, \ \pi_{P_1 H_1}(1) = \frac{2-N}{N}, \ \pi_{P_1 H_1}(g) = \frac{1}{N} \ \forall g = 2, \ldots, N-1.$$

With such a choice we have that $PH_1 = PY = 0$. Notice moreover that $P_1 \chi_0 = \lambda_1 \chi_0$ implies that

$$\lambda_1 = \sum_{g=0}^{N-1} \pi_{P_1}(g) = \sum_{g=1}^{N-2} \frac{g+1-N}{N} = \sum_{g=1}^{N-2} -\frac{g}{N} = -\frac{(N-1)(N-2)}{2N}$$

and so

$$b = \frac{1}{N} \delta_1^2 |\lambda_1|^2 = \delta_1^2 \frac{(N-1)^2 (N-2)^2}{4N^3}.$$

Moreover we have that

$$\|H_1 P_1\|^2 = N \sum_{g=0}^{N-1} |\pi_{P_1 H_1}(g)|^2 = \frac{(2-N)^2}{N} + (N-2)\frac{1}{N} = \frac{(N-1)(N-2)}{N}$$

which implies that

$$L = \frac{1}{N} \delta_1^2 \|H_1 P_1\|^2 = \delta_1^2 \frac{(N-1)(N-2)}{N^2}.$$

Finally notice that $YP_1 = (I - P)P_1 = P_1 - \lambda_1 P$ and so

$$||YP_1||^2 = N \sum_{g=0}^{N-1} |\pi_{P_1}(g) - \lambda_1 \pi_P(g)|^2 = 2N \frac{(N-1)^2(N-2)^2}{4N^4} +$$

$$N \sum_{g=1}^{N-2} \left| -\frac{g}{N} + \frac{(N-1)(N-2)}{2N^2} \right|^2 = \frac{(N-1)^2(N-2)^2}{4N^2} +$$

$$\frac{1}{N} \sum_{g=1}^{N-2} \frac{N^2 g^2 - (N-1)(N-2)}{N^2} \sum_{g=1}^{N-2} g = \frac{(N-1)(N-2)(5N^2-3N-6)}{12N^2}$$

which implies that

$$a = N^{-1} \delta_1^2 ||YP_1||^2 = \delta_1^2 \frac{(N-1)(N-2)(5N^2-3N-6)}{12N^3} .$$

For big N we have that $L \simeq \delta_1^2$, $a \simeq \delta_1^2 \frac{5N}{12}$ and $b \simeq \delta_1^2 \frac{N}{4}$. In this case, since we have that $\rho(P) = 0$, applying Theorem 4.1, we obtain that

$$\mathbb{E}||\alpha^* \chi_0 - x(t)||^2 \leq B \delta_1^{2t}$$

where

$$B \quad = \quad \left(\frac{5}{12} + \frac{\delta_1^2}{4(1-\delta_1)^2} \right) N (\mathbb{E}||Hx(0)||^2)^{1/2}$$

Let $\delta_1 = 1/2$, then we have that the strategy proposed in this case allows a convergence rate $\rho \simeq 1/2$. We need in total N uniform quantizers and $N(N-2)$ logarithmic quantizers. Thus, the total number of symbols L_{tot} that needs to be transmitted during each sampling period is

$$L_{u,\ell}^{\text{Cayley}} = NC + \frac{2}{\log 3} N(N-2) \log C.$$

Without the logarithmic quantizers we need only $L_u^{\text{Cayley}} = NC$ symbols, but we obtain a convergence rate $\rho \simeq 1 - \frac{2\pi^2}{N^2}$ (from Theorem 3.1). Observe that for large C the total number of symbols in the two cases are slightly different, but we obtain a manifest improvement in terms of rate of convergence.

If we assume that $N = 2^\nu$ and we take as an alternative method the one proposed in Proposition 3.3, thus without quantization, it can be shown that in this way we obtain a convergence rate

$$\rho \simeq 1 - \frac{\pi^2}{2 \log N} ,$$

with the total number of symbols $L_\ell^{\text{Cayley}} = CN \log N$. Also in this case it is clear that in some situations the technique based on the use of logarithmic quantizers proposed above presents much better convergence performance through the use of a comparable total number of symbols.
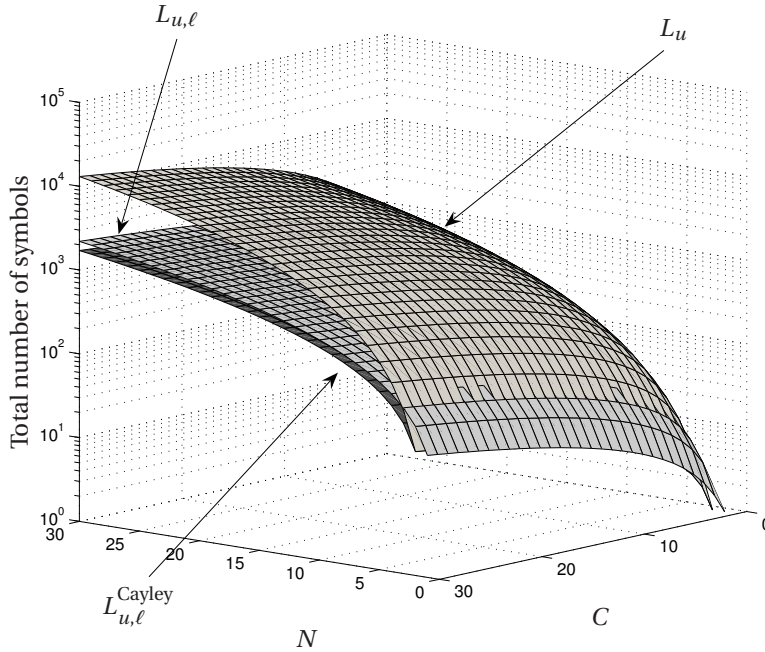
Figure 4.7: Total number of communicated symbols for the proposed control strategies for various choices of N and C. Plots show that the strategy with only uniform quantizers requires a large amount of symbols compared to the strategies with logarithmic quantizers particularly when N and C are large. The two strategies with logarithmic quantizers are comparable.

4.7   Comparisons and numerical results

4.7.1   Total number of symbols

An interesting comparison between the different strategies we have considered is on the total number of symbols that each strategy requires. The total number of symbols is related to the total amount of data circulating in the network at each time instance. In Figure 4.7 are shown three plots shown how the number of symbols changes as function of the number of vehicles N and the contraction rate C. The plots refer to the three strategies: uniform L_u, uniform-logarithmic $L_{u,\ell}$ and Cayley uniform-logarithmic $L_{u,\ell}^{\text{Cayley}}$. As it can be seen comparing the three plots, when the number of vehicle and the contraction rate increase the total number of symbols needed is much lower when logarithmic quantizers are used.
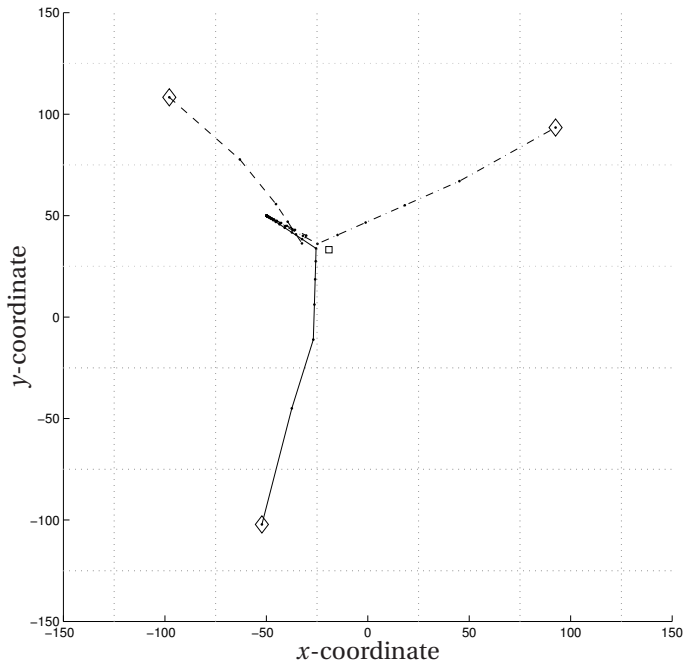
4.7.2 Simulations

Computer simulations were performed to illustrate the behavior of the proposed strategies. Figure 4.8 shows the trajectories of three vehicles moving on a plane. The vehicles are modelled as point masses and with independent controllers for the x and y coordinates. In particular in Figure 4.8(a) is shown the strategy where only uniformly quantized data is used. The grid in the picture divides the plane in cells corresponding to quantization regions of the quantizer. Notice, as expected, the vehicles converges to the center of one of the cells. The square indicates the consensus point that would be reached if no quantization data is used.

In Figure 4.8(b) are shown three vehicles that exchange data both uniformly and logarithmically according to the Topology 1 shown in Figure 4.6. Also in this case consensus is achieved.

In Figure 4.9 it is shown the stable limit cycle for two vehicles when only uniform quantized data is used. In particular Figure 4.9(b) are shown the x-coordinate for the two vehicles as function of time, showing clearly the limit cycle.

4.8 Summary

In this chapter we have considered the consensus problem under quantized communication data. In particular we have designed controller and communication strategies that solve the consensus problem when either uniform quantizers or a mixture of uniform and logarithmic quantizers are used. Results have been extended to the case of communication networks that can be modelled as Cayley graphs. Expressions of the total number of symbols needed to achieve consensus have also been derived. This allowed us to compare the different strategies.
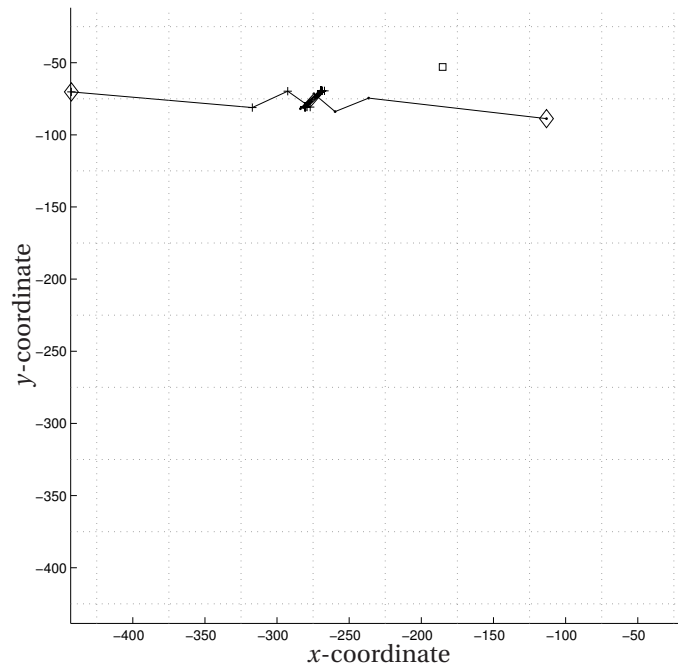
(a) Trajectories of three vehicles exchanging uniformly quantized data.
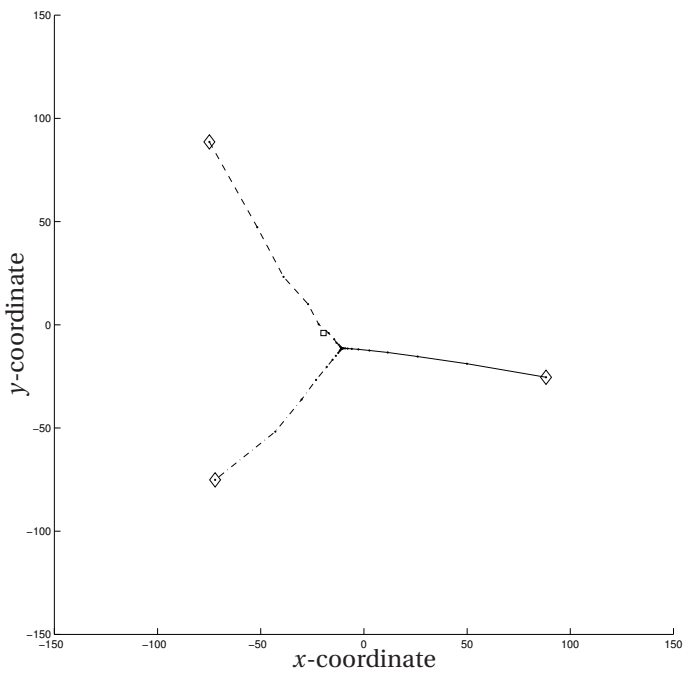
(b) Trajectories of three vehicles exchanging uniformly and logarithmically quantized data.

Figure 4.8: Simulations of three vehicles moving on plane.

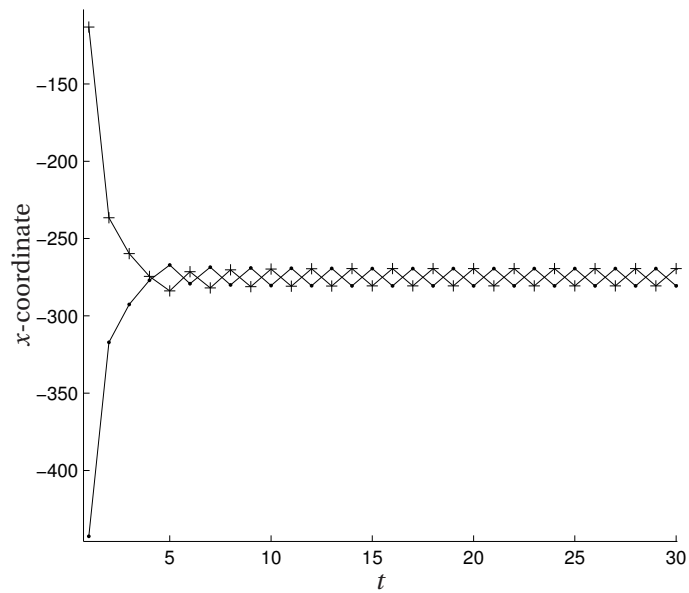(a) Trajectories of two vehicles exchanging uniformly quantized data

(b) Evolution of the x-coordinate for the two vehicles exchanging uniformly quantized data.

Figure 4.9: Simulations for two vehicles exchanging uniformly quantized data.

MODEL PREDICTIVE CONSENSUS

In this chapter we study the consensus problem, introduced in Chapter 4, in a different setting. In particular, we assume that the agents are described by general linear dynamics, possibly time-varying and different for each agent, that the inputs are constrained and that a linear combination of the states needs to converge to a common value, the consensus point, after a fixed time. Furthermore, we assume the consensus point is negotiated by the agents so that an overall cost function would be minimized. In order to accommodate all the constraints a distributed model predictive control (MPC) strategy is used to design the controller and to determine an optimal consensus point. In distributed MPC, a static finite-horizon optimization problem is decomposed into a set of subproblems, each solved by an individual agent. The coordination of the subproblems is, generally, achieved by an active communication, or sensing, among the agents [Componogara et al. 2002]. Distributed MPC for coordinating swarms of mobile agents was recently proposed in the literature. Distributed MPC strategies for steering agents to a stable formation are studied in [Dunbar and Murray 2004, 2005; Borrelli et al. 2005]. In [Dunbar and Murray 2004, 2005] the authors propose a scheme where the equilibrium is given a priori, while in [Borrelli et al. 2005] each agents need to know the models and constraints of the other teammates, in order to solve a local optimal control problem. In this chapter we consider a less restrictive setup.

The main contribution of this chapter is to propose a decentralized control strategy that yields consensus in fixed time. In this solution, agents can be described by arbitrary linear difference equations and their input subject to convex constraints. The proposed algorithms require the communication of possible consensus point among the agents in order to determine an optimal point. Contrary to related work, the agents do not

need any model of the dynamics of their teammates, nor exchange complete planned trajectories. We explore various communication, computation, and control structures, and demonstrate the performance of the algorithms by numerical examples.

5.1   Outline

The chapter is organized as follows. In Section 5.2 we formally define the subsystem models and the distributed model predictive control problem. In Section 5.3 it is shown how primal decomposition techniques and incremental subgradient methods allow us to find a distributed solution to this consensus problem, in which each agent performs individual planning of its trajectory and exchanges critical information with neighbors only. We explore different computation and control structures needed in order to cope with disturbances and changes in the system configuration, in Section 5.4. The performance of these different structures are demonstrated by numerical examples in Section 5.5.

5.2   Problem formulation

Consider $N > 1$ agents whose dynamics are described by the following discrete time state equations

$$x_i(t+1) = A_i x_i(t) + B_i u_i(t)$$
$$y_i(t) = C_i x_i(t), \qquad\qquad i = 1,\dots,N,$$

where $A_i \in \mathbb{R}^{n_i \times n_i}$, $B_i \in \mathbb{R}^{n_i \times p_i}$ and $C_i \in \mathbb{R}^{s_i \times n_i}$. We assume that the inputs are constrained according to

$$u_i(t) \in \mathcal{U}_i := \{v : \underline{u}_i \leqslant v \leqslant \overline{u}_i\}, \tag{5.1}$$

where $\underline{u}_i, \overline{u}_i \in \mathbb{R}^{p_i}$ and the inequalities are element-wise.

Let $\tau > 0$ be a finite and fixed time. We want to find a sequence of inputs $u_i(0),\dots,u_i(\tau-1)$, with $i = 1,\dots,N$ and $u_i(t) \in \mathcal{U}_i$ for all $t = 0,\dots,\tau-1$, such that

$$y_i(\tau) = \theta, \tag{5.2}$$

where $\theta \in \Theta$ is the consensus point and Θ is a given convex and compact set. Namely we are seeking a control sequence so that in fixed time we reach a consensus, meaning that all the outputs are equal at time τ.

In order for (5.2) to hold, the outputs need to have the same dimensions, i.e., we require that $s_i = s_j$ for all i, j. We assume that the following cost function is associated to the i-th system,

$$V_i(y_i(t), u_i(t), \theta) = \big(y_i(t) - \theta\big)^T Q_i \big(y_i(t) - \theta\big) + u_i(t)^T R_i u_i(t) \tag{5.3}$$

where $Q_i \in \mathbb{R}^{s \times s}$ and $R_i \in \mathbb{R}^{p_i \times p_i}$ are positive definite symmetric matrices (i.e., we penalize deviations from the consensus point and the use of control effort). Let us introduce the following vectors

$$\mathbf{x}_i = \begin{pmatrix} x_i(1) \\ x_i(2) \\ \vdots \\ x_i(\tau) \end{pmatrix}, \quad \mathbf{u}_i = \begin{pmatrix} u_i(0) \\ u_i(1) \\ \vdots \\ u_i(\tau-1) \end{pmatrix},$$

and the matrices $\mathbf{Q}_i = I \otimes Q_i$, $\mathbf{R}_i = I \otimes R_i$, where I is the identity matrix and $\otimes$ is the Kronecker matrix product. We have that the following holds

$$\mathbf{x}_i = \underbrace{\begin{pmatrix} A_i \\ A_i^2 \\ \vdots \\ A_i^\tau \end{pmatrix}}_{\mathbf{E}_i} x_i^0 + \underbrace{\begin{pmatrix} B_i & 0 & 0 & \dots & 0 \\ A_i B_i & B_i & 0 & \dots & 0 \\ \vdots & & \ddots & & \vdots \\ A_i^{\tau-1} B_i & A_i^{\tau-2} & A_i^{\tau-3} B_i & \vdots & B_i \end{pmatrix}}_{\mathbf{F}_i} \mathbf{u}_i.$$

We consider next the following optimization problem.

$$\begin{aligned}
\underset{\mathbf{u}_1,\dots,\mathbf{u_N},\theta}{\text{minimize}} \quad & \sum_{i=1}^N \mathbf{V}_i(\mathbf{u}_i,\theta) \\
\text{s.t.} \quad & \mathbf{H}_i(\mathbf{E}_i x_i^0 + \mathbf{F}_i \mathbf{u}_i) = \theta \\
& \theta \in \Theta \\
& \mathbf{u}_i \in \prod_{i=1}^\tau \mathcal{U}_i,
\end{aligned} \tag{5.4}$$

where cost function is

$$\mathbf{V}_i(\mathbf{u}_i,\theta) = \sum_{t=1}^\tau V_i(y_i(t), u_i(t), \theta) = (\mathbf{H}_i(\mathbf{E}_i x_i^0 + \mathbf{F}_i \mathbf{u}_i) - \mathbb{1} \otimes \theta)^T \mathbf{Q}_i (\mathbf{H}_i(\mathbf{E}_i x_i^0 + \mathbf{F}_i \mathbf{u}_i)$$
$$- \mathbb{1}_\tau \otimes \theta) + \mathbf{u}_i^T \mathbf{R}_i \mathbf{u}_i$$

with $\mathbb{1}$ the vector $(1,1,\dots,1)^T$, and where the second constraint in the optimization problem corresponds to the consensus condition $y_i(\tau) = \theta$, which has been rewritten as

$$y_i(\tau) = C_i x_i(\tau) = \underbrace{\begin{pmatrix} 0 & \dots & 0 & C_i \end{pmatrix}}_{\mathbf{H}_i} \mathbf{x}_i = \mathbf{H}_i(\mathbf{E}_i x_i^0 + \mathbf{F}_i \mathbf{u}_i) = \theta.$$

In order to make the problem well posed the following assumptions need to be satisfied. First, the dynamical systems are assumed to be controllable and observable. Second, the meeting time τ is large enough so that all θ in the set Θ is feasible, i.e., all θ in the set Θ are possible consensus points. Third, for all $\theta \in \Theta$ and $i = 1,\dots,N$, there exists $\mathbf{u}_i$ in the relative interior of $\prod_{i=1}^\tau \mathcal{U}_i$ such that $y_i(\tau) = \theta$. This condition means that it should be possible to reach θ without saturating the control signal.

5.3   Distributed negotiation

In this section we show how the optimal consensus point, θ, can be computed in a distributed way. This is particularly important in multi-agent applications since generally an agent do not have all the information available. More precisely, we assume that the agents can exchange data over a communication network modelled by a directed graph $\mathscr{G} = (V, \mathscr{E})$, which we will call the communication graph. The set V is the vertex set and $\mathscr{E}$ is the arc set. We associate to each agent a vertex of the graph and we have that an arc $(i, j) \in \mathscr{E}$ if and only if agent i can transmit data to agent j.

In order to transform the optimization problem (5.4) in a distributed way we use primal decomposition in combination with incremental subgradient methods (*e.g.*, [Bertsekas et al. 2003]). One important feature of this type of problems is that they can be solved in a decentralized way by an iterative algorithm. The main limitation is that the convergence to the optimum is guaranteed only for particular classes of communication graphs $\mathscr{G}$, which we will describe in detail in the next section.

Since $\mathbf{H}_i(\mathbf{E}_i x_i^0 + \mathbf{F}_i \mathbf{u}_i) = \theta$, we can eliminate the dependence from θ in $\mathbf{V}_i(\mathbf{u}_i, \theta)$. Thus we have

$$\mathbf{V}_i(\mathbf{u}_i) = \left(\mathbf{H}_i(\mathbf{E}_i x_i^0 + \mathbf{F}_i \mathbf{u}_i) - \mathbb{1} \otimes (\mathbf{H}_i(\mathbf{E}_i x_i^0 + \mathbf{F}_i \mathbf{u}_i))\right)^T \mathbf{Q}_i \left(\mathbf{H}_i(\mathbf{E}_i x_i^0 + \mathbf{F}_i \mathbf{u}_i)\right.$$
$$\left. - \mathbb{1} \otimes (\mathbf{H}_i(\mathbf{E}_i x_i^0 + \mathbf{F}_i \mathbf{u}_i))\right) + \mathbf{u}_i^T \mathbf{R}_i \mathbf{u}_i \,.$$

We can then define $q_i(\theta)$ as follows

$$q_i(\theta) = \operatorname*{minimum}_{\mathbf{u}_1, \dots, \mathbf{u}_N} \quad \mathbf{V}_i(\mathbf{u}_i) \tag{5.5}$$
$$\text{s.t.} \quad \mathbf{H}_i(\mathbf{E}_i x_i^0 + \mathbf{F}_i \mathbf{u}_i) = \theta$$
$$\mathbf{u}_i \in \mathscr{U}_i^\tau \,.$$

Then the optimization problem (5.4) can be written as

$$\operatorname*{minimize}_\theta \quad \sum_{i=1}^N q_i(\theta) \tag{5.6}$$
$$\text{s.t.} \quad \theta \in \Theta \,.$$

since the only coupling between the agents is θ. We will later use subgradients to find the consensus point and therefore we give the following definition.

Definition 5.1 *([Bertsekas et al. 2003]) Let $f : \mathbb{R}^n \to \mathbb{R}$ be a convex function. We say that a vector $\lambda \in \mathbb{R}^n$ is a subgradient of f at point $x \in \mathbb{R}^n$ if*

$$f(z) \geqslant f(x) + \lambda^T(z - x)$$

for all $z \in \mathbb{R}^n$.

Proposition 5.1 *The cost function $q_i(\theta)$ defined in (5.5) is a convex function and a subgradient λ_i is given by the Lagrange multipliers corresponding to the constraint $\mathbf{H}_i(\mathbf{E}_i x_i^0 + \mathbf{F}_i \mathbf{u}_i) = \theta$.*

Proof. We start by showing that a subgradient is given by the Lagrange multipliers corresponding to the constraint $\mathbf{H}_i(\mathbf{E}_i x_i^0 + \mathbf{F}_i \mathbf{u}_i) = \theta$. By Lagrangian relaxation we can define

$$L(\mathbf{u}_i, \theta, \lambda_i) = \mathbf{V}_i(\mathbf{u}_i) - \lambda_i^T(\mathbf{H}_i(\mathbf{E}_i x_i^0 + \mathbf{F}_i \mathbf{u}_i) - \theta),$$

where λ_i are Lagrange multipliers. We also introduce the dual function

$$d(\lambda_i, \theta) = \min_{\mathbf{u}_i \in \mathcal{U}_i^\tau} \mathbf{V}_i(\mathbf{u}_i) - \lambda_i^T(\mathbf{H}_i(\mathbf{E}_i x_i^0 + \mathbf{F}_i \mathbf{u}_i) - \theta).$$

Since the constraint $\mathbf{H}_i(\mathbf{E}_i x_i^0 + \mathbf{F}_i \mathbf{u}_i) = \theta$ is linear in $\mathbf{u}_i$ and there exist a solution to this equation (by assumption) within the relative interior of $\mathcal{U}_i^\tau$ and the function $\mathbf{V}_i$ is convex and the set $\mathcal{U}_i^\tau$ is convex, strong duality follows from Theorem 6.4.4 (p. 373) in [Bertsekas et al. 2003]. Now $q_i(\theta)$ can be expressed as

$$q_i(\theta) = \max_{\lambda_i} d(\lambda_i, \theta).$$

Consider two feasible points, $\theta^\dagger$ and $\theta^\ddagger$, and let $\lambda_i^\dagger$ be the Lagrange multipliers corresponding to the relaxed constraint for $\theta^\dagger$, then

$$q_i(\theta^\ddagger) = \max_{\lambda_i} \left\{ \min_{\mathbf{u}_i \in \mathcal{U}_i} \left\{ \mathbf{V}_i(\mathbf{u}_i) - \lambda_i^T(\mathbf{H}_i(\mathbf{E}_i x_i^0 + \mathbf{F}_i \mathbf{u}_i) - \theta^\ddagger) \right\} \right\} \geq$$

$$\geq \min_{\mathbf{u}_i \in \mathcal{U}_i^\tau} \left\{ \mathbf{V}_i(\mathbf{u}_i) - (\lambda_i^\dagger)^T(\mathbf{H}_i(\mathbf{E}_i x_i^0 + \mathbf{F}_i \mathbf{u}_i) - \theta^\ddagger) \right\} =$$

$$= \min_{\mathbf{u}_i \in \mathcal{U}_i^\tau} \left\{ \mathbf{V}_i(\mathbf{u}_i) - (\lambda_i^\dagger)^T(\mathbf{H}_i(\mathbf{E}_i x_i^0 + \mathbf{F}_i \mathbf{u}_i) - \theta^\dagger) \right\}$$

$$+ (\lambda_i^\dagger)^T(\theta^\ddagger - \theta^\dagger) = q(\theta^\dagger) + (\lambda_i^\dagger)^T(\theta^\ddagger - \theta^\dagger)$$

Hence, by the definition of a subgradient, $\lambda_i^\dagger$ is a subgradient of $q_i(.)$ at $\theta^\dagger$. Now $q_i(\theta^\ddagger)$ can be expressed as

$$q_i(\theta^\ddagger) = \max_{\lambda_i} \left\{ \min_{\mathbf{u}_i \in \mathcal{U}_i^\tau} \left\{ \mathbf{V}_i(\mathbf{u}_i) - \lambda_i^T \mathbf{H}_i(\mathbf{E}_i x_i^0 + \mathbf{F}_i \mathbf{u}_i) \right\} + \lambda_i^T \theta^\ddagger \right\} =$$

$$= \max_{\lambda_i} \left\{ g(\lambda_i) + \lambda_i \theta^\ddagger \right\}$$

where $g(\lambda_i)$ is some function and $g(\lambda_i) + \lambda_i \theta^\ddagger$ is convex in $\theta^\ddagger$. Since $q_i(\theta^\ddagger)$ is the pointwise maximum of a family of convex functions, $q_i(\theta^\ddagger)$ is convex. □

To find the consensus point θ, we next use incremental and randomized subgradient methods.

5.3.1 Incremental subgradient algorithms

We present in the following two algorithms that compute the optimal consensus point, θ, for two classes of communication graphs. These algorithms are based on the incremental subgradient methods from optimization theory [Bertsekas et al. 2003]. The main
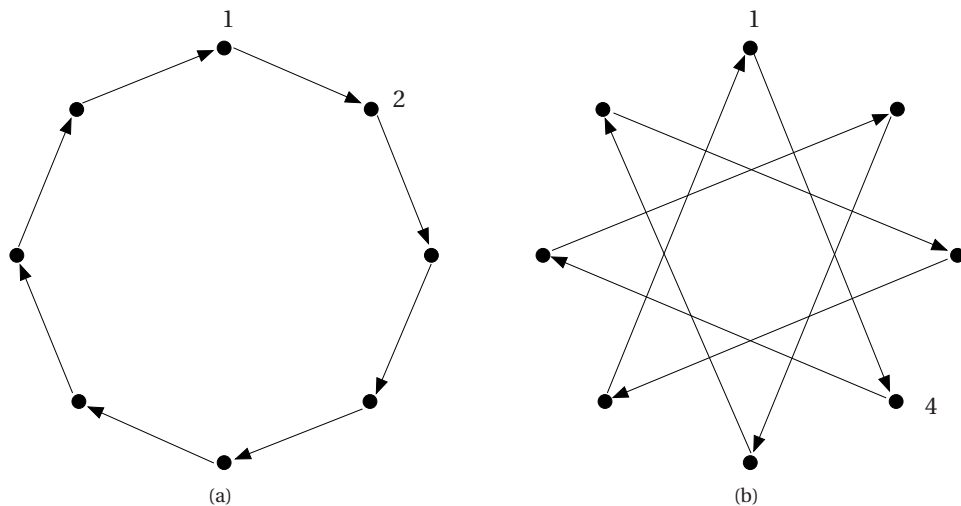
(a)   (b)

Figure 5.1: Two examples of communication graphs over which is possible the solve
the optimization problem with an incremental algorithm. On the right a Cayley graph
defined on $\mathbb{Z}_8$ with $S = \{1\}$. On the left a Cayley graph defined on the same group with
$S = \{3\}$.

drawback of such algorithms is that the convergence is guaranteed only asymptotically
with respect to the number of iterations. Let for the rest of the section assume that in
the time horizon τ we do not include the iterations need to the subgradient algorithm
to converge. We will propose, in the next session, some way of circumventing this prob-
lem.

Subgradient methods work in a way that is similar to gradient methods, i.e., the up-
date is made in the opposite direction of the subgradient. The update equation is

$$\theta_{k+1} = \mathscr{P}_\Theta\{\theta_k - \alpha_k \lambda_k\} \tag{5.7}$$

where $\mathscr{P}_\Theta\{\cdot\}$ denotes the Euclidean projection on the set Θ and α_k is the step-size. The
subgradient λ_k is, in the standard approach, computed for the total cost $\sum_i q_i(\theta)$, and
thus independent of i. In this chapter we describe two algorithms where the generic
agent i computes the subgradient $\lambda_{i,k}$ corresponding to the function q_i based on the
information received by the neighbor agents.

In the first algorithm we assume that the communication graph is a Cayley graph,
see Chapter 3 for the definition, defined on an additive Abelian group G of order $|G| = N$.
We consider $S \subset G$ such that $|S| = 1$ and with $\langle S \cup \{0\} \rangle = G$, that is S generates the group G
(see Chapter 2). Two examples of such communication graphs are shown in Figure 5.1.
Let us consider the example shown in Figure 5.1(a). Starting with an arbitrary initial
condition $\theta_0 \in \Theta$, the first agent computes the subgradient $\lambda_{1,0}$ corresponding to $q_1(\theta_0)$.

Algorithm 1: Cyclic Incremental Algorithm

1. Initialize θ_0 and α_0
2. $k := 0$
3. $s :=$ element of the set S
4. **loop**
5.   **for** $j := 1$ to N **do**
6. $i := (j \cdot s) \bmod N$
7.   Compute a subgradient, $\lambda_{i,k}$, corresponding to $q_i(\theta_k)$
8. $\theta_{k+1} := \mathscr{P}_\Theta \{\theta_k - \alpha_k \lambda_{i,k}\}$
9. $k := k + 1$
10. $\alpha_k := \alpha_0 / k$
11.   **end for**
12. **end loop**

Algorithm 2: Randomized Algorithm

1. Initialize θ_0 and α_0
2. $k := 0$
3. **loop**
4.   Choose $i \in \{1, ..., N\}$ accordingly to uniform probability mass function
5.   Compute a subgradient, $\lambda_{i,k}$, corresponding to $q_i(\theta_k)$
6. $\theta_{k+1} := \mathscr{P}_\Theta \{\theta_k - \alpha_k \lambda_{i,k}\}$
7. $\alpha_k := \alpha_0 / k$
8. $k := k + 1$
9. **end loop**

Using (5.7) an update of the consensus point θ_1 is computed and communicated to the next agent. This agent then computes in the same way the update of the consensus point, θ_2. The algorithm then proceeds iteratively. A pseudocode version of the algorithm is summarized in Algorithm 1.

In the second algorithm, at each time step k the agent that has performed the last update of the consensus point, accordingly to (5.7), randomly selects another agent, among all the available agents, and sends the update to the selected agent. The advantage of the method is that there is no need for a particular communication structure, the communication graph is random, however at each time step every agent must be able to communicate with any other agent. The algorithm is summarized in Algorithm 2.

We then have the following proposition.

Proposition 5.2 *Algorithms 1 and 2 converge in the sense that* $\lim_{k \to \infty} \theta_k = \theta^*$, *where* θ^* *is the solution to the optimization problem* (5.6).

The proof follows from Theorem 8.2.6 (p. 480) and Theorem 8.2.13 (p. 496) in [Bertsekas et al. 2003], since the set Θ is convex and compact (so the norms of all possible subgra-

dients have an upper bound), and the step-size a_k is square summable over k but not summable over k.

5.4   Implementation

In this section we present two new classes of control algorithms that address some implementation issues in the consensus problem. Figure 5.2 shows the logical flow of the incremental subgradient algorithms presented together with show the two new classes, cf., [Skogestad and Postlethwaite 2005, p. 386].

More specifically, the logical flow of the scheme presented in the previous section is summarized in Figure 5.2(a). In the negotiation phase, the optimal consensus point is computed in a distributed way using Algorithm 1 or Algorithm 2. After the distributed negotiation, which in general requires al long time before the consensus point is computed is closed to the optimum, the corresponding control action is applied to the agent in open loop during the execution phase. If there are no disturbances the system will reach the consensus point at time τ. The main advantage of the scheme proposed is that it is possible to formally guarantee that the optimal consensus point is computed in a distributed way. Moreover only a small amount of information, the current consensus point, needs to be exchange at each step. However, such strategy, being completely open loop, is very sensitive to disturbances.

In Figure 5.2(b), a second control strategy is proposed. In this case, as the previous strategy, the negotiation phase yields a consensus point that is optimal in the absence of disturbances. The controller that drives the agents towards the consensus during the execution phase uses the negotiated consensus point as fixed reference. Each agent can then use a receding horizon (MPC) control strategy for reaching the consensus point: in each step we recompute the optimal control sequence for reaching the consensus point at time τ, apply the first component, sense the current state and recompute the control sequence.

The third control strategy is shown in Figure 5.2(c). The negotiation phase, in this case, is carried out at each time step and we assume that the negotiation is stopped after that all the agents have communicated only $\beta \in Z$ times, namely we assume that the negotiation is interrupted at $k = \beta N$. In this case we then have N different reference signals, one for each agent. Similarly to above, in the execution the optimal control sequence for reaching the consensus point is computed and the first component is applied. The negotiation phase is then repeated.

Similarly to classical MPC, the control strategies in Figure 5.2(b) and Figure 5.2(c) can cope with disturbances due to the receding horizon operation. The main advantage of the strategy in Figure 5.2(c) is that the negotiation is not carried out to the optimum and thus we do not need to wait for the incremental subgradient algorithms to converge. This solution can also cope with changes in the agent dynamics and/or input constraints. Indeed the agent affected can include these changes locally in its optimization algorithm. As we will see later, the strategy can also handle the situation when the
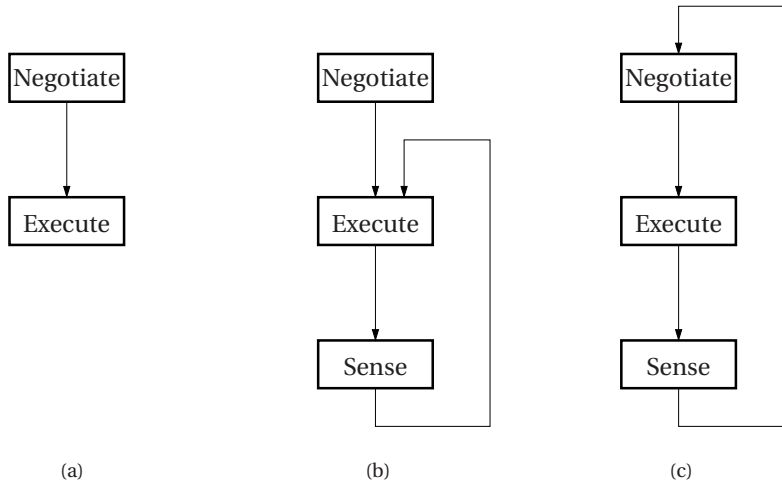
Figure 5.2: The logical flow of the different control strategies. (a) open loop strategy: θ is negotiated once at the beginning, then the corresponding control action is applied. (b) set-point strategy: θ is negotiated once at the beginning and the corresponding control action is then computed at every time step and applied to the system. (c) renegotiation strategy: θ is renegotiated at every time step. The corresponding control action is then computed and applied to the system.

number of agents in the consensus problem increases or decreases. In this case the new agent can be included in the negotiation and the consensus point can be recomputed.

Compared to the open-loop solution of Figure 5.2(a), the control strategies of Figure 5.2(b) and Figure 5.2(c) are much harder to analyze formally. Still, since they are relevant from a practical perspective, we will demonstrate the potential of such strategies via simulations.

5.5   Numerical examples

In this section we explore the performance of the three control strategies through numerical examples. The setup is that a number of agents with double integrator dynamics and input constraints should reach the same coordinates at time τ.

5.5.1   Disturbance free scenario

The first case is the ideal case, where we assume that there is no noise, the number of agents is constant, and the dynamics of the agents do not change. There is no need for feedback and the optimal consensus point is negotiated in the beginning, and then the corresponding control actions are applied to the systems in open-loop. In this specific

(a) The agents meet at θ at time τ.

(b) The agents meet at a formation, parameterized as the consensus point θ + individual offsets, at time τ.
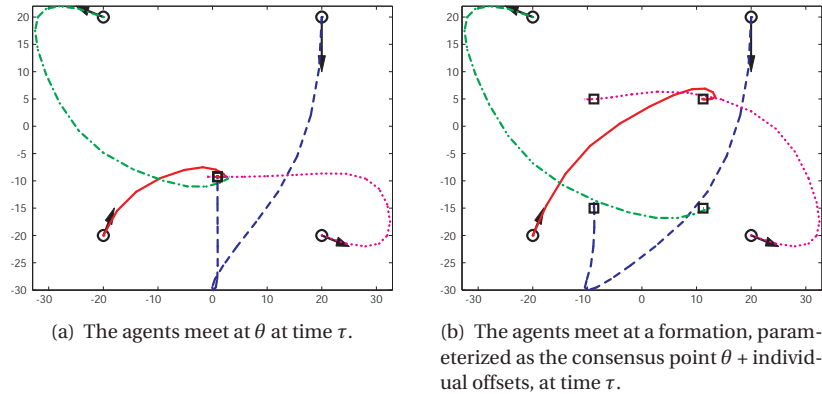
Figure 5.3: The trajectories of four agents with double integrator dynamics. The circles are the starting points and the squares are the ending points. The arrows show the initial velocities.

example there are four agents with double integrator dynamics, identical control signal constraints, but different initial positions and velocities. The agents should meet after 20 time samples. The trajectories are shown in Figure 5.3(a). As we expect the agents meet after 20 samples. With the same setup we also introduce the extension that the agents can meet in a formation. This is done by adding an individual bias to the consensus point. The configuration is identical with the ideal case except that the system now should meet in a square formation. As can be seen in Figure 5.3(b), the agents meet in a square formation after 20 samples.

5.5.2   Noisy scenario

In the second case, we add Gaussian noise with standard deviation 0.5. Two variants are compared: the open-loop variant (Figure 5.2(a)) and the setpoint variant (Figure 5.2(b)). In the setpoint variant, the consensus is negotiated before the agents start moving, and then the consensus is used as a setpoint. The control signals are recalculated at every time step, yielding a closed loop control. The trajectories of the open loop variant are shown in Figure 5.4(a), and as expected the agents do not reach consensus. Figure 5.4(b) demonstrates the results for the setpoint variant: the agents are very close to achieving consensus in 20 samples despite the persistent disturbances.

5.5.3   Scalability scenario

The third case starts with three agents and adds a fourth agent after 10 samples. The total time of the simulation is 30 samples. Also in this scenario, two variants are compared: the setpoint variant discussed above and the renegotiation variant (Figure 5.2(c)). In the setpoint variant the consensus point is negotiated between the three agents in the be-

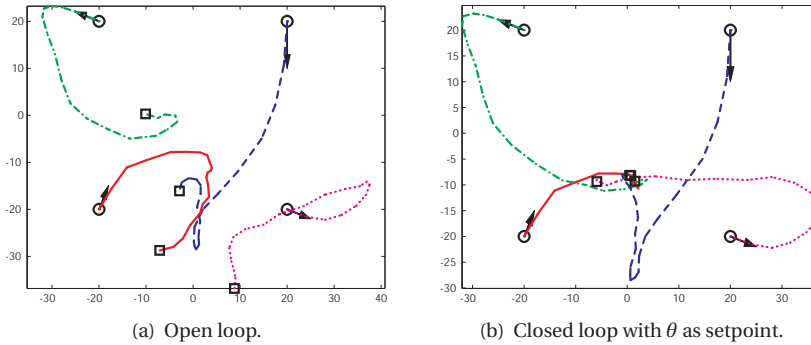(a) Open loop.   (b) Closed loop with θ as setpoint.

Figure 5.4: The trajectories of four agents with double integrator dynamics and noise added to the states at each sample. The circles are the starting points and the squares are the ending points. The arrows show the initial velocities.

ginning. When the fourth agent is added, it is given θ as a setpoint. Figure 5.5(a) shows the trajectories of the setpoint variant. The agents reach consensus as expected but the initial condition of the fourth system does not influence the consensus point at all, irrespectively of how hard it is to control and how expensive its control efforts are. In the renegotiation algorithm, the cyclic algorithm is executed with 10 iterations at each step. The trajectories are shown in Figure 5.5(b), and as can be seen the final consensus is closer to the added agent in this case compared with the previous algorithm. Another advantage is that the agents can start moving before the consensus point is completely agreed upon. However, this is also a drawback since if the current θ is far from optimal, then the agents can start moving in the wrong direction. The behavior depends on the setup, e.g., the dynamics and initial conditions, and warrants further theoretical investigations.

5.6 Summary

We have formulated a consensus problem where the output of a number of different agents should coincide after a specified time. The dynamics of the agents can be arbitrary, as long as they are linear, and input constraints can be accommodated for. We have shown that it is possible to find the consensus point in a distributed way where the only information needed to be communicated is the current consensus point suggestion. Moreover, we have proposed three different control schemes suited for more realistic scenarios and we have explored the performance by numerical simulation. The control schemes are very flexible and can handle several difficulties in multi-agent coordination. The drawback is that the general behavior is difficult to analyze for the more complex control schemes.

(a) Closed loop with θ negotiated once,   (b) θ is renegotiated at every time step.
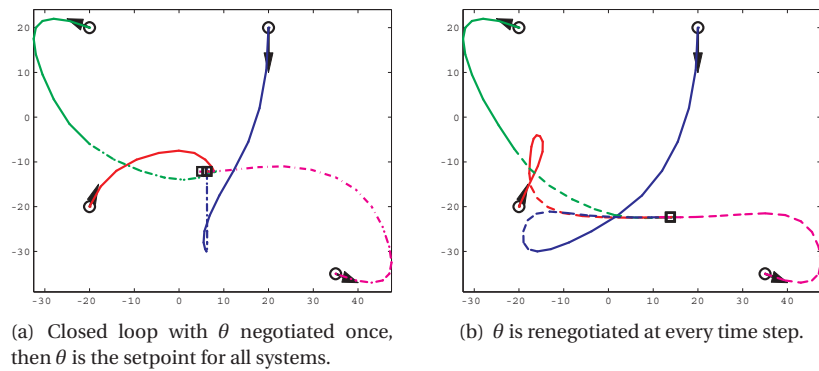then θ is the setpoint for all systems.

Figure 5.5: The trajectories of four agents with double integrator dynamics. The system starts with three agents and after 10 samples a fourth agent is added to the system. The circles are the starting points and the squares are the ending points. The solid lines denote the trajectories before the fourth system is added, and the dashed lines denote the trajectories after that the fourth system has been added. Finally, the arrows show the initial velocities.

6

COLLABORATIVE ESTIMATION

An interesting application area where a system comprised of a lager number of independent agents have a tremendous potential, is that of collaborative estimation and tracking. Indeed, noisy data, coming from different agents, can be fused to obtain a more accurate information about a dynamical process. Typical scenarios include tracking of moving objects [Zhao et al. 2003; Mazo et al. 2004], monitoring of the temperature or salinity of large geographical areas such as forests and lakes [Szewczyk et al. 2004; Borges de Sousa et al. 2005], and synchronization of the agents clocks [Giridhar and Kumar 2006].

In this chapter we assume that the agents are stationary nodes equipped with sensors and a wireless communication device that allows internode data exchange. We also assume that the nodes measure the same dynamic process. An example is shown in Figure 6.1, where a wireless sensor network (WSN) is deployed in order to estimate the position of a moving vehicle. Under the assumption that the dynamic process is not too fast, or that the sampling frequency of the nodes is fast enough, we propose an algorithm where neighbor nodes combine estimates and measurements so that the overall estimation error variance is minimized. In particular each node linearly weights the data coming from neighbors to obtain a more accurate estimate of the time-varying signal measured, where the weights are optimally chosen online. A similar approach, where the weights are fixed and based on the Laplacian matrix of the graph modelling the communication network, was proposed by [Olfati-Saber and Shamma 2005]. Related work to the present chapter is the solution discussed in [Xiao et al. 2005] and [Xiao et al. 2006]. The authors consider the problem of estimating a constant parameter from noisy data. The estimation is based on a distributed average consensus, which is shown
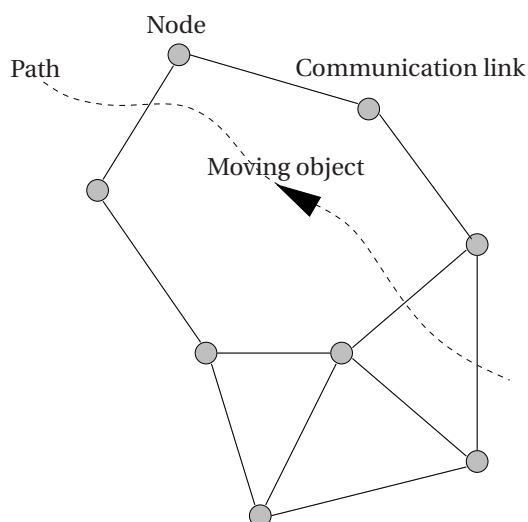
Figure 6.1: A possible scenario where collaborative estimation can be applied. A set of communicating nodes measure the position, with respect to a common coordinate frame, of a moving vehicle. The communication of measurements and estimates results in an accurate measure of the vehicle position.

to converge to the global maximum-likelihood estimate of the parameter.

6.1 Outline

The chapter is organized as follows. In Section 1 we formalize the problem. We also define a model of the communication network based on undirected graphs. A centralized solution based on the minimization of the overall estimate variance is discussed in Section 2. Since a centralized solution requires a large amount of data flowing from the nodes to a central station and back, we propose a decentralized solution in Section 3. The detailed algorithm, corresponding to the decentralized solution, and some implementation issues are discussed in Section 4. Numerical results, where the proposed algorithm is compared with other solutions, are reported in Section 5.

6.2 Problem formulation

Let us consider $N > 1$ nodes randomly distributed in the plane. We assume that each node can measure a common scalar signal $d(t)$ corrupted by additive noise:

$$u_i(t) = d(t) + v_i(t), \qquad i = 1, \dots, N,$$

where v_i is a zero-mean Gaussian random variable. This is a common assumption to characterize the noise fluctuations, e.g., [Gustafsson and Gunnarsson 2005; Olfati-Saber and Shamma 2005], and can be motivated by the central limit theorem. Defining the vectors $u(t) = (u_1(t),\dots,u_N(t))^T$ and $v(t) = (v_1(t),\dots,v_N(t))^T$, we can rewrite the previous equation as

$$u(t) = d(t)\mathbb{1} + v(t),$$

where $\mathbb{1} = (1,\dots,1)^T$. We assume that the covariance matrix of the random vector $v(t)$ is $\Sigma = \sigma^2 I$, so that v_i and v_j, for $i \neq j$, are uncorrelated.

Since the nodes are connected through a communication network, each node has available extra data, transmitted by the neighbors, in order to reconstruct the signal $d(t)$. We thus assume that a node i builds an estimate, $x_i(t)$, of the signal $d(t)$ as

$$x_i(nt + n) = \sum_{j=1}^{N} k_{ij}(nt)x_j(nt) + \sum_{j=1}^{N} h_{ij}(nt)u_j(nt), \tag{6.1}$$

where n represents the sampling period. Thus each node computes an estimates of the a linear combination of its estimates and measurements with the estimates and measurements received from neighbors nodes. If node i is not connected with node j at time t, then $k_{ij}(nt) = k_{ij}(nt) = 0$ and $h_{ij}(nt) = h_{ji}(nt) = 0$. This estimation model is similar, though more general, to the one proposed in [Olfati-Saber and Shamma 2005].

Remark 6.1
From the model (6.1) *that we propose, it is clear that one could try to design $k_{ii}(t)$ and $h_{ii}(t)$ so that a single node, without exchanging data with neighbors, is able to estimate $d(t)$. This would have the advantage of saving power for communication. However for a single node it would require a longer time before achieving a good estimate of $d(t)$. Moreover measurements taken too close in time, by the same node, are generally corrupted by correlated noise*

$$E\{v_i(t)v_i(t-\tau)\} = r(\tau),$$

where $r(\tau)$ is the autocorrelation function of the noise. Measurements taken by different nodes are instead corrupted by uncorrelated noise.

Let us assume, for simplicity that the sampling period is $n = 1$, we rewrite the estimator (6.1) in a more compact way as

$$x(t+1) = K(t)x(t) + H(t)u(t) \tag{6.2}$$

where $x(t) = (x_1(t),\dots,x_N(t))^T$, $[K(t)]_{ij} = k_{ij}(t)$ and $[H(t)]_{ij} = h_{ij}(t)$.

It is convenient to model the communication network as an undirected graph $\mathcal{G} = (\mathcal{V},\mathcal{E})$, where $\mathcal{V} = \{1,\dots,N\}$ is the vertex set and $\mathcal{E} \subseteq \mathcal{V} \times \mathcal{V}$ the edge set. Note that $(i, j) \in \mathcal{E}$ implies that $(j, i) \in \mathcal{E}$ since the graph is undirected. The graph $\mathcal{G}$ is said to be connected if there is a sequence of edges in $\mathcal{E}$ that can be traversed to go from any vertex to any

other vertex. We associate to each edge $(i, j) \in \mathscr{E}$ a time-varying weight $w_{ji}(t)$. In general, it may hold that the weights $w_{ij}(t)$ and $w_{ji}(t)$ are different. We introduce the adjacency matrix $W(t)$ as

$$[W(t)]_{ij} = \begin{cases} w_{ij}(t), & \text{if } (j, i) \in \mathscr{E} \\ 0, & \text{otherwise}. \end{cases}$$

We say that a matrix $W(t)$ is compatible with $\mathscr{G}$, if $W(t)$ defines an adjacency matrix for $\mathscr{G}$. We denote this by $W(t) \simeq \mathscr{G}$. We interpret the matrices $K(t)$ and $H(t)$ of equation (6.2) as the adjacency matrices of two weighted graphs, one associated to the communication of estimates $x(t)$ and the other associated to the communication of measurements $u(t)$. It is convenient to introduce the neighbors of a node i as the set $\mathscr{N}_i$ of all nodes that can communicate with i, namely

$$\mathscr{N}_i = \{j \in \mathscr{V} : (j, i) \in \mathscr{E}\}.$$

We can now state the main problem of the paper. Given a wireless sensor network modelled by a connected graph $\mathscr{G}$, find time-varying matrices $K(t)$ and $H(t)$, compatible with $\mathscr{G}$, such that the signal $d(t)$ is consistently estimated and the variance of the estimate is minimized. Moreover, the solution should be distributed in the sense that the computations of $k_{ij}(t)$ and $h_{ij}(t)$ should be performed by node i.

6.3   Centralized estimation

Let us assume that $x(0)$ and $u(0)$ are independent and identically distributed random variables. We construct the difference

$$\begin{aligned} y(t+1) &= x(t+1) - d(t+1)\mathbb{1} \\ &= K(t)y(t) + K(t)d(t)\mathbb{1} + H(t)d(t) - d(t+1)\mathbb{1} + H(t)v(t). \end{aligned}$$

If the signal $d(t) = d$ is constant then, taking the expected value with respect to the noise $v(t)$, we obtain

$$\mathbb{E}y(t+1) = K(t)\mathbb{E}y(t) + (K(t) + H(t))\mathbb{1}d - d\mathbb{1}. \tag{6.3}$$

The convergence of $\mathbb{E}y(t)$ to zero is clearly guaranteed if

$$(K(t) + H(t))\mathbb{1} = \mathbb{1} \tag{6.4}$$

and

$$\gamma_{\max}(K(t)) < 1$$

for all t, where $\gamma_{\max}(.)$ is the largest singular value of $K(t)$. It follows that the estimate is consistent also if $d(t)$ is time-varying, as long as the variations are sufficiently slow.

The degree of freedom in the choice of $K(t)$ and $H(t)$, can be used to minimize the variance of the estimate. For this purpose we study how the covariance matrix changes

with time. Let us assume that $x(t)$ and $u(t)$ are independent random vectors. Introduce the matrix

$$P(t) = \mathbb{E}y(t)y^T(t) = \mathbb{E}(x(t) - d(t)\mathbb{1})(x(t) - d(t)\mathbb{1})^T.$$

Then,

$$P(t+1) = K(t)P(t)K(t)^T + \sigma^2 H(t)H(t)^T. \tag{6.5}$$

One option now is to choose $K(t)$ and $H(t)$ such that $P(t+1)$ is minimized at each time instance. Hence, we have the following optimization problem

$$\min_{K(t),H(t)} \quad \text{tr}(K(t)P(t)K^T(t)) + \sigma^2 \text{tr}(H(t)H^T(t)) \tag{6.6}$$
$$\text{s.t.} \quad (K(t) + H(t))\mathbb{1} = \mathbb{1},$$
$$\gamma_{\max}(K(t)) < 1,$$
$$K(t) \simeq \mathscr{G},$$
$$H(t) \simeq \mathscr{G}.$$

This optimization problem is solved iteratively, starting with some initial guess $P(0)$. Notice that the objective function is quadratic in $K(t)$ and $H(t)$ for a given $P(t)$. The first constraint is the linear matrix inequality (6.4). The second constraint, which ensures that the estimation error converges to zero, it can be written as a linear matrix inequality using Schur complement [Boyd et al. 1994]. The last constraints, which impose structure on the matrices $K(t)$ and $H(t)$, correspond to equality constraints on the elements of the matrices $H(t)$ and $K(t)$.

Although the optimization problem (6.6) could be solved using standard numerical optimization tools, it clearly requires a powerful central node collecting the data, computing the new weights and dispatching them to the sensors.

Beside the typical disadvantage of a centralized solution which is not robust to failures, in this case we would have large delays due to the propagation of the data from the farthest nodes to the central node. Although this could be overcome having directed paths from every node to the central node, this would require, in general, a total power consumption which is prohibitive for small nodes. We propose in the following a decentralized solution where each node computes its weights minimizing the variance of its estimate.

6.4 Decentralized estimation

In order to state a decentralized optimization problem, we need to introduce the following vectors

$$\tilde{y}_i(t) = \left(y_{i_1}(t), \ldots, y_{i_{M_i}}(t) \right) \in \mathbb{R}^{M_i}$$

where $M_i = |\mathcal{N}_i|$, and such that $y_{i_j}(t) = y_j(t)$ if $j \in \mathcal{N}_i$. Thus $\mathbf{y}_i$ is a vector that contains all the estimation errors of the neighbors of sensors i, including itself. In a similar way

is defined the vector

$$\tilde{k}_i(t) = \left(k_{i_1}(t), \ldots, k_{i_{M_i}}(t) \right)^T \in \mathbb{R}^{M_i}$$

where $k_{i_s}(t) = k_{ij}(t)$ if and only if $j \in \mathcal{N}_i$. The vector $\tilde{k}_i(t)$ contains all the non-zero elements of the i-row of the matrix K. Similarly we define $\tilde{h}_i(t)$ with respect to the matrix H.

The variance for the node i is then

$$\mathbb{E}y_i(t+1)^2 = \tilde{k}_i(t)^T \Gamma_i(t) \tilde{k}_i(t) + \sigma^2 \tilde{h}_i(t) \tilde{h}_i(t)^T,$$

where $\Gamma_i(t) = \mathbb{E}\tilde{y}_i(t)\tilde{y}_i(t)^T$ is the covariance matrix associated to the sensors i based on its estimates and the estimates received from its neighbors. We will discuss in the next session how this matrix can be computed. Notice that $\mathbb{E}y_i(t+1)^2 = P_{ii}(t+1)$, with $P(t+1)$ defined in (6.5).

We then can state the following optimization problem for node i

$$\min_{\tilde{k}_i(t),\tilde{h}_i(t)} \quad \tilde{k}_i(t)^T \Gamma_i(t) \tilde{k}_i(t) + \sigma^2 \tilde{h}_i(t) \tilde{h}_i(t)^T \tag{6.7}$$

$$s.t. \quad \left(\tilde{k}_i^T(t) + \tilde{h}_i^T(t) \right) \mathbb{1} = 1 \tag{6.8}$$

$$\gamma_{\max}(K(t)) < 1. \tag{6.9}$$

The first constraint, which comes from the condition (6.4), depends only on variables that are local for node i, whereas the last constraint is a global constraint involving the entire matrix $K(T)$ and thus it cannot be computed locally. In order to make the optimization problem (6.7) distributed we need to find conditions on the $\tilde{k}_i$ and $\tilde{h}_i$ that would guarantee that $\gamma_{\max}(K(t)) < 1$. In particular we use the following result.

Proposition 6.1 *If it holds*

$$\sum_{j=1}^{N} k_{ij}(t)^2 < 1/2, \qquad and \qquad \sum_{j=1}^{N} |k_{ij}(t)| < 1 \tag{6.10}$$

then $\gamma_{\max}(K(t)) < 1$, for any $t \geqslant 0$.

Proof. Since the result does not depend on t, in order to have lighter notation, in the following we drop the time dependence. We need to prove that if the given inequalities hold, then $\gamma_{\max}(K) < 1$. This means that it must hold $\lambda_{\max}(KK^T) < 1$, where with $\lambda_{\max}(.)$ we denote the maximum eigenvalue. We have that

$$[KK^T]_{ij} = \sum_r k_{ir} k_{jr}$$

and in particular

$$[KK^T]_{ii} = \sum_s k_{is}^2.$$

Let λ be a generic eigenvalues of KK^T. Then we know, from the Gerschgorin's circle theorem, that

$$\lambda \in \left\{ z \in \mathbb{C} \mid \bigcup_{i=1}^{N} \left| z - \sum_s k_{is}^2 \right| \leqslant \sum_{j \neq i} \left| \sum_s k_{is} k_{js} \right| \leqslant \sum_{j \neq i} \sum_s |k_{is}||k_{js}| \right\}.$$

If we now consider the following sum we have that

$$\left(\sum_s |k_{is}| \right)^2 = \sum_s k_{is}^2 + \sum_s \sum_{s \neq \ell} |k_{is}||k_{i\ell}|.$$

Since $(\sum_s |k_{is}|)^2 < 1$ by hypothesis then we have that

$$\sum_s \sum_{s \neq \ell} |k_{is}||k_{i\ell}| < 1 - \sum_s k_{is}^2.$$

And thus we have that

$$\lambda \in \left\{ z \in \mathbb{C} \mid \bigcup_{i=1}^{N} \left| z - \sum_s k_{is}^2 \right| < 1 - \sum_s k_{is}^2 \right\}.$$

Since, by hypothesis, $\sum_s k_{is}^2 < 1/2$, we easily conclude that $|\lambda| < 1$, and thus we have the sought results. $\qquad\square$

Remark 6.2
Notice that the bounds on $\tilde{k}_i$ and $\tilde{h}_i$ are quite conservative since Gerschgorin's bounds are in general not tight.

From the definition of $\tilde{k}_i$ and $\tilde{h}_i$ it follows that the two inequalities (6.10) are equivalent to

$$\sum_{j=1}^{M_i} k_{i_j}(t)^2 < 1/2, \qquad \text{and} \qquad \sum_{j=1}^{M_i} |k_{i_j}(t)| < 1$$

since the other $N - M_i$ coefficient are zero. Let us define the following set

$$\Theta = \left\{ \tilde{k}_i \in \mathbb{R}^{M_i} \mid \sum_{j=1}^{M_i} k_{i_j}(t)^2 < \frac{1}{2} \text{ and } \sum_{j=1}^{M_i} |k_{i_j}(t)| < 1 \right\}. \tag{6.11}$$

It is not difficult to see that the set Θ is convex. We can then rewrite (6.7) as the following problem, where all the variable to be optimized are local for node i

$$\min_{\tilde{k}_i, \tilde{h}_i} \quad \tilde{k}_i(t)^T \Gamma_i(t) \tilde{k}_i(t) + \sigma^2 \tilde{h}_i(t) \tilde{h}_i(t)^T \tag{6.12}$$
$$s.t. \quad \left(\tilde{k}_i^T(t) + \tilde{h}_i^T(t) \right) \mathbb{1} = 1$$
$$\tilde{k}_i \in \Theta$$

Notice that the problem is quadratic in $\tilde{k}_i$ and $\tilde{h}_i$ for a given $\Gamma_i(t)$, with one linear constraint and two nonlinear constraints. Since the cost function of the primal optimization problem (6.12) is convex in Θ, the constraint $(\tilde{k}_i^T + \tilde{h}_i^T)\mathbb{1} = 1$ is linear in $\tilde{k}_i(t)$ and $\tilde{h}_i(t)$, and we if we assume the solution is in the set Θ, then strong duality follows [Bertsekas et al. 2003]. The problem can then be transform in its dual. We consider the Lagrangian

$$L(\eta, \tilde{k}_i(t), \tilde{h}_i(t)) = \tilde{k}_i^T(t)\Gamma_i\tilde{k}_i(t) + \sigma^2\tilde{h}_i(t)\tilde{h}_i^T(t) + \eta((\tilde{k}_i^T(t) + \tilde{h}_i^T(t))\mathbb{1} - 1)$$

where $\eta \in \mathbb{R}$ is a Lagrangian multiplier. We introduce the dual function

$$g(\eta) = \inf_{\tilde{k}_i(t), \tilde{h}_i(t)} L(\eta, \tilde{k}_i(t), \tilde{h}_i(t)),$$

and the dual optimization problem becomes

$$\max_{\eta} g(\eta).$$

In particular we obtain that

$$\tilde{k}_i = -\frac{\eta\Gamma_i^{-1}\mathbb{1}}{2} \tag{6.13}$$

$$\tilde{h}_i = -\frac{\eta\mathbb{1}}{2\sigma^2}. \tag{6.14}$$

We then minimize the dual optimization function $g(\eta)$ with respect to η. Simple algebraic calculation yields the optimal values

$$\tilde{k}_i(t) = \frac{\Gamma_i(t)^{-1}\mathbb{1}}{\sigma^{-2}M_i + \mathbb{1}^T\Gamma_i(t)^{-1}\mathbb{1}}$$

$$\tilde{h}_i(t) = \frac{\mathbb{1}}{M_i + \sigma^2\mathbb{1}^T\Gamma_i(t)^{-1}\mathbb{1}}.$$

which are the optimal weights for each sensor, for a given $\Gamma_i(t)$. We should now show that these optimal weights are feasible for the problem (6.12), which corresponds to prove that the solution belong to the set Θ defined in (6.11). This so far has not been shown formally, however extensive simulations show that the obtained solution is feasible.

As we have pointed out before the optimal weights $\tilde{k}_i(t)$ and $\tilde{h}_i(t)$ depend on the covariance matrix $\Gamma_i(t)$. Since each node receives measurements and estimates from the neighbors, it is possible to compute, or estimate, the covariance matrix $\Gamma_i(t)$ at each time step.

6.5   Implementation issues

Algorithm 3 below shows the implementation of the estimator in each node of the network. First, each sensor initializes its local covariance matrix estimate with the noise

---

Algorithm 3: Estimation algorithm for node i

---

1. $t := 0$
2. $\widehat{\Gamma}_i := \sigma^2 I$
3. **while** forever **do**
4. $\qquad M_i := |\mathcal{N}_i|$
5. $\qquad \hat{d} := 0$
6. $\qquad$ **if** $t \leqslant 2$ **then**
7. $\qquad\qquad$ **for** $j \in \mathcal{N}_i$ **do**
8. $\qquad\qquad\qquad \hat{d} := \hat{d} + \dfrac{u_j(t)}{M_i}$
9. $\qquad\qquad$ **end for**
10. $\qquad$ **else**
11. $\qquad\qquad$ **for** $j \in \mathcal{N}_i$ **do**
12. $\qquad\qquad\qquad \hat{d} := \hat{d} + \dfrac{x_j(t) + u_j(t)}{2M_i}$
13. $\qquad\qquad$ **end for**
14. $\qquad\qquad$ **for** $j \in \mathcal{N}_i$ **do**
15. $\qquad\qquad\qquad \hat{y}_{i_j}(t) := x_j(t) - \hat{d}$
16. $\qquad\qquad$ **end for**
17. $\qquad$ **end if**
18. $\qquad \widehat{\Gamma}_i(t) := \dfrac{t-1}{t}\widehat{\Gamma}_i(t-1) + \dfrac{1}{t}\hat{\mathbf{y}}_i(t)\hat{\mathbf{y}}_i^T(t)$
19. $\qquad \tilde{k}_i(t) := \dfrac{\widehat{\Gamma}_i(t)^{-1}\mathbb{1}}{\sigma^{-2}M_i + \mathbb{1}^T\widehat{\Gamma}_i(t)^{-1}\mathbb{1}}$
20. $\qquad \tilde{h}_i(t) := \dfrac{\mathbb{1}}{M_i + \sigma^2\mathbb{1}^T\widehat{\Gamma}_i(t)^{-1}\mathbb{1}}$
21. $\qquad \hat{\mathbf{y}}_i(t) := \left(\hat{y}_{i_1}(t), \ldots, \hat{y}_{i_{M_i}}(t)\right)^T$
22. $\qquad x_i(t) := \sum_{j \in \mathcal{N}_i(t)}\left(k_{i_j}x_j(t) + h_{i_j}u_j(t)\right)$
23. $\qquad t := t + 1$
24. **end while**

---

covariance, i.e. $\widehat{\Gamma}_i(0) = \sigma^2 I$ (see line 2 in the algorithm), where we remark using the "hat" it is only an estimate of the real noise covariance. In order to compute the optimal weights (6.14) we need at each time step the matrix $\widehat{\Gamma}_i(t)$. This can be computed using measurements and estimates communicated to the node by the neighbors. Let $\hat{\tilde{y}}_i = x_i(t) - \hat{d}(t)\mathbb{1}$, where $\hat{d}(t)$ is a "rough" estimate of the signal $d(t)$ based on an average between the available estimates and measurements (see lines 8 and 12 in the algorithm). Indeed, as an estimate of $d(t)$ we cannot use $x(t-1)$. The reason is that, even tough the signal is evolving rather slowly, the prediction (6.2) (which was computed at time $t-1$) is not accurate enough to avoid the propagation of an error. Simulations results show that this has catastrophic effects on the estimation of $\widehat{\Gamma}_i(t)$ and we need to rely on a simple average. However, as it will be shown in the next session, this is sufficient to obtain good results.

At the time instant t each node updates the estimate of the covariance matrix as follows (see line 18)

$$\widehat{\Gamma}_i(t) = \frac{t-1}{t}\widehat{\Gamma}_i(t-1) + \frac{1}{t}\hat{\tilde{y}}_i(t)\hat{\tilde{y}}_i(t)^T.$$

After computing the covariance matrix the new weights can be computed as shown in lines 19 and 20 of the Algorithm. The estimate at time t is then updated as shown in line 23. In the algorithm a matrix inversion should be computed. This is not a difficult operation in resource constrained sensor network, since each node has generally a rather limited number of neighbors, and thus the size of the matrix $\widehat{\Gamma}_i$ is very small.

Note that the algorithm is implemented under the assumption that each node is able to compute and communicate data within the sampling instance and that the nodes have a synchronous clock.

6.6   Numerical results

Numerical simulations have been carried out to compare the proposed algorithm with order possible approaches. In particular the proposed algorithm is compared with two other algorithms, one we called *arithmetic mean estimator*, namely such that
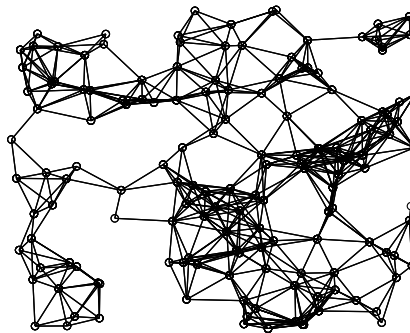
$$k_{ij}(t) = h_{ij}(t) = \begin{cases} \dfrac{1}{2|\mathcal{N}_i|} & \text{if } i \sim j \\ 0 & \text{otherwise}. \end{cases}$$

The other one is based on the normalized Laplacian [Godsil and Royle 2001], and we will called it *Laplacian based estimator*, namely

$$k_{ij}(t) = h_{ij}(t) = \begin{cases} 1 - \dfrac{|\mathcal{N}_i|}{\max_i |\mathcal{N}_i|} & \text{if } i = j \\ \dfrac{|\mathcal{N}_i|}{\max_i |\mathcal{N}_i|} & \text{if } i \sim j \\ 0 & \text{otherwise}. \end{cases}$$
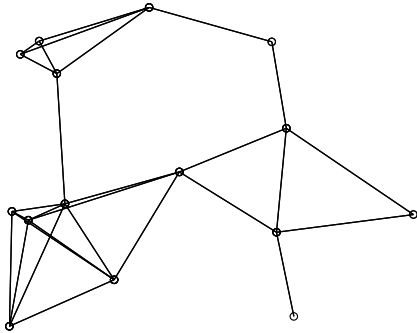
(a) Random generated network with $N = 15$.
Each node has 3.6 neighbors, in average.

(b) Random generated network with $N = 150$.
Each node has 8.3 neighbors, in average.

Two random generated networks have been considered. The first, shown in Figure 6.2(a) with $N = 15$ nodes and the second with $N = 150$ nodes in Figure 6.2(b). The signal to be tracked is $d(t) = 3\sin(2\pi t/780) - \cos(2\pi t/620)$ with a noise normally distributed around $d(t)$ with variance $\sigma^2 = 1.2$. The sensor network is generated distributing randomly distributed on an a squared area of side $N/2$. Two nodes are connected if and only if their relative distance is less than $1.5\sqrt{N}$.

Realizations are shown for the two cases in Figure 6.2 and Figure 6.3. The first plot of the two figures shows the signal corrupted by noise, and the second refers the the realization for the arithmetic mean based estimator, the third to the Laplacian based and the last refers to the proposed algorithm. In particular it is possible to appreciate, visually, the improvements due to the solution proposed.

In the following table are collected the standard deviation of the means square error.

Estimator	Std. dev. MSE $N = 15$	Std. dev. MSE $N = 150$
Arithmetic mean	0.296	0.209
Laplacian based	0.350	0.356
Decentralized	0.175	0.132

In the first case the proposed algorithm yields and improvement of about 70% and of about 60% in the second case, with respect to the arithmetic mean estimator and of about 103% and of about 173% compared with the Laplacian based estimator.

6.7   Summary

In this chapter, we have presented a decentralized cooperative estimation algorithm for the estimation of time-varying signal using a wireless sensor network. Specifically, the
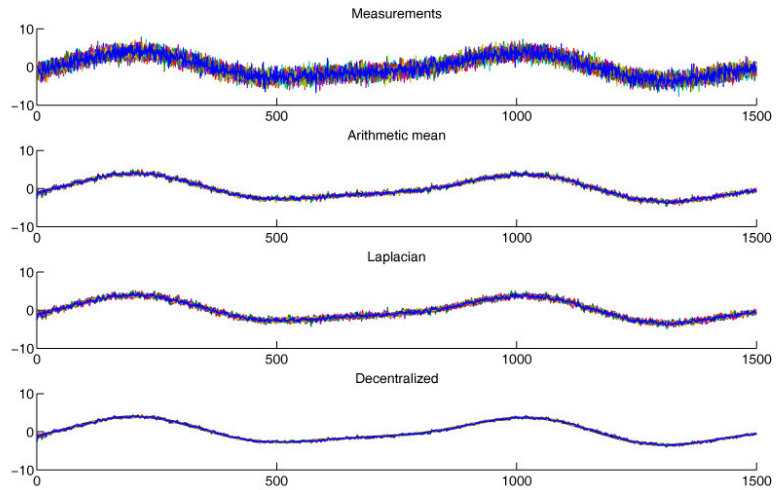
Figure 6.2: Realization of the different estimators versus time. The first plot show the measurements. The second shows the arithmetic mean estimator, the second the Laplacian based and the last show the proposed distributed estimator. The noise variance is of 1.2.
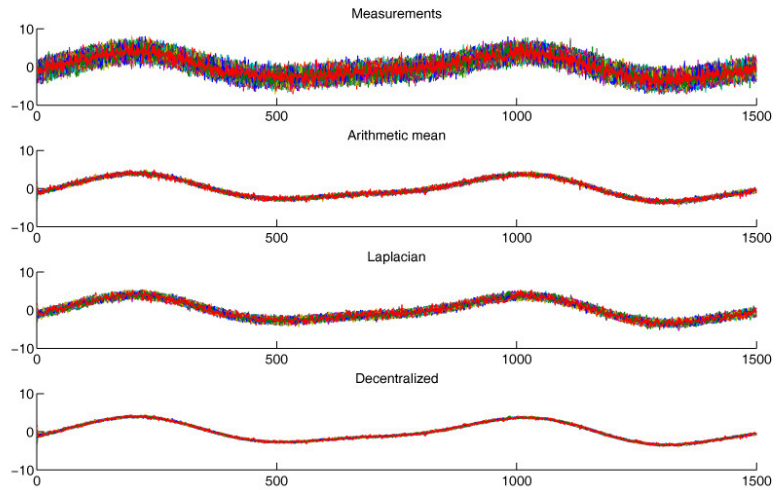

Figure 6.3: Realization of the different estimators versus time. The first plot show the measurements. The second shows the arithmetic mean estimator, the second the Laplacian based and the last show the proposed distributed estimator. The noise variance is of 1.2.

algorithm allows for accurate refinements of the estimates by employing previous esti-
mates and noisy measurements of the signal to be estimated. We provide optimal time-
varying weights to be used in combining the information, where the cost function is the
variance of the estimate. Numerical results shows that the proposed algorithm exhibits
very good performance in terms of standard deviation of the measurement errors and
that it outperform other common solutions.

HIERARCHICAL COORDINATION ARCHITECTURE

In this chapter we present a control architecture for the implementation of a class of coordination strategies for a team of autonomous vehicles. This class is characterized by the alternation between two phases: a communication phase where the team exchanges messages to define waypoints for each vehicle; and a motion phase where the vehicles move in the absence of communications to the designated waypoints, where a new communication phase will take place. The coordination strategy is encoded as an automata based specification.

Several difficulties must be faced in developing a control architecture for the implementation of this class of coordination strategies. We illustrate these difficulties and discuss our contributions in the context of the coordinated search for the extremum of a scalar field by a team of autonomous underwater vehicles with limited communication capabilities. The coordination strategy is inspired by a class of optimization algorithms with phased operations: each phase starts with the selection of points to sample and terminates when these points have been sampled.

First, there are severe limitations on communications. For example, autonomous underwater vehicles use acoustic communications which pose significant restrictions on range and bandwidth [Sozer et al. 2000; Kilfoyle and Baggeroer 2000]. This precludes the use of communications for low-level feedback control. We address this difficulty by restricting communications to the exchange of a few coordination messages.

The second difficulty is in that the design space of the team search is large and heterogeneous. The design involves generating sampling points and arrival times to ensure communications at the end of each phase; assigning vehicles to the sampling points; and designing real-time feedback strategies for each vehicle. We address this difficulty

by structuring the design into two pieces: generation of sampling points and execution control. We present conditions for the generation of sampling points and arrival times with the required properties; this is done in the setting of dynamic optimization and reach set computations. We introduce a layered design for the execution control with a team controller, a vehicle supervisor and several maneuver controllers per vehicle; this is done in the framework of hybrid automata. The coordination strategy is implemented through the interactions of the team controllers during the coordination phase. In this phase, one team controller, the master controller, receives the samples sent by the other team controllers, calculates the sampling points and arrival times for the next motion phase and sends them to the other team controllers. The motion phase is executed independently by each vehicle. Each vehicle supervisor commands the maneuver controller of that vehicle to reach the designated sampling point within a given tolerance of the arrival time.

The third difficulty originates in the requirement that the execution control must indeed implement the search strategy. We address this difficulty by layering the execution control and designing each layer to ensure that their controllers produce guaranteed results under the assumption that the controllers at the adjacent layers also produce guaranteed results. This is done in a modular fashion. The vehicle supervisor and the maneuver controllers guarantee that each sampling point is visited within a given tolerance of the arrival time. Under these assumptions the composition of the team controllers is shown to implement the specification. This is done using automata-based techniques. This modularity decouples the behavior of the controlled team from that of the optimization algorithm; the team inherits the search properties of the optimization algorithm.

Our contributions concern the design of a modular architecture and the proof that the modules and the interactions within the architecture implement a given specification. This is done in the framework of automata-theoretic techniques and bisimulation analysis. Our design touches upon several related problems: finding the minimizer of a scalar field through the coordinated motions of multiple vehicles; guaranteed maneuver design; waypoint based coordination schemes, and control architectures.

There is a substantial body of work on the formalization of control architectures. Examples include the use of Petri nets and stochastic hybrid automata [Saridis and Valavanis 1988; Lima and Saridis 1996], hybrid systems [Varaiya 1993; Varaiya and Shladover 1991; Varaiya 1997; Godbole et al. 1995], and linear temporal logic [Fainekos et al. 2005]. Our work is related to the layering concepts presented in [Varaiya 1997]. The ideas used in execution control are inspired by [Varaiya 1997, 1993; de Sousa et al. 2000]. The case study we present in the last part of chapter, is related to find the minimum of a scalar field with the coordinated motions of autonomous vehicles. This problem has received large attention in the last decade. A significant body of this work concerns the adaptation of optimization algorithms to single- or multi-vehicle search strategies. Search strategies for single vehicle operations which include a combination of the underlying principles of different optimization algorithms are reported in [Burian et al. 1996] along with illustrative examples which use real data, such as depth profiles of a lake. Pure gradient-based methods for scenarios where a vehicle platoon searches the minimum

of general convex and smooth scalar fields are presented in [Bachmayer and Leonard 2002]. Lyapunov-based arguments are used in [Fiorelli et al. 2003] for the gradient descent of a scalar field. These approaches result in feedback control laws that require closing the control loop around communicated measurements. We take the view of considering limited and sporadic communications, which preclude the use of these techniques.

7.1 Outline

The paper is organized as follows. In Section 7.2 we introduce the problem formulation. In particular we highlight the constraints and assumptions under which the control architecture is developed. Moreover we define the system specification, namely a mathematical description of the overall system behavior. Section 7.3 describes the hierarchical control structure in the framework of interacting hybrid automata. The main results are reported in Section 7.4 where properties of the hierarchical control structure are discussed and it is shown that such architecture implements the given system specification. In Section 7.5 we present simulation results to illustrate the implementation of our design in a team search mission for a team of underwater vehicles.

7.2 Problem formulation

Let us consider a set $V = \{v_1, v_2, \ldots, v_N\}$ of $N > 1$ vehicles. Each vehicle v_i is modelled as a nonlinear control system

$$\dot{x}_i(t) = f_i(x_i(t), u_i(t)),$$

where $x_i(t) \in \mathcal{X} \subset \mathbb{R}^n$ is the state of the vehicle, $u_i(t) \in \mathcal{U} \subset \mathbb{R}^m$ the control, and $f_i : \mathcal{X} \times \mathcal{U} \to T\mathcal{X}$ the vector field.

The main problem is that of designing a control architecture that allows to implement control strategies for coordinating the team of vehicles V, so that a given task is completed. Moreover the architecture should be robust to typical faults and errors that can occur in a multi-vehicle system (such as communication data losses, vehicle failures, etc.) guaranteeing that some given overall specification is fulfilled. In the following, we describe in detail the main assumptions under which the architecture is built.

7.2.1 Team coordination via waypoints generation

The first assumption relates to the control strategy that coordinates the whole team of vehicles. In this work we assume that the team is coordinated by an event-based controller that generates *waypoints*, namely a point $w = (w_1, \ldots, w_N) \in \mathcal{W} \subseteq \mathcal{X}^N$. The team coordination is defined by the following update map

$$(w^+, t^+) = \varphi(w, t, e),$$

where e is an event defined on an event alphabet Σ and $t \in \mathcal{T} \subset \mathbb{R}_+$ is the time step. With notation w^+ we indicate the next value of w. Similarly for t. We call $\varphi(.)$ the team coordination strategy. Based on w_i and w_i^+, the control u_i is derived for each vehicle i.

7.2.2 Vehicle models

The vehicle models we consider are those that can be approximated by a unicycle. We then have that each vehicle is described by the differential equation

$$\begin{bmatrix} \dot{x} \\ \dot{y} \\ \dot{\psi} \end{bmatrix} = \begin{bmatrix} v\cos\psi \\ v\sin\psi \\ \omega \end{bmatrix}, \tag{7.1}$$

where (x, y) is the location of the vehicle with respect some fixed coordinate frame, v is the linear forward velocity, ψ is the orientation of the vehicle and ω is the angular velocity. In the following we will also consider the case of external slowly-varying disturbances acting on the vehicles. Typical example are wind disturbances for airplanes or water streams for underwater vehicles. We then have the following modified dynamic equations

$$\begin{bmatrix} \dot{x} \\ \dot{y} \\ \dot{\psi} \end{bmatrix} = \begin{bmatrix} v\cos\psi + v_d\cos\psi_d \\ v\sin\psi + v_d\sin\psi_d \\ \omega \end{bmatrix}.$$

where v_d and ψ_d is the velocity and the direction, respectively, of the disturbance acting on the vehicle.

Many vehicles used can be approximately described by a unicycle model together with extra kinematic constraints. Let us consider some examples. Synchro drive vehicles can be precisely described by the previous kinematic model. In this type of vehicle, indeed, the linear and angular velocities can be controlled independently and are the same for all wheels. Differential drive vehicles, where the locomotion system is composed of two parallel driving wheels that can be controlled independently, are described by a unicycle model if we impose that $v = (v_1 + v_2)/2$ and $\omega = (v_1 - v_2)/\ell$, where v_1 and v_2 are the right and left wheel speeds and ℓ is the distance between them. Notice the kinematic constraint between angular and linear speed. Tricycle and car-like vehicles, where only the front wheels are actuated, can be modelled by the previous kinematic model. In this case if α is the angle of the turning wheel with respect to the heading of the vehicle, then $v = v_s\cos\alpha$ and $\omega = v_s/d\sin\alpha$ where v_s is the linear velocity of the steering wheel and d is the distance between passive axle and the steering wheel. See [Laumond et al. 1998; Oriolo et al. 2002; Beard et al. 2002; LaValle 2006] for further discussions. Also underwater vehicles and aerial vehicles that move on a plane can be approximated with the unicycle model [Ögren 2003; McGee et al. 2005]. For this type of vehicles the extra kinematic constraints impose that $v_{\min} > 0$, that is the vehicle requires a minimum velocity ("stall" velocity) to maintain controllability, and the angular velocity depends on the linear velocity $\omega = c\,v$ where c is a constant related to the maximum curvature of the trajectory that the vehicle can follow.
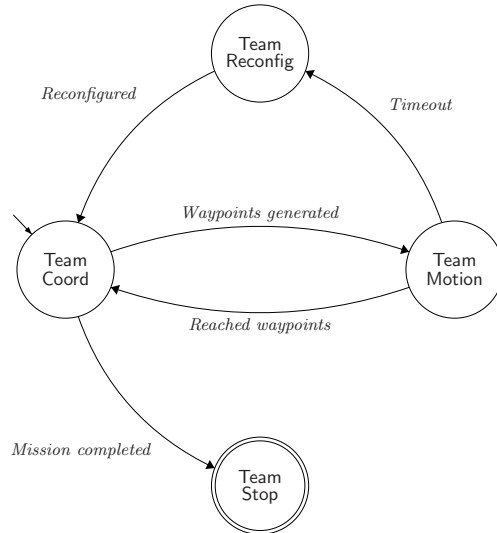
Figure 7.1: System specification for the team coordination.

7.2.3   System specification

In order to guarantee that a control architecture can steer the vehicles so that a given task is fulfilled, we need to have a model of the desired system behavior, the system specification. Introducing such a model allows us to relate properties of a control architecture and the specification. The system specification should also model the interaction between communication and control.

In this chapter we present the system specification as a transition system.

Definition 7.1 (Transition system [Puri and Varaiya 1996]) *A transition system T is a tuple*

$$T = (Q, \rightarrow, I, O, Init, Final),$$

where

- *Q is the set of states*

- *I and O is the set of inputs and outputs, respectively*

- *$\rightarrow \subset Q \times I \times Q \times O$ is the transition relation*

- *$Init \in Q$ is the initial state*

- *$Final \in Q$ is the final state*

The interpretation is that an input $i \in I$ cause the system to move from one state $q \in Q$ to another state $q' \in Q$ producing the output $o \in O$. It is convenient to write $q \xrightarrow{i/o} q'$ instead of $(q, i, q', o) \in \rightarrow$. The graphical representation of T is a directed graph with vertices representing Q and arcs representing $\xrightarrow{i/o}$, an arc with empty origin representing Init and a vertex with an extra circle representing Final.

We define the system specification for the team coordination as the transition system

$$T_{\mathrm{Spec}} = (Q_{\mathrm{Spec}}, \rightarrow, I_{\mathrm{Spec}}, \emptyset, \mathsf{Team\ Coord}, \mathsf{Team\ Stop})$$

shown in Figure 7.1. It has four discrete states: Team Coord, Team Reconfig, Team Motion, Team Stop. The mission proceeds in phases. Each phase is described by a loop

$$\mathsf{Team\ Coord} \rightarrow \mathsf{Team\ Motion} \rightarrow \mathsf{Team\ Coord}.$$

This loop is repeated until the mission is successfully completed, namely when a termination condition is satisfied. Note that the loop describes the interaction between communication and control. Namely, in the Team Coord state the vehicles exchange data, while in the state Team Motion the vehicles move.

The system specification implies the following behaviour of the overall multi-vehicle system. The system starts in the Team Coord state. A transition to Team Stop takes place if the termination condition is true. Otherwise in Team Coord the vehicles exchange part of their state information, including their current waypoint w_i, prior to the generation of the new waypoints. The transition to Team Motion takes place upon the reception of next waypoints w_i^+. While in Team Motion, the low-level controllers drive each vehicle to their waypoint. When the vehicles have reached their waypoints, the system switch back to Team Coord to exchange new vehicle state information. If a vehicle did not succeed to reach its waypoint, a timeout event is generated and the system goes to Team Reconfig. Then the team executes an reconfiguration operation, which means that they adjust their team behaviour due to the faulty vehicle. (For simplicity, we assume that only one vehicle did not reach its waypoint at each reconfiguration). After reconfiguration, the system goes to Team Coord, where the (currently active) vehicles exchange their state information and new waypoints are generated. If the team has reached its goal, the mission is completed and the system go to the state Team Stop.

Note that the system specification defined here is fairly general, and captures a rather wide class of multi-vehicle control problems. In the next section we define a hierarchical control structure and then, in Section 7.4, we will show that the proposed architecture fulfills the given specifications.

7.3   Hierarchical control architecture

The problem of coordinating vehicles is inherently a hybrid control problem. Indeed it has both discrete dynamics, related to the coordination strategy, and continuous dynamics, related to the model description of the individual vehicle. There is a distinct

$$(w^+, t^+) = \varphi(w, t, e) \qquad \text{Team Controller}$$

e $(w, \text{command})$

Vehicle Supervisor

e' maneuver type

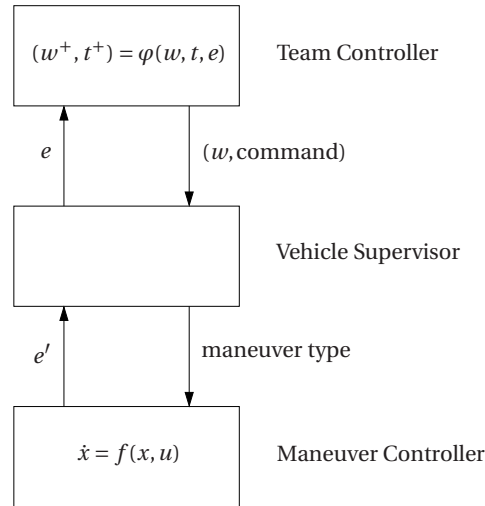$$\dot{x} = f(x, u) \qquad \text{Maneuver Controller}$$

Figure 7.2: Hierarchical control structure for each vehicle.

interaction between the discrete and continuous parts. The team coordination is obtained computing a set of waypoints according to the team coordination strategy. The vehicles are steered by a local feedback control strategy from one waypoint to the next one. Upon reaching a waypoint, the next waypoint is computed by the team coordination strategy, and so on. The hierarchical control structure allows us to formally prove correctness of the implementation. It also enables a modular design of the control system for which modules can be developed and implemented independently as long as their interfaces are appropriate. The control structure provides an intuitive structure for program developers and system operators.

7.3.1 Master-slave control structure

We propose a hierarchical control structure, for each vehicle, organized in three layers, as shown in Figure 7.2. It consists of a team controller, a vehicle supervisor and a maneuver controller. The team controller handles the event-based coordination of the vehicles by assigning new waypoints. Thus it implements the team coordination strategy $\varphi(.)$. It also determines when the mission is completed and when the team needs to reconfigure. The vehicle supervisor provides a set of maneuvers onto which it maps the coordination commands from the team controller. Such intermediate layer is an interface between the high-level coordination in the team controller and the low-level implementation in the maneuver controller, which allows abstraction of the lower layer. The vehicle supervisor signals back to the team controller an event e, which is used by the team controller to handle possible faults. The maneuver controller interprets the maneuvers specified by the vehicle supervisor. It computes low-level control commands
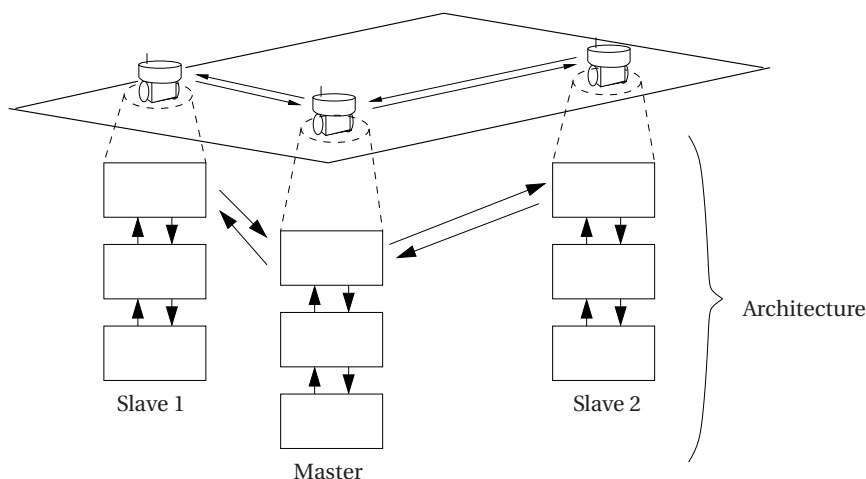
Figure 7.3: Control architecture for multi-vehicle system with three vehicles. Each hierarchical structure corresponds to a vehicle controller. Arrows between hierarchies represent communication links between vehicles. Arrows inside each hierarchical stack represents signals between different layers.

and executes them on the vehicle. Hence, the maneuver controller specifies $u_i(t)$ for the individual vehicle control systems $\dot{x}_i(t) = f_i(x_i(t), u_i(t))$ as described in Section 7.2. It signals back to the vehicle supervisor the success or the failure of the maneuver.

The hierarchical control architecture for each vehicle needs to be extended to the case in which there are many cooperating vehicles. The (local) team controller of each vehicle takes care of the co-operation with the other vehicles and takes decision on the event-based coordination of the team. The team controller is either in mode *master* or *slave*. During each mission, we assume that there is only one master in the team and, for simplicity, that this role is fixed for the whole mission. The master team controller provides inputs to the slave team controllers of the other vehicles, and the slave team controllers report to the master. The interaction between master and slaves is achieved over a communication network. The (local) vehicle supervisor and the (local) maneuver controller work exactly as described previously, but note that maneuvers, events, etc., are now local variables. The overall architecture is illustrated in Figure 7.3.

7.3.2   Team controller

The team controller for each vehicle is modelled as a transition system. Since the team controller can be in either the master or slave mode, we have two team controller transition systems. They are further described below. The master team controller

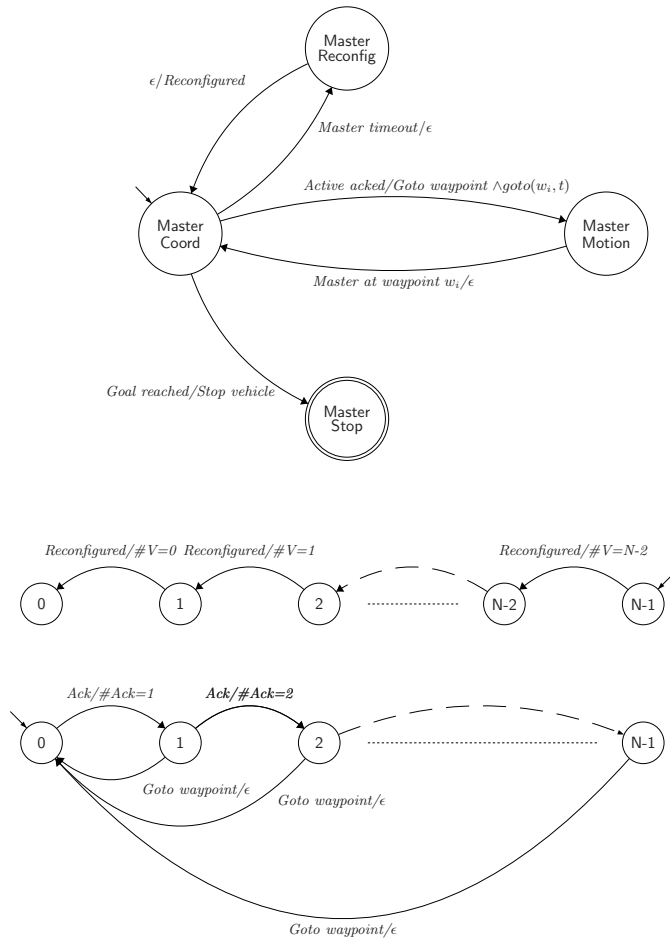$$T_M = (Q_M, \rightarrow, I_M, O_M, \mathrm{Init}_M, \mathrm{Final}_M)$$

Figure 7.4: The master team controller is the parallel composition of three transition systems.

is shown in detail in Figure 7.4 The master team controller consists of the parallel composition of three transition systems. The main functionality is provided by the upper transition system with the four states Master Coord, Master Reconfig, Master Motion, Master Stop. The other two transition systems are counters: one counter stores the number of active slaves and the other counter keeps track of the number of received acknowledgments from the slaves. In the state Master Coord, the master waits for data transmitted by the slaves. As data are received, acknowledgments ("Acks") are being counted until all active slaves have been acknowledged. Then the master computes the new set of waypoints and send them to the slaves. An event *Goto to waypoint* is triggered

and a command $goto(w_i, t)$ is signaled to the vehicle supervisor. Notice that t here represents a constant time within which the command needs to executed. This transition, which is represented by the state transition from Master Coord to Master Motion, resets the ack counter. When the master reaches its waypoint, it returns to Master Coord where it waits for the slave team controllers to report. This transition takes place when the vehicle supervisor has received a "done" event from the maneuver controller. If some of the slaves do not succeed to reach their assigned waypoints within a given timeout time, *Master timeout* will trigger, signalled by the vehicle supervisor, and the master will go to Master Reconfig where a team reconfiguration will take place. The number of active slaves is then updated through a state transition in the active slaves counter given by the middle transition system in Figure 7.4. When the master is in Master Coord and has received data from all active slaves, it determines if the goal is reached. If that is the case, the master issues stop commands to the slaves and goes to Master Stop. The stop command is also sent to the vehicle controller for a suitable action on the vehicles.

The slave team controller transition system is shown in Figure 7.5. The team controllers of the $N-1$ slaves are identical and denoted

$$T_{S_1} = \cdots = T_{S_{N-1}} = (Q_S, \rightarrow, I_S, O_S, \text{Init}_S, \text{Final}_S).$$

The states are Slave Coord, Slave Motion, Slave Stop. The initial state is Slave Coord, where the slave team controller is waiting for the next waypoint and a motion command from the master team controller. When the command has been received, the slave goes to Slave Motion and the vehicle moves to its new waypoint. This is done signalling the vehicle supervisor with $goto(w_i, t)$, where t is a constant, similarly as for the master team controller. If the vehicle reaches its waypoint before the slave timeout expires, the slave team controller sends an ack to the master team controller together with the partial state information required by the waypoint generating algorithm and the system goes to Slave Coord waiting for the next waypoint. If instead the slave vehicle does not reach the waypoint, the slave team controller goes to Slave Stop. The event *Slave timeout* is trigged by the vehicle supervisor. The slave team controller may also go to Slave Stop from Slave Coord. This transition typically takes place when the master has decided that the goal is reached and therefore forces all slaves to stop.

7.3.3 Vehicle supervisor

Each vehicle is described as a provider of maneuvers; different maneuvers are required for different missions. External controllers, such as the master team controller, request the vehicle to execute maneuvers. Interactions are mediated by the vehicle supervisor, which resides onboard the vehicle. It is introduced for the purpose of modularity: there is a library of maneuvers and of maneuver controllers. The vehicle supervisor checks requests for the execution of a given maneuver against the list of maneuvers available in a library. In this way we can extend the vehicle capabilities, by adding new maneuvers to the library, without recoding the existing control code. In the reminder of this paper we show that the search mission can be executed with two maneuvers, goto and hold,
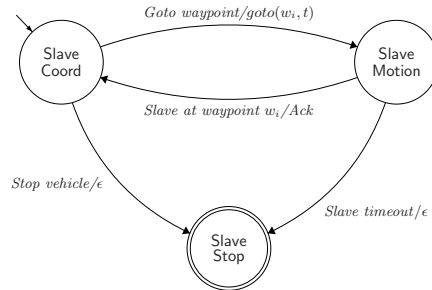
Figure 7.5: Slave team controller.

which can be collapsed to just one maneuver for the purpose of simplicity. This simplification would eliminate the need for the vehicle supervisor. However, for the sake of generality, we present it next.

The vehicle supervisor interfaces the team controller with the maneuver controllers. The vehicle supervisor (for the master)

$$T_V = (Q_V, \rightarrow, I_V, O_V, \text{Init}_V, \text{Final}_V)$$

is shown in Figure 7.6, where

- $Q_V = \{\text{Idle}, \text{Motion}, \text{Stop}\}$

- $I_V = \{goto(w_i,t), doneGoto, MtimeOut, Stop\ vehicle\}$

- $O_V = \{Master\ at\ waypoint(w_i), startGoto(w_i,t)\}$

- $\text{Init}_V = \text{Idle}$ and $\text{Final}_V = \text{Stop}$.

The vehicle supervisor for the slave is similar with the exception that signals refers to those of the slave. In the following we refer to the master vehicle supervisor.

The input and output events model interactions with the team controller and with the maneuver controller. The vehicle supervisor receives the events $goto(w_i,t)$ and *Stop vehicle* from the team controller to execute a goto maneuver to waypoint w_i in time less than t and to stop the vehicle; it receives the events *doneGoto* and *MtimeOut* from the current maneuver controller to indicate the termination of the maneuver because of a time out; it sends the events $startGoto(w_i,t)$ and $startHold(w_i)$ to the maneuver controller to go to waypoint w_i in time less than t and to hold the position; and it sends the events *Master at waypoint(w_i)* and *Master timeout* to the team controller to indicate that the waypoint was reached and a that time out has occurred.

A normal execution cycle alternates between the states Idle and Motion. The transition to Motion is taken when the event $goto(w_i,t)$ is received from the team controller. The transition to the Idle state takes place when the event *doneGoto* is received from the maneuver controller and the event *Master at waypoint* is signalled to the team controller together with the reached waypoint w_i.
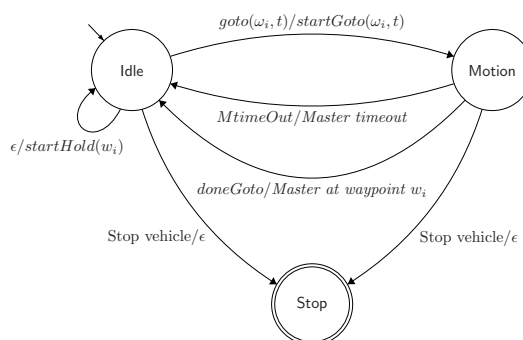
Figure 7.6: Vehicle supervisor.

Note that there are no clocks in the vehicle supervisor. The reasons for this are that (i) both the supervisor and the maneuver controllers reside on the same vehicle and we can therefore assume reliable communications between them; and (ii) maneuver timeouts are extended locally within the maneuver controllers.

7.3.4   Maneuver controller

The low level control is organized in terms of maneuvers. For the purpose of modularity, there is one maneuver controller for each type of maneuver. In this way we can easily add maneuver controllers to the existing ones to extend the capabilities of the vehicle, without changing the vehicle supervisor. Each maneuver controller is a hybrid automaton which encodes the corresponding control logic. The maneuver controller takes as input a maneuver specification and generates commands to the actuators.

7.4   System properties

This section shows how to verify that the proposed control architecture implements the specification. The verification is done in a modular fashion. We observe that the execution proceeds in phases and thus we need to verify the behavior of the control architecture for each phase. First, we show that the high-level team coordination through the interconnected master and slave team controllers are consistent with the system specification. Second, we state a set of properties for the waypoint generation procedure to generate waypoints and times of arrival that are both reachable and allow for the master and the slave team controllers to follow the required patterns of coordination. We show how to ensure these properties for a general nonlinear system. Third, we prove that the on-line execution control generates the interactions among the team controller and the vehicle supervisors which ensure that the sampling points are reached within the allowed time intervals under the assumption that the maneuver controllers produce

guaranteed results. The described modularity decouples efficiently the behavior of the controlled team from that of the underlying optimization algorithm.

7.4.1 Team coordination

We will in this section define a quotient transition system $T/\sim$ based on the system T derived from the interconnected master and slave team controllers. We will show that $T/\sim$ is isomorphic to the team coordination specification T_{Spec} in Section 7.2. Since T is bisimilar with $T/\sim$ by construction, we will conclude that the closed-loop system based on the interconnected team controllers fulfills the specification.

The interconnection of the master team controller

$$T_M = (Q_M, \rightarrow, I_M, O_M, \text{Init}_M, \text{Final}_M)$$

with $N-1$ identical slave team controllers

$$T_{S_1} = \cdots = T_{S_{N-1}} = (Q_S, \rightarrow, I_S, O_S, \text{Init}_S, \text{Final}_S)$$

is illustrated in Figure 7.3. To simplify notation we do not distinguish the transition relations, but the interpretation in each case should be clear from the context. The overall transition system $T = (Q, \rightarrow, I, O, \text{Init}, \text{Final})$ is given by the parallel composition

$$T = T_M \| T_{S_1} \| \ldots \| T_{S_{N-1}}.$$

The state of T is denoted

$$q = (q_M, q_{S_1}, \ldots, q_{S_{N-1}}, k) \in Q = Q_M \times Q_S^{N-1} \times \{0, \ldots, N-1\},$$

where q_M is the state of the main part of the master team controller (upper transition system in Figure 7.4), q_{S_i} is the state of slave i team controller (Figure 7.5), and k is the number of active slaves (middle transition system in Figure 7.4). (We disregard the lower transition system in Figure 7.4.)

We introduce the quotient transition system $T/\sim = (Q/\sim, \rightarrow, I, O, \text{Init}/\sim, \text{Final}/\sim)$ with equivalence relation $\sim \subset Q \times Q$, which partitions the state space of T into four equivalence classes $Q_R, Q_C, Q_M, Q_S \subset Q$. (The indices indicate "Reconfiguration", "Coordination", "Motion" and "Stop", which reveals the idea behind the partition.) The equivalence classes are defined as follows:

$$Q_R = \big\{ q = (\text{Master Reconfig}, q_1, \ldots, q_{N-1}, \cdot) \in Q : q_i \in \{\text{Slave Coord}, \text{Slave Stop}\} \big\}$$
$$Q_C = \big\{ q = (\text{Master Coord}, q_1, \ldots, q_{N-1}, \cdot) \in Q : q_i \in \{\text{Slave Coord}, \text{Slave Stop}\} \big\}$$
$$Q_M = \big\{ q = (\text{Master Motion}, \cdot, \ldots, \cdot) \in Q \big\}$$
$$Q_S = \big\{ q = (\text{Master Stop}, \text{Slave Stop}, \ldots, \text{Slave Stop}, \cdot) \in Q \big\}.$$

Consider four elements $q_R \in Q_R$, $q_C \in Q_C$, $q_M \in Q_M$ and $q_S \in Q_S$. The transition relation for $T/\sim$ is then defined as follows:

- $q_R \to q_C$ provided that Master Reconfig $\to$ Master Coord and
        Slave Coord $\to$ Slave Stop

- $q_C \to q_M$ provided that Master Coord $\to$ Master Motion and
        Slave Coord $\to$ Slave Motion

- $q_C \to q_S$ provided that Master Coord $\to$ Master Stop and
        Slave Coord $\to$ Slave Stop

- $q_M \to q_R$ provided that Master Motion $\to$ Master Reconfig,
        Slave Motion $\to$ Slave Coord and Slave Motion $\to$ Slave Stop

- $q_M \to q_C$ provided that Master Motion $\to$ Master Coord,
        Slave Motion $\to$ Slave Coord and Slave Motion $\to$ Slave Stop.

The inputs I, outputs O, initial states $Init/\sim$ and final states $Final/\sim$ of $T/\sim$ are easily derived from T.

Recall the definition of simulation and bisimulation for transition systems, e.g., [Puri and Varaiya 1996].

Definition 7.2 (Simulation and bisimulation)   *Given two transition systems*

$$T_1 = (Q_1, \to, I_1, O_1, Init_1, Final_1)$$

and

$$T_2 = (Q_2, \to, I_2, O_2, Init_2, Final_2),$$

we say that T_2 simulates T_1 with relation $R \subset Q_1 \times Q_2$ if $(x, y) \in R$ and $x \to x'$ implies that there exists $y' \in Q_2$ such that $y \to y'$ and $(x', y') \in R$. If T_1 simulates T_2 and T_2 simulates T_1, we say that T_1 and T_2 are bisimilar.

The following result follows from construction with R being the equivalence relation defined previously.

Lemma 7.1   *T and $T/\sim$ are bisimilar.*

We next show that $T/\sim$ and T_{Spec} are isomorphic. We recall the following definition.

Definition 7.3 (Isomorphic transition systems)   *Two transition systems*

$$T_1 = (Q_1, \to, I_1, O_1, Init_1, Final_1)$$

and

$$T_2 = (Q_2, \to, I_2, O_2, Init_2, Final_2)$$

are isomorphic if there is a bijection $h : Q_1 \to Q_2$ such that for all $x, y \in Q_1$ it holds that $x \to y$ if and only if $h(x) \to h(y)$.

In order to relate $T/\sim$ and T_{Spec}, we need to identify the inputs of $T/\sim$ with the inputs of T_{Spec}. It can easily be done by relating each transition of $T/\sim$ with a transition of T_{Spec}:

- $q_R \to q_C$ corresponds to Team Reconfig $\to$ Team Coord

- $q_C \to q_M$ corresponds to Team Coord $\to$ Team Motion

- $q_C \to q_S$ corresponds to Team Coord $\to$ Team Stop

- $q_M \to q_R$ corresponds to Team Motion $\to$ Team Reconfig

- $q_M \to q_C$ corresponds to Team Motion $\to$ Team Coord.

A suitable bijective map $h : Q/\sim \to Q_{Spec}$ of Definition 7.3 is simply the relabelling:

- $h(Q_R) =$ Team Reconfig

- $h(Q_C) =$ Team Coord

- $h(Q_M) =$ Team Motion

- $h(Q_S) =$ Team Stop.

It then follows that $T/\sim$ and T_{Spec} are isomorphic. Two transition systems that are isomorphic are obviously also bisimilar. Since T and $T/\sim$ are bisimilar (Lemma 7.1) and thus also $T/\sim$ and T_{Spec} are bisimilar, we have the following main result.

Theorem 7.1 T and T_{Spec} are bisimilar.

The transition systems T and T_{Spec} are hence equivalent in the sense of a bisimulation relation. The implementation of the interconnected team controllers will thus fulfills the system specification.

7.4.2 Waypoint generation

The generation of the waypoints by the team controller according to a team coordination strategy $\varphi(.)$ needs to fulfill some conditions so that the generated waypoints are reachable for the vehicles. Let us recall the definition of the reach set.

Definition 7.4 (Backward Reach set) *Consider a control system $\dot{x} = f(x, u)$. The backward reach set $R[t_\alpha, t_\beta, \mathcal{M}]$ at time $t_\alpha < t_\beta$ is the set of points $z \in \mathcal{X}$ such that there exists a control $u(\cdot)$ that drives the trajectory of the system $\dot{x} = f(x, u)$ with initial condition $x(t_\alpha) = z$ to some closed target set $\mathcal{M} \subset \mathcal{X}$ at time $\tau \in [t_\alpha, t_\beta]$.*

It is possible to extend the definition to capture uncertainties and disturbances, see [Kurzhanskii and Varaiya 2001, 2002b,a]. Although that is useful for underwater vehicles facing uncertain currents etc., we limit the discussion to the basic definition of reach set given above.

We define next the notion of admissible waypoint. Vehicle i reaches its waypoint w_i^+, after a goto maneuver, if no faults occurred. After the goto maneuver it executes an hold maneuver around w_i^+ awaiting for new commands. Let us consider d_h the maximum distance the vehicle can be from w_i^+ executing an holding maneuver. Notice that for systems that cannot be stopped, such as airplanes or underwater vehicles, a holding maneuver corresponds to hover around the point w_i^+. Let r_{com} be the limited range within which inter-vehicle communication is possible. We then have the following definition.

Definition 7.5 (Admissible waypoint) *A waypoint is admissible if the following conditions hold for every i and j,*

$$\|w_i^+ - w_j^+\| \leq r_{com} - d_h$$
$$w_i \in R[t, \bar{t}, w_i^+]\,,$$

where $\bar{t}$ is the time within which the control action must be completed.

An admissible waypoint generation procedure is one which is generates admissible waypoints. In order to determine admissibility we need to compute the reach sets for each vehicle. This is a non-trivial task. Some recent literature have proposed been tackling the problem of computing the reach set of a system [Varaiya 1998; Lafferriere et al. 2001; Mitchell and Tomlin 2003; Kurzhanski and Varaiya 2004], however for a general nonlinear system the problem is still open.

In the following we study a particular example where the waypoints belong to a grid in the two-dimensional space and the distance between waypoints is chosen so that a feasible trajectory for vehicles modelled as unicycles exists.

7.5   Autonomous underwater vehicles in search mission

In this section we show how the proposed architecture can be used to implement a search algorithm for autonomous underwater vehicles (AUVs). We assume that the AUVs move at a constant depth, they are equipped with acoustic modem for inter-vehicle communication and they can measure the temperature, or some other scalar variable, at their position. The objective is to search for the minimum of a temperature field. The search algorithm is based on a fixed-size version of the simplex optimization algorithm introduced in [Spendley et al. 1962]. This is a very effective algorithm for finding the extremum of a scalar field from few samples. Some other optimization algorithms have been previously used in vehicle-based search strategies, e.g., [Bachmayer and Leonard 2002; Burian et al. 1996]. The simplicity and robustness properties of the simplex algorithm makes it a good candidate, particularly for a team of AUVs under severe communication constraints. What also makes this method appealing is the fact that it allows reasoning about vehicle motion in discrete terms: indeed the simplex algorithm imposes a discretization of the configuration space, so it can be implemented in the proposed hierarchical structure.
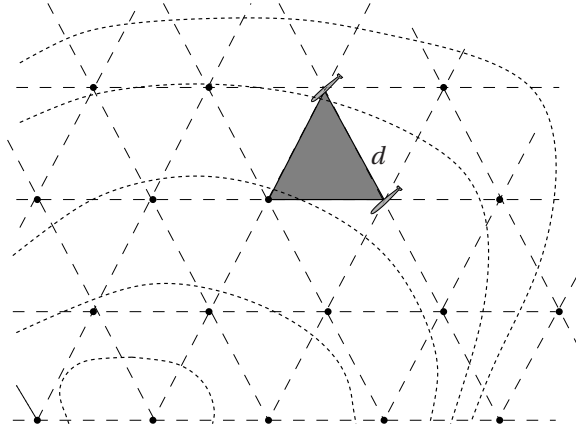
Figure 7.7: A triangular grid with aperture d over a scalar field depicted through its level curves (dark dashed lines). The shaded triangle illustrates the simplex location, which evolves on the grid.

7.5.1 Simplex algorithm

The simplex optimization algorithm is a direct search method which behaves much like a gradient descent method but with no explicit gradient calculation. It is usually applied in situations where computation capability is limited and gradient calculation is difficult, as happens in scalar fields corrupted by noise. We are interested in executing a search operation for finding the minimum of a planar field defined over a convex set $\Omega \subset \mathbb{R}^2$, see Figure 7.7. The simplex optimization method starts by evaluating the scalar field at the vertices of a three-sided simplex, placed at an initial guess position. It then proceeds by creating a new simplex, obtained by reflecting the vertex associated to the sample with higher field value. The reflection is with respect to the line passing through the two remaining vertices. The algorithm stops when the newly generated simplex coincides with the simplex generated two iterations before, namely after two reflections step we need to reflect the starting vertex. This procedure is described with more details below.

Consider a triangular grid $\mathcal{G} \subset \Omega$ with aperture d, as depicted in Figure 7.7. Introduce an arbitrary point $p_0 \in \Omega$ and a base of vectors given by b_1, b_2 such that $b_1^T b_1 = b_2^T b_2 = d^2$ and $b_1^T b_2 = d^2 \cos \pi/3$. The grid is then the set of points

$$\mathcal{G} = \{ p \in \Omega | \ p = p_0 + k b_1 + \ell b_2, \ k, \ell \in \mathbb{Z} \}.$$

A simplex $z = (z_1, z_2, z_3) \in \mathcal{G}^3$ is defined by three neighboring vertices of $\mathcal{G}$, which belong to a triangle. Let $F : \Omega \to \mathbb{R}$ the scalar field. The reflection rule updates the simplex in the following way. Suppose, without loss of generality, that $F(z_3) \geq F(z_i)$, $i = 1, 2$. Given a simplex $z = (z_1, z_2, z_3)$ the next simplex is

$$z^+ = (z_1, z_2, z_3)^+ = (z_1, z_2, z_1 + z_2 - z_3).$$

Algorithm 4: Simplex algorithm.

1. $z(0) := (z_1(0), z_2(0), z_3(0))$

2. $k := 0$

3. **while** $k < 2 \vee z(k) \neq (k-2)$ **do**

4. $i := \arg\max_i F(z_i(k))$

5. $z_i' := z_j + z_h - z_i$ with $j, h \in \{1, 2, 3\}$ and $j \neq h, j \neq i, h \neq i$

6. $z_j' := z_j$

7. $z_h' := z_h$

8. $z(k+1) := (z_1', z_2', z_3')$

9. $k := k + 1$

10. **end while**

The algorithm implementing the simplex is shown in Algorithm 4.

We see from the condition on line 3 that the algorithm stops at iteration $\bar{k}$ when $z(\bar{k}) = z(\bar{k} - 2)$. Since the algorithm is deterministic, it follows that a continuation after step $\bar{k}$ would lead to an oscillation between the two discrete states $z(\bar{k})$ and $z(\bar{k} - 1)$. The main limitation of the simplex algorithm is that we are not guaranteed that when the algorithm stops we have reached a neighbor of the minimum. However the simplex could be used as a first strategy to get close to the minimum.

7.5.2   Team controller design

The team controller implements the simplex algorithm. The master team controller will receive the acknowledgements from the slaves together with the measurement taken at the current position. The master then runs the simplex search algorithm in order to compute the next waypoint, computed reflecting the current waypoint at which the measured field is higher. Let assume $N = 3$.

The team controller of the master needs to compute the next simplex, which gives the next set of waypoint. It should also assign waypoints to the various slaves. Let us denote with (w_1, w_2, w_3) the current simplex and with $(w_1, w_2, w_3)^+$ the next simplex. For simplicity of notation we defined the reflecting operator

$$\xi : \mathcal{G}^3 \to \mathcal{G}^3 : (w_1, w_2, w_3) \mapsto \gamma(w_1, w_2, w_3) = w_3 + w_2 - w_1,$$

that is $\gamma(w_1, w_2, w_3)$ takes the first argument and computes its reflection with respect to the second and third argument. Thus the simplex algorithm can be then described by the map $(w^+, t^+) = \varphi_{\text{simplex}}(w, t, e)$ where $w \in \mathcal{G}^3$ is a simplex, w^+ is computed through the reflecting operator and an event e is related to the fact a vehicle arrived in a neighborhood of the waypoint.

The master team controller is the transition system $T_M = (Q_M, \rightarrow, I_M, O_M, \text{Init}_M, \text{Final}_M)$ as defined in Section 7.3 with input and outputs
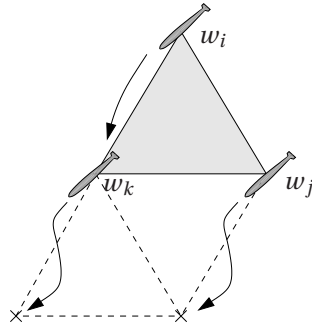
Figure 7.8: Assignment of the next waypoints for the three AUVs, by the master team controller, when $F(w_i) \geqslant F(w_j) \geqslant F(w_k)$.
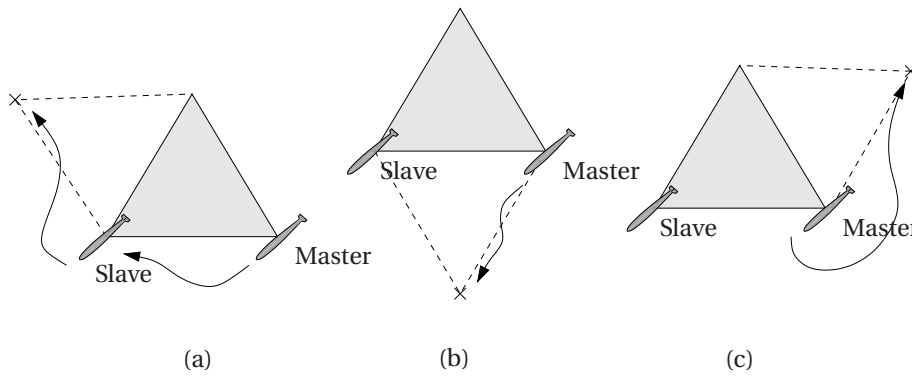

(a)   (b)   (c)

Figure 7.9: Assignment, by the master team controller, of the next waypoints when only one slave AUV is present.

- $I_M = \mathbb{R}^3$ is a vector with the three samples taken by the three vehicles,

- $O_M = \mathcal{G}^3$, is the new simplex. The vertexes are the new waypoints. (We assume that the triple is ordered so that in position i there is the next waypoint for vehicle i.)

Before defining the transition relation we notice that the master can compute two steps of the simplex algorithm, without knowing the new samples. Let us assume, without loss of generality that we start with the simplex (w_1, w_2, w_3) such that $F(w_1) \geqslant F(w_2) \geqslant F(w_3)$. Applying the simplex algorithm we have $(w_1, w_2, w_3)^+ = (\gamma(w_1, w_2, w_3), w_2, w_3)$. However in this situation the master can already compute the next simplex. Indeed two situations could occur. The case $F(\gamma(w_1, w_2, w_3)) \geqslant \max(F(w_2), F(w_3))$ implies that $(\gamma(w_1, w_2, w_3), w_2, w_3) = (w_1, w_2, w_3)$, and thus the algorithm stops. Otherwise we compute the reflected waypoint of w_2 with respect to $\gamma(w_1, w_2, w_3)$ and w_3. We have that

the transition

$$\text{Team Coord} \xrightarrow{\;Active\,acked\big/(w_1,w_2,w_3)^+\;} \text{Team Motion} \qquad (7.2)$$

is such that

$$(w_i, w_j, w_k)^+ = (w_k, \gamma(w_i, w_j, w_k), \gamma(w_j, w_k, \gamma(w_i, w_j, w_k)))$$

with $F(w_i) \geqslant F(w_j) \geqslant F(w_k)$. The situation is represented in Figure 7.8.

Notice that if any of the two slave vehicles break down or is not able to reach its assigned waypoint, the algorithm can still work. However in this case, during the reconfiguration, transition (7.2) needs to be changed. Notice that the master, just before a reconfiguration, knows the field value at each vertex of the previous simplex, and thus the next simple can always be computed. With two only vehicles the waypoint assignment is as shown in Figure 7.9.

7.5.3   Vehicle supervisor design

The vehicle supervisor consists of two possible maneuvers in this case: a Goto and a Hold maneuver. The first is issued by the master when the next waypoint is different from the previous one, whereas the second is issued when the vehicle needs to stay at the same waypoint. In this case the vehicle supervisor is as the one we presented in Section 7.3, but to the Hold state corresponds the Idle state. Indeed whenever a AUV is waiting for critical information it needs to hover around the current position.

7.5.4   Maneuver controller design

The maneuver controller is responsible of steering the AUVs from the current waypoint to the next one. If the next waypoint is the same as the current one, then the AUV will be in Hold state which means that it will follow a circular trajectory that pass through the waypoint. For the problem we are interested in, we propose the hybrid system as shown in Figure 7.10. The continuous state space $X \subseteq \mathbb{R}^4$ since we have the state of the vehicle $(x, y, \psi)^T$ and the time t.

The system starts in the Hold state. In this state the controller maintains a constant velocity so that the vehicle follows a circular trajectory. If the vehicle supervisor send a $startGoto(w_i^+, \bar{t})$ command, then the maneuver controller of vehicle i needs to steer the vehicle tracking a trajectory of the type shown in Figure 7.11. Depending on the heading of the vehicle with respect to the final waypoint, the system will jump either to the state Turn CW or Turn CCW, following an arc of circle clockwise or counter clockwise, respectively. The arc of circle in boldface shown in Figure 7.11. The minimum radius of the circle will depend on the minimum curvature of the trajectory that the vehicle can follow. When the angle of the vehicle ψ is close to the angle ψ_{ref} the vehicle switches control jumping to the Straight state. In this state the controller will make the system following a straight line passing through the next waypoint. When the distance between the vehicle and the final waypoint w_i^+ is less than a given threshold, r_{tol},
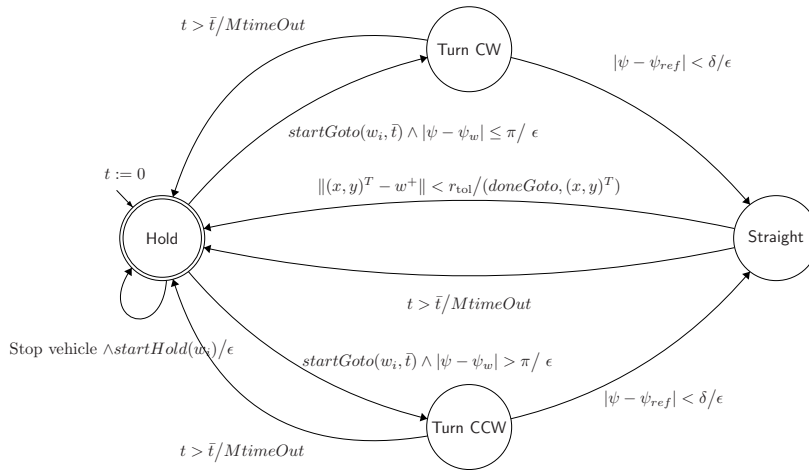
Figure 7.10: Hybrid automaton modelling the maneuver controller.

the maneuver controller returns in the Hold state maintaining the vehicle around the reached point. If something goes wrong and the maneuver controller is not able to complete the $startGoto(.)$ command within time $\bar{t}$, then an error signal is communicated to the vehicle supervisor. In case of success a $doneGoto$ together with the coordinate of the reached point are signalled to the vehicle supervisor.

This is a very simple, though instructive, example of how to build a maneuver control for this type of architecture. Complex control strategies, such as those discussed in [Souères et al. 2001], could be considered in this framework. In the case of disturbances acting on the vehicles, such as water streams, techniques as those in [Aicardi et al. 2001] could be used in order to counteract the disturbances.

7.5.5 Simulations results

Computer simulations were performed to illustrate the behavior of the proposed hierarchical control structure applied to a team of AUVs. We considered the simplex based search with three AUVs in a time-varying planar scalar field (which could represent salinity, temperature, etc.).

Figure 7.12 shows four snapshots of the evolution of the AUVs' positions in a scalar field. The field is quadratic with additive white noise and a constant drift of $(-0.4, 0)$ m/s. The approximately ellipsoidal lines are the level curves of the scalar field. Notice that we have added noise to the measurements, which is the reason why the level curves are not smooth. The simulation starts with the AUVs at the desired depth and at the vertices of a predefined initial simplex $w = ((100, 50), (122, 62), (100, 75))$. Figure 7.12(a) shows the initial trajectory of the AUVs. The grid implicitly imposed by the simplex algorithm is
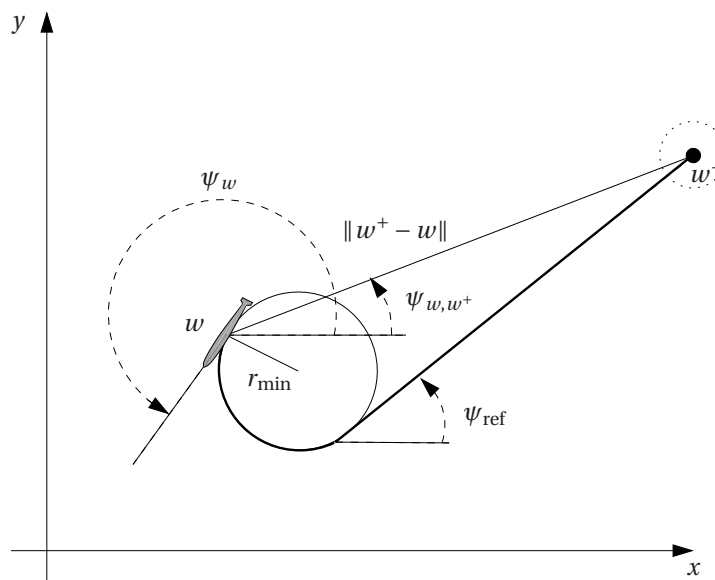
Figure 7.11: Example of a trajectory followed by a vehicle, for moving from w to w^+.

illustrated in this plot. The multi-vehicle system completes the search procedure after 135 s.

Figure 7.13 shows another scenario for the evolution of three AUVs towards the extremum of the scalar field. The initial simplex is $w = ((400, 300), (422, 312), (400, 275))$. The figure is labelled with the discrete states of the team controllers (TC), vehicle supervisors (VS) and maneuver controllers (MC) for different phases of the operation. During the progression, one of the AUVs fails to reach its waypoint. In the figure, it corresponds to the AUV with the dotted trajectory. The other two AUVs reach their corresponding waypoints and wait there until the timeout occurs. Note the circular trajectories of these two AUVs while waiting. At timeout, the system is reconfigured and the team, now composed of two vehicles, proceeds with the execution of the search. The team is able to progress towards the extremum of the field, despite the failure of one of the vehicles.

7.6   Summary

We presented a hierarchical control architecture for implementing coordination strategy for a team of autonomous vehicles. A general coordination problem was mapped onto the architecture decomposing it into waypoint generation and online execution control. The waypoint generation procedure generates the waypoints for the team in accordance to a given high-level coordination algorithm and was mapped onto the top layer of the hierarchy called team controller. The execution control was organized into

(a) AUVs' trajectories after the first iteration.

(b) Situation after 70 seconds.

(c) Situation after 100 seconds.
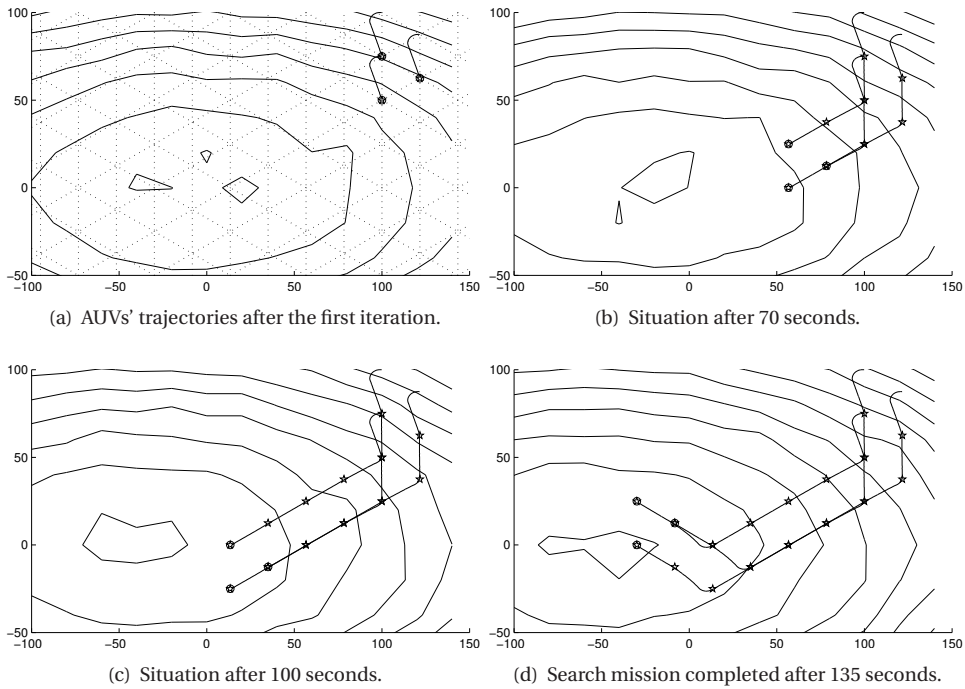
(d) Search mission completed after 135 seconds.

Figure 7.12: Simplex coordination algorithm executing a search in a noisy quadratic field with drift.

two additional layers, the vehicle supervisor and maneuver controller.

It was shown that the controller implementation is consistent with the system specification on the desired team behavior. This was done in a modular fashion by layering the execution control and designing each layer to ensure that the controllers produce suitable results.

We considered a case study, the design of a search mission for autonomous underwater vehicles and we discussed the design of all the three layers of the proposed architecture. Computer simulations illustrated the overall system performance.

(a) One step of the search algorithm

(b) The vehicle with the dotted trajectory does not reach the assigned waypoint

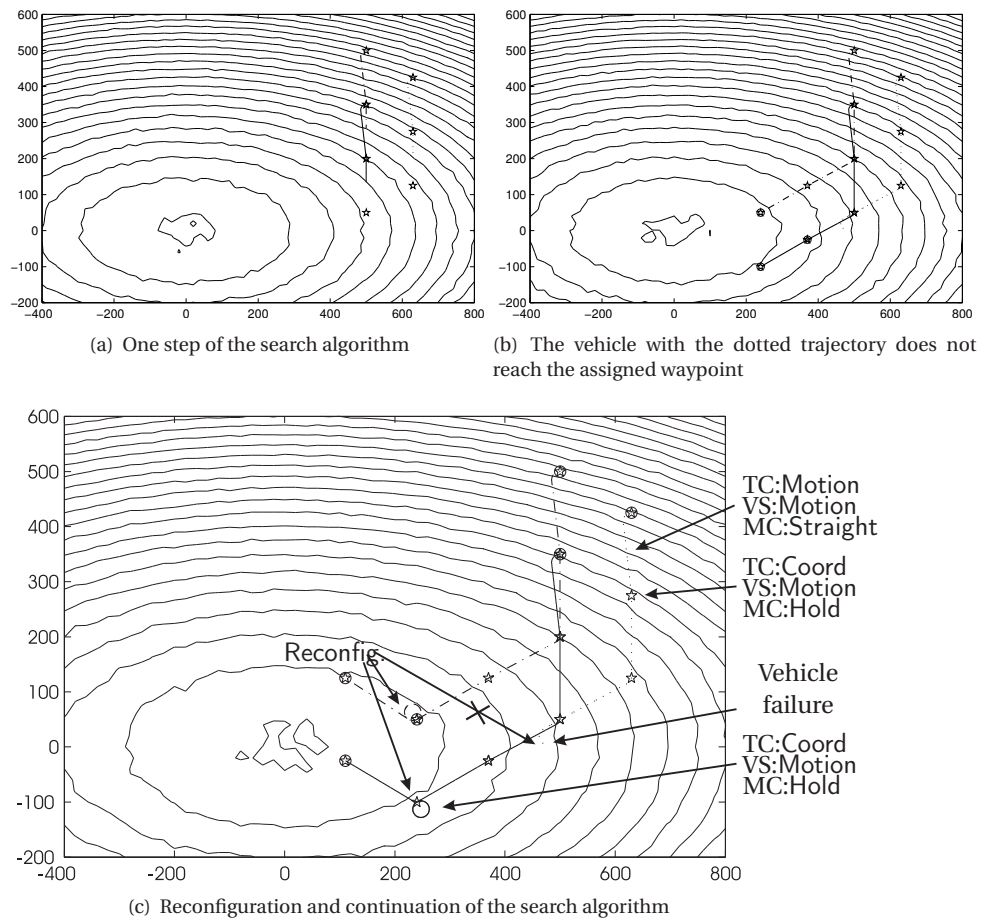(c) Reconfiguration and continuation of the search algorithm

Figure 7.13: Trajectories of three AUVs (solid, dotted, dash-dot) moving towards the minimizer of a scalar field. The stars correspond to the generated waypoints. Note the reconfiguration after a vehicle failure.

8

CONCLUSIONS AND FUTURE WORK

8.1 Conclusions

In this thesis analysis, design and implementation of cooperative control strategies for multi-robot systems under communication constraints were discussed. In particular, a problem was researched in detail in which the group of agents is supposed to agree on a common state without any centralized coordination: the consensus problem. We analyzed the tradeoffs between how fast agents can coordinate and the amount of information that needs to be exchanged. Under the assumption that the communication network has a certain symmetry, that is, it can be described by a Cayley graph on an Abelian group we determined a bound of the convergence rate to consensus. Furthermore, we proved that the convergence rate to the barycenter of the initial configuration decreases as the number of agents increases, if the amount of information does not scale with the number of agents. We also considered some particular random strategies that consist in randomly choosing a communication graph from a predefined family of graphs. In particular we considered stochastically time-varying Cayley graphs and graphs with bounded in-degree. It turns out these strategies yield a significant improvement of the performance compared to time-invariant communication graphs. Since digital communication involves quantization in order to cope with bandwidth limitations, we also analyzed the consensus problem under quantized communication data. In particular, we studied control and communication strategies that solve the consensus problem when either uniform quantizers or a mixture of uniform and logarithmic quantizers are used. Results were extended to the case of communication networks that can be modelled as Cayley graphs. Estimates of the total number of symbols needed to

achieve consensus were also derived, which allowed us to compare the different strategies.

We formulated a control design problem for which the output of the agents should coincide after a pre-specified time. The dynamics of the agents are supposed to be time-invariant and linear and subject to input constraints. A receding horizon control strategy was investigated. We showed that it was possible to design strategies where the consensus point was negotiated among the agents in a distributed way. We explored the performance by numerical simulations. The control schemes is very flexible and can handle several difficulties in multi-agent coordination. The drawback is that the general behavior is difficult to analyze for the more complex control schemes. We also designed a decentralized cooperative estimation algorithm for the estimation of time-varying signals based on a consensus filter. Specifically, the algorithm allows for accurate refinements of the estimates by employing previous estimates and noisy measurements. We provided optimal time-varying filter weights.

The implementation of multi-robot control systems is difficult due to the high system complexity. We presented a hierarchical control architecture for implementing coordination strategies for a team of autonomous vehicles. A general coordination problem was mapped onto the architecture decomposing it into waypoint generation and online execution control. The waypoint generation procedure generates waypoints in accordance to a given high-level team coordination algorithm. The execution control was organized into two additional layers: the vehicle supervisor and the maneuver controller. It was shown that the controller implementation is consistent with the system specification of the desired team behavior. This was done in a modular fashion by layering the execution control and designing each layer to ensure that the controllers produce suitable results. We considered a case study on a search mission for autonomous underwater vehicles and we discussed the design of all the three layers of the proposed architecture. Computer simulations illustrated the overall system performance.

8.2   Future work

The thesis presents original contributions to several problem in multi-robot coordination, but it also suggests may research issues for further studies. One important limitation of the considered consensus problem is on the assumption of the communication. Certain classes of time-invariant and time-varying communication graphs were studied. These simplified models allowed us to analyze also controller performance. One would need to consider more realistic network models. One such model is that where the communication graph changes with the relative position of the agents. This type of model arises when agents are considered as omnidirectional antennas with a short reliable communication range. In the literature, dynamic networks have been considered in the consensus problem, but performance analysis and quantization issues, in this type of networks, are still open questions that would be interesting to study.

Modular and flexible architectures for implementation of coordination algorithms offer many new research challenges. Verification of hierarchical control architectures

for multi-agent systems is quite an open question. The hierarchical organization is important since verification could be tackled layer by layer, assuming the other layers fulfill some specifications. Important extensions on modelling dynamic reconfiguration and uncertainty for multi-agent systems should be considered

In this thesis we focused on a master-slave architecture. In order to tackle the class of multi-agent systems we have considered in the first part of the thesis, decentralization issues need to be addressed.

REFERENCES

M. Aicardi, G. Casalino, G. Indiveri, A. Aguiar, P. Encarnação, and A. Pascoal. A planar path following controller for underactuated marine vehicles. In *Proc. 9th Mediterranean Conference on Control and Automation*, 2001.

D. J. Aldous and J. A. Fill. *Reversible Markov Chains and Random Walks on Graphs*. Book in preparation, `http://www.stat.berkeley.edu/~aldous/book.html`, 200X.

N. Alon. Eigenvalues and expanders. *Combinatorica*, 6(2):83–86, 1986.

N. Alon and Y. Roichman. Random Cayley graphs and expanders. *Random Structures and Algorithms*, 5:271–284, 1994.

K. J. Åström and B. Witternmark. *Computer-Controlled Systems*. Prenticel Hall, 1997.

L. Babai. Spectra of Cayley graphs. *Journal of Combinatorial Theory, Series B*, 27:180–189, 1979.

R. Bachmayer and N. E. Leonard. Vehicle networks for gradient descent in a sampled environment. In *Proceedings of IEEE Conference on Decision and Control*, pages 112–117, 2002.

R. W. Beard, T. W. McLain, M. Goodrich, and E. P. Anderson. Coordinated target assignment and intercept for unmanned air vehicles. *IEEE Transactions on Robotics and Automation*, 18(6):911–922, 2002.

E. Behrends. *Introduction to Markov Chains (with Special Emphasis on Rapid Mixing)*. Vieweg Verlag, 1999.

D.P. Bertsekas, A. Nedić, and A. E. Ozdaglar. *Convex Analysis and Optimization*. Athena Scientific, 2003.

P. Bolzen, P. Colaneri, and G. De Nicolao. On almost sure stability of discrete-time Markov jump linear systems. In *IEEE Conference on Decision and Control*, 2004.

J. Borges de Sousa, K. H. Johansson, A. A. Speranzon, and J. Silva. A control architecture for multiple submarines in coordinated search missions. In *16th IFAC World Congress on Automatic Control*, 2005.

F. Borrelli, T. Keviczky, K. Fregene, and G. J. Balas. Decentralized receding horizon control of cooperative vehicle formations. In *Proceedings of the 44th IEEE Conference on Decision and Control / European Control Conference*, 2005.

S. Boyd, L. El Ghaoui, E. Feron, and V. Balakrishnan. *Linear Matrix Inequalities in System and Control Theory*. Studies in Applied Mathematics. SIAM, Philadelphia, 1994.

S. Boyd, P. Diaconis, and L. Xiao. Fastest mixing Markov chain on a graph. *SIAM Review*, 46:667–689, 2004.

P. Bremaud. *Markov chains, Gibbs fields, Monte Carlo simulation, and queues.* Springer-Verlag, 2nd edition, 2001.

R.W. Brockett and D. Liberzon. Quantized feedback stabilization of linear systems. *IEEE Transaction on Automatic Control*, 45(7):1279–1289, 2000.

W. Burgard, M. Moors, C. Stachniss, and F. Schneider. Coordinated multi-robot exploration. *IEEE Transaction on Robotics*, 21(3):376–378, 2005.

E. Burian, D. Yoerger, A. Bradley, and H. Singh. Gradient search with autonomous underwater vehicles using scalar measurements. In *IEEE Symp. Autonomous Underwater Vehicle Technology*, pages 86–89, 1996.

M. Campbell, R. D'Andrea, D. Schneider, A. Chaudhry, S. Waydo, J. Sullivan, J. Veverka, and A. Klochko. Roboflag games using systems based, hierarchical control. In *Proceedings of the American Control Conference*, 2003.

N. Carter. Group explorer - software. `http://groupexplorer.sourceforge.net/`, 2005.

CNN. Trapped sub surfaces, crew safe. *CNN Online News*, 2005. `http://www.cnn.com/2005/WORLD/europe/08/06/russia.sea/index.html`.

E. Componogara, D. Jia, B. H. Krogh, and S. Talukdar. Distributed model predictive control. *IEEE Control Systems Magazine*, February 2002.

J. Cortés, S. Martínez, and F. Bullo. Robust rendezvous for mobile autonomous agents via proximity graphs in arbitrary dimensions. *IEEE Transaction on Automatic Control*, 2004a. To appear.

J. Cortés, S. Martínez, T. Karatas, and F. Bullo. Coverage control for mobile sensing networks. *IEEE Transaction on Automatic Control*, 20(2):243–255, 2004b.

J. Cortés, S. Martínez, T. Karatas, and F. Bullo. Coverage control for mobile sensing networks. *IEEE Transaction on Robotics and Automation*, 20(2):243–255, 2004c.

R. E. Curry. *Estimation and control with quantized measurements.* The MIT Press, 1970.

R. D'Andrea and G. E. Dullerud. Distributed control design for spatially interconnected systems. *IEEE Transactions on Automatic Control*, 48(9):1478–1495, 2003.

C. De Persis. On stabilization of nonlinear systems under data-rate constraints: The case of discrete-time systems. In *In Proceedings of the 16th International Symposium on Mathematical Theory of Networks and Systems*, 2004.

J. B. de Sousa, A. Girard, and Hedrick K. Real-time hybrid control of mobile offshore base scaled models. In *Proceedings of the American Control Conference*, 2000.

D. F. Delchamps. Stabilizing a linear system with quantized state feedback. *IEEE Transactions on Automatic Control*, 1990.

P. Diaconis. *Group Representations in Probability and Statistics*, volume 11 of *IMS Lecture Notes - Monograph Series, S. S. Gupta (ed.)*. Institute of Mathematical Statistics, Hawyard Ca, 1988.

R. Diestel. *Graph Theory*, volume 173 of *Graduate Texts in Mathematics*. Springer-Verlag, Heidelberg, third edition edition, 2005.

W. B. Dunbar and R. M. Murray. Receding horizon control of multi-vehicle formations: A distributed implementation. In *Proceedings of the IEEE Conference on Decision and Control*, 2004.

W. B. Dunbar and R. M. Murray. Distributed receding horizon control with application to multi-vehicle formation stabilization. *Automatica*, 2005. Submitted.

M. Egerstedt and X. Hu. Formation constrained multi-agent control. *IEEE Transaction on Robotics and Automation*, 17(6), 2001.

N. Elia and S. J. Mitter. Stabilization of linear systems with limited information. *IEEE Transactions on Automatic Control*, 46(9), 2001.

F. Fagnani and S. Zampieri. Quantized stabilization of linear systems: complexity versus performances. *IEEE Transactions on Automatic Control*, 49:1534–1548, 2004.

G. Fainekos, H. Kress-Gazit, and G. Pappas. Hybrid controllers for path planning : a temporal logic approach. In *Proceedings IEEE Conference Decision and Control*. IEEE Control Society, 2005.

Y. Fang and K. A. Loparo. Stochastic stability of jump linear systems. *IEEE Transaction on Automatic Control*, 47(7):1204–1208, 2002.

G. Ferrari-Trecate, A. Buffa, and M. Gati. Analysis of coordination in multiple agents formations through partial difference equations. Technical Report 5-PV, Istituto di Matematica Applicata e Tecnologie Informatiche, C.N.R., Pavia, Italy, 2005. Submitted for publication.

E. Fiorelli, P. Bhatta, and N. E. Leonard. Adaptive sampling using feedback control of an autonomous underwater glider fleet. In *Proc. 13th Int. Symp. on Unmanned Untethered Submersible Technology (UUST)*. IEEE, 2003.

D. Fox, W. Burgard, H. Kruppa, and S. Thrun. A probabilistic approach to collaborative multi-robot localization. *Autonomous Robots*, 2000.

J. B. Fraleigh. *A first course in Abstract Algebra*. Addison Wesley, 1998.

J. Friedman. A proof of Alon's second eigenvalue conjecture. *Accepted to the Memoirs of the A.M.S.*, 2004.

F. R. Gantmacher. *The theory of matrices*. New York : Chelsea publ., 1959.

A. Giridhar and P. R. Kumar. Distributed clock synchronization over wireless networks: Algorithms and analysis. In *Submitted to 45th IEEE Conference on Decision and Control*, 2006.

D. N. Godbole, J. Lygeros, and S. Sastry. Hierarchical hybrid control: An ivhs case study. In A. Nerode P. Antsaklis and S. Sastry, editors, *Hybrid Systems II*, LNCS, pages 166–90. Birkhauser, 1995.

Datta N. Godbole, John Lygeros, and Shankar Sastry. Hierarchical hybrid control: A case study. In *Hybrid Systems*, pages 166–190, 1994.

C. Godsil and G. Royle. *Algebraic Graph Theory*. Springer, 2001.

F. Gustafsson and F. Gunnarsson. Mobile positioning using wireless networks. *IEEE Signal Processing Magazine*, 2005.

Y. Hatano and M. Mesbahi. Agreement of random networks. In *IEEE Conference on Decision and Control*, 2004.

J. P. Hespanha, H. J. Kim, and S. Sastry. Multiple-agent probabilistic pursuit–evasion games. In *IEEE Conference on Decision and Control*, volume 3, pages 2432–2437, 1999.

A. Jadbabaie, J. Lin, and A. S. Morse. Coordination of groups of mobile autonomous agents using nearest neighbor rules. *IEEE Transactions on Automatic Control*, 48(6): 988–1001, 2003.

J.W. Jaromczyk and G.T. Toussaint. Relative neighborhood graphs and their relatives. *Proceedings of IEEE*, 80:1502–1517, 1992.

D. B. Kilfoyle and A. B. Baggeroer. The state of the art in underwater acoustic telemetry. *IEEE Journal of Oceanic Engineering*, 25(1):4–27, 2000.

T. J. Koo and S. Sastry. Bisimulation based hierarchical system architecture for single-agent multi-modal systems. In *Hybrid Systems: Computation and Control*, volume 2289. Lecture Notes in Computer Science, Springer-Verlag, 2002.

A. B. Kurzhanski and P. Varaiya. Ellipsoidal techniques for hybrid dynamics: the reachability problem. In *In Proceedings of MTNS*, 2004.

A. B. Kurzhanskii and P. Varaiya. Dynamic optimization for reachability problems. *Journal of Optimization Theory & Applications*, 108(2):227–51, 2001.

A. B. Kurzhanskii and P. Varaiya. On reachability under uncertainty. *Siam Journal of Control and Optimization*, 41(1):181–216, 2002a.

A. B. Kurzhanskii and P. Varaiya. Optimization methods for target problems of control. In *Proceedings of Mathematical Theory of Networks and Systems Conference*, 2002b.

G. Lafferriere, G. J. Pappas, and S. Yovine. Symbolic reachability computations for families of linear vector fields. *Journal of Symbolic Computation*, 32(3):231–253, 2001.

J.-P. Laumond, S. Sekhavat, and F. Lamiraux. *Guidelines in Nonholonomic Motion Planning for Mobile Robots*, volume 299, chapter 1. Lectures Notes in Control and Information Sciences, 1998. `http://www.laas.fr/~jpl/book.html`.

S. M. LaValle. *Planning Algorithms*. Cambridge University Press, 2006. Also available at http://msl.cs.uiuc.edu/planning/.

N. E. Leonard and E. Fiorelli. Virtual leaders, articial potentials and coordinated control of groups. In *Proceedings of IEEE Decision and Control Conference*, pages 2968–2973. IEEE, 2001.

P. Lima and G. N. Saridis. *Design of Intelligent Control Systems Based on Hierarchical Stochastic Automata*. Intelligent Control and Intelligent Automation. World Scientific Publisher Co., 1996.

Z. Lin, B. Francis, and M. Maggiore. On the state agreement problem for multiple nonlinear dynamical systems. In *Proceedings of 16th IFAC World Congress*, 2005.

M. Lindhé, P. Ögren, and K. H. Johansson. Flocking with obstacle avoidance: A new distributed coordination algorithm based on voronoi partitions. In *In Proceedings of IEEE ICRA*, 2005.

J. Lygeros, D. N. Godbole, and S. Sastry. Optimal control approach to multiagent, hierarchical system verification. In *In Prooceedings of IFAC World Congress*, 1996.

M. Marodi, F. d'Ovidio, and T. Vicsek. Synchronization of oscillators with long range interaction: Phase transition and anomalous finite size effects. *Phisical Review E*, 66, 2002.

M. Mazo, A. Speranzon, K. H. Johansson, and X. Hu. Multi-robot tracking of a moving object using directional sensors. In *Proceedings of the International Conference on Robotics and Automation (ICRA)*, 2004.

T.G. McGee, R. Sengupta, and K. Hedrick. Obstacle detection for small autonomous aircraft using sky segmentation. In *In Proceeedings of IEEE Conference on Robotics an Automation*, 2005.

I. Mitchell and c. Tomlin. Overapproximating reachable sets by hamilton-jacobi projections. *Journal of Scientific Computing*, 19(1-3):323–346, 2003.

S. K. Mitter. Control with limited information: the role of systems theory and information theory. *IEEE Information Theory Society Newsletter*, 4(50):122–131, 2000.

M. R. Murty. Ramanujan graphs. *Journal of Ramanujan Mathematical Society*, 18(1): 1–20, 2003.

P. Ögren. *Formation and obstacle avoidance in mobile robot control*. PhD thesis, Royal Institute of Technology, Stockholm, Sweden, 2003.

R. Olfati-Saber and R. M. Murray. Consensus problems in networks of agents with switching topology and time-delays. *IEEE Transactions on Automatic Control*, 49(9): 1520–1533, 2004.

R. Olfati-Saber and J. S. Shamma. Consensus filters for sensor networks and distributed sensor fusion. *In Proc. of IEEE CDC*, 2005.

R. Olfati-Saber, W. B. Dunbar, and R. M. Murray. Cooperative control of multi-vehicle systems using cost graphs and optimization. In *Proceedings of the American Control Conference*, 2003.

G. Oriolo, A. Luca, and M. Vendittelli. Wmr control via dynamic feedback linearization: Design. *IEEE Transactions on Control Systems Technology*, 2002.

A. Puri and P. Varaiya. Decidable hybrid systems. *Computer and Mathematical Modeling*, 11(23):191–202, 1996.

B. Recht and R. D'Andrea. Distributed control of systems over discrete groups. *IEEE Transactions on Automatic Control*, 49(9):1446–1452, 2004.

W. Ren and R. W. Beard. Consensus seeking in multiagent systems under dynamically changing interaction topologies. *IEEE Transaction on Automatic Control*, 50(5), 2005.

W. Ren and R. W. Beard. A decentralized scheme for spacecraft formation flying via the virtual structure approach. *AIAA Journal of Guidance, Control and Dynamics*, 27(1): 73–82, 2004.

L. Saloff-Coste. Random walks on finite groups. In Harry Kesten, editor, *Encyclopaedia of Mathematical Sciences*, pages 263–346. Springer, 2004.

G. N. Saridis and K. P. Valavanis. Analytical design of intelligent machines. *Automatica*, 24(2):123–33, 1988.

S. Skogestad and I. Postlethwaite. *Multivariable Feedback Control*. John Wiley & Sons, New York-Chichester-Brisbane, 2005.

S. L. Smith, M. E. Broucke, and B. A. Francis. A hierarchical cyclic pursuit scheme for vehicle networks. *Automatica*, 41(6):1045–1053, 2005.

P. Souères, A. Balluchi, and A. Bicchi. Optimal feedback control for line tracking with a bounded-curvature vehicle. *International Journal of Control*, 74(10):1009–1019, 2001.

E. M. Sozer, M. Stojanovic, and J. G. Proakis. Underwater acoustic networks. *IEEE Journal of Oceanic Engineering*, 25(1):72–83, 2000.

W. Spendley, G. R. Hext, and F. R. Himsworth. Sequential applications of simplex designs in optimization and evolutionary operation. *Technometrics*, 4:441–461, 1962.

A. Speranzon and K. H. Johansson. On some communication schemes for distributed pursuit-evasion games. In *In Proceedings of IEEE Conference on Decision and Control*, 2003.

S. H. Strogatz. From Kuramoto to Crawford: exploring the onset of synchronization in populations of coupled oscillators. *Physica D: Nonlinear Phenomena*, 143(1-4):1–20, 2000.

R. Szewczyk, A. Mainwaring, J. Polastre, and D. Culler. An analysis of a large scale habitat monitoring application. In *In Proceedings of the Second ACM Conference on Embedded Networked Sensor Systems*, 2004.

H. G. Tanner, A. Jadbabaie, and G. J. Pappas. Stable flocking of mobile agents, part II: Dynamic topology. In *IEEE Conference on Decision and Control*, 2003.

H. G. Tanner, A. Jadbabaie, and G. J. Pappas. Flocking in fixed and switching networks. *IEEE Transaction on Automatic Control*, 2005. Submitted.

S. Tatikonda and S. K. Mitter. Control under communication constraints. *IEEE Transactions on Automatic Control*, 49:1056–1068, 2004.

A. Terras. *Fourier analysis on finite groups and applications*, volume 43 of *London Mathematical Society Student Texts*. Cambridge University Press, Cambridge Ma, 1999.

UNEP. Wildland fires, a double impact on the planet. Technical report, United Nation Environment Program, 2003. `http://www.grid.unep.ch/product/publication/download/ew_fire.en.pdf`.

P. Varaiya. Smart cars on smart roads: problems of control. *IEEE Transactions on Automatic Control*, 38(3):195–207, February 1993.

P. Varaiya. Towards a layered view of control. In *IEEE Conference on Decision and Control*, volume 2, pages 1187–1190, 1997.

P. Varaiya. A question about hierarchical systems. In In T. Djaferis and I. Schick, editors, *System Theory: modeling, analysis and control*. Kluwer, 2000.

P. Varaiya. Reach set computation using optimal control. In *KIT Workshop*, 1998.

P. Varaiya and S. E. Shladover. Sketch of an ivhs systems architecture. In *Proceedings of the VNIS '91. Vehicle Navigation and Information Systems Conference*, pages 909–922. IEEE, 1991.

R. Vidal, O. Shakernia, J. Kim, D. Shim, and S. Sastry. Probabilistic pursuit-evasion games: Theory, implementation and experimental evaluation. *IEEE Transactions on Robotics and Automation*, 8(5):662–669, 2002.

B. Widrow, I. Kollar, and M. Liu. Statistical theory of quantization. *IEEE Transaction on Instrumentation and Measurement*, 45(6), 1995.

W. S. Wong and R. W. Brockett. Systems with finite communication bandwidth constraints. i. state estimation problems. *IEEE Transactions on Automatic Control*, vol.42 (no.9):1294–9, 1997.

L. Xiao, S. Boyd, and S. Lall. A scheme for robust distributed sensor fusion based on average consensus. *In Proc. of IEEE IPSN*, 2005.

L. Xiao, S. Boyd, and S. Lall. A space-time diffusion scheme for peer-to-peer least-squares estimation. In *In Proceedings of Fifth International Conference on Information Processing in Sensor Networks*, 2006. To appear.

F. Zhao, Liu J., J. Liu, L. Guibas, and J. Reich. Collaborative signal and information processing: an information-directed approach. *Proceedings of the IEEE*, 91(8), 2003.